National Library of Canada
Acquisitions and Bibliographic Services
395 Wellington Street
Ottawa ON K1A 0N4
Canada

Bibliothèque nationale du Canada
Acquisitions et services bibliographiques
395, rue Wellington
Ottawa ON K1A 0N4
Canada

Your file Votre référence

Our file Notre référence

The author has granted a non-exclusive licence allowing the National Library of Canada to reproduce, loan, distribute or sell copies of this thesis in microform, paper or electronic formats.

L'auteur a accordé une licence non exclusive permettant à la Bibliothèque nationale du Canada de reproduire, prêter, distribuer ou vendre des copies de cette thèse sous la forme de microfiche/film, de reproduction sur papier ou sur format électronique.

The author retains ownership of the copyright in this thesis. Neither the thesis nor substantial extracts from it may be printed or otherwise reproduced without the author's permission.

L'auteur conserve la propriété du droit d'auteur qui protège cette thèse. Ni la thèse ni des extraits substantiels de celle-ci ne doivent être imprimés ou autrement reproduits sans son autorisation.

0-612-46821-6

Canada

**University of Alberta**

**Library Release Form**

**Name of Author:** Mario Costa Sousa

**Title of Thesis:** Computer-Generated Graphite Pencil Materials and Rendering

**Degree:** Doctor of Philosophy

**Year this Degree Granted:** 1999

Permission is hereby granted to the University of Alberta Library to reproduce single copies of this thesis and to lend or sell such copies for private, scholarly or scientific research purposes only.

The author reserves all other publication and other rights in association with the copyright in the thesis, and except as hereinbefore provided, neither the thesis nor any substantial portion thereof may be printed or otherwise reproduced in any material form whatever without the author's prior written permission.

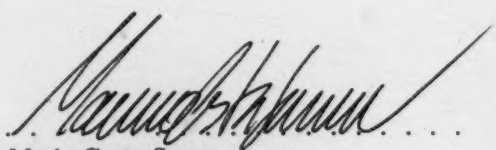

Mario Costa Sousa
Estrada da Saudade 1660
Petropolis, Rio de Janeiro
Brazil 25610-350

**Date:** AUGUST. 9, 1999

"A #2 pencil and a dream can take you anywhere."
-Joyce A. Myers

**University of Alberta**

**Faculty of Graduate Studies and Research**

The undersigned certify that they have read, and recommend to the Faculty of Graduate Studies and Research for acceptance, a thesis entitled **Computer-Generated Graphite Pencil Materials and Rendering** submitted by Mario Costa Sousa in partial fulfillment of the requirements for the degree of **Doctor of Philosophy**

. . . . . .

Dr. John W. Buchanan (Supervisor)

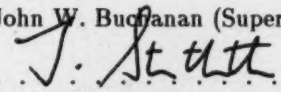

. . . . . .

Dr. Thomas Strothotte (External)

. . . . . .

Dr. Mark Green (Examiner)

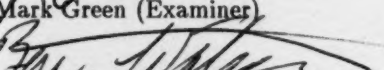

. . . . . .

Dr. Benjamin Watson (Examiner)

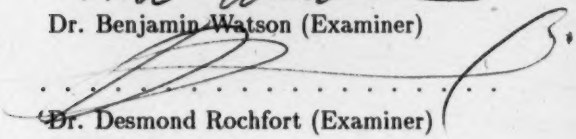

. . . . . .

Dr. Desmond Rochfort (Examiner)

**Date:** July 26, 1999

# Abstract

During the past decades, photorealism has been the driving research effort in computer graphics and has become the method of choice for rendering 3D models. Despite much recent progress in efficiency and quality of photorealistic rendering methods, there is one very important open issue remaining: Photorealistic images are not always the best option for representing information in certain application domains (architecture design, technical and artistic illustration). Therefore, alternative display methods are necessary. The main thrust of research in Non-Photorealistic Rendering (NPR) is to devise such alternative display methods. Several approaches have been proposed, and they can be categorized in two main research directions: 1) simulation of natural media for drawing (pencil, charcoal, pen-and-ink) or painting (watercolor, oil), including their correspondent rendering tools and primitives (brush, boards, strokes); and 2) rendering methods applied to reference images and/or 3D models directly. This research contributes to both directions by presenting an automatic 3D pencil rendering system. We have broken the problem of simulating pencil drawing down into four basic parts: (1) simulating the drawing materials (graphite pencil and drawing paper, blenders and kneaded eraser) (2) modeling the drawing primitives (individual pencil strokes and mark-making to create tones and textures) (3) simulating the basic rendering techniques used by artists and illustrators familiar with pencil rendering, and (4) modeling the control of the drawing composition. Each part builds upon the others and is essential to developing the framework for higher-level rendering methods and tools. We demonstrate the capabilities of our approach with a variety of images generated from 3D models.

In memory of my dear father Roberto Ferraz Costa Sousa who once encouraged me to pursue a Bachelor's degree in Computer Science back in 1985. I've always been interested on art (drawing and painting) and by that time I've also gained interested on computers. He told me "Why don't you get a degree in computer science, and then one day try to figure out how to apply computers to art making them draw for you. You will enjoy the best of both worlds." Thank you very much dad. Your suggestion really worked out.

# Acknowledgements

I wish to acknowledge all those who have contributed in some way to this work. First, I wish to express my appreciation and gratitude to my supervisor and friend John W. Buchanan. Under his guidance, I successfully overcame many difficulties and learn a lot about computer graphics and the craft of research.

It was a pleasure to work and collaborate with the University of Alberta Computer Graphics Research Group. I thank its members, Mark Green, John Buchanan and Ben Watson for helping me put the final version of the thesis and research papers together, through their reviews, comments, patience, and constant support. I would like to thank my external examiner Thomas Strothotte of the Department of Simulation and Graphics, University of Magdeburg, Germany, for his reviews, constructive criticism and positive comments, which has provided a valuable input to the final version of the thesis. My thanks also go to Desmond Rochfort, Barbara Maywood, and John Freeman of the Department of Art and Design, for their comments, discussions, and suggestions.

Many thanks to all of my colleagues from the Render Group: Oleg Veryovka, Lisa Streit, Paul Ferry, Jean-Paul Samson. We shared many hours of inspiring and fruitful discussions about work, punctuated with much fun and mutual respect all the way. We all gained insights in problems that helped to shape our personal attitudes in many respects. Together, we built up ideas and most importantly a friendship. I also thank the students and staff members of the computer graphics lab for their comments and suggestions.

Further thanks are due to the following people from the Department of Computing Science: Jim Hoover and Tony Marsland for their reviews, comments and suggestions, Xiaobo Li and Lorna Stewart for chairing my thesis defense and candidacy respectively, Roman Fedoriw for his expansive comments and suggestions, Randy Goebel for his support, and Edith Drummond for her efficient administrative support and help.

I would like to thank from the Department of Chemical and Materials Engineering, Zhenghe Xu for his insights and comments on the simulation models and Tina Barker for generating the SEM images. My thanks also go to David Clyburn of the Academic Support Centre for his valuable review of the text, and to Paul Lalonde from Electronic Arts Canada for his comments.

I couldn't forget to acknowledge all the past, present, and future pencil illustrators and artists for inspiring me on this research, and all the architects, designers, illustrators, and artists for their valuable suggestions, insights, and comments from the very beginning until the conclusion of this work.

I would also like to thank the National Council of Scientific and Technological Development of Brazil (CNPq) for funding my entire PhD program, and to the Natural Sciences and Engineering Council of Canada (NSERC) for also sponsoring this research.

On the very top of all those who I owe more than can be expressed here is my beloved wife Patricia Rebolo Medici for her support, encouragement, patience, and friendship. She always believed in me.

Finally, I am eternally in debt to my parents, Roberto Ferraz Costa Sousa and Ana Etel Costa Sousa, for their unconditional and priceless love and encouragement during all my endeavors. My affectionate thoughts also go to my siblings, relatives, and my parents-in-law for their constant support despite the great distance that separate us nowadays.

# Table of Contents


**1 Introduction** 1
- 1.1 Non-photorealistic rendering . . . 1
- 1.2 The research problem . . . 1
- 1.3 Methodology . . . 2
- 1.4 Contributions . . . 4
- 1.5 Overview . . . 4

**2 Related Work** 6
- 2.1 General overview . . . 6
- 2.2 Classification and reviews . . . 9
  - 2.2.1 Category 1: Drawing media . . . 10
  - 2.2.2 Category 2: Direct 3D rendering methods . . . 13
  - 2.2.3 Category 3: Post-processing 3D rendering methods . . . 25
- 2.3 Wrap-up . . . 29

**3 Pencil and Paper Model** 30
- 3.1 The observational approach . . . 30
- 3.2 Pencil model . . . 32
  - 3.2.1 Hard and soft pencils . . . 32
  - 3.2.2 Pencil points . . . 34
- 3.3 Paper model . . . 36
  - 3.3.1 Paper grain . . . 36
- 3.4 Pencil and paper interaction . . . 37
  - 3.4.1 Polygonal tip shape evaluation . . . 40
  - 3.4.2 Pressure distribution . . . 40
  - 3.4.3 Paper porous volume . . . 41
  - 3.4.4 How much lead material is "bitten" . . . 43
  - 3.4.5 Paper damage computation . . . 47
  - 3.4.6 Intensity value of deposited lead material . . . 47
- 3.5 Results . . . 48
  - 3.5.1 Lead material distribution and tone blending . . . 48
  - 3.5.2 Paper damage . . . 52
  - 3.5.3 Alternative drawing surfaces . . . 52
- 3.6 Wrap-up . . . 53

**4 Blender and Eraser Model** 61
- 4.1 The observational approach . . . 61
- 4.2 Model description . . . 62
  - 4.2.1 Tip shapes . . . 63
  - 4.2.2 Pressure distribution coefficients . . . 63
- 4.3 Blender and erasers interacting with lead and paper . . . 64
  - 4.3.1 Polygonal shape evaluation . . . 66
  - 4.3.2 Blender buffer . . . 66
  - 4.3.3 Pressure distribution . . . 73
  - 4.3.4 Deposit and removal of lead material . . . 73
- 4.4 Results . . . 74

4.4.1 Blender and eraser swatches . . . 74
4.4.2 Tone rendering using smudge . . . 75
4.5 Wrap-up . . . 83

**5 Drawing Primitives** **84**
5.1 Pencil stroke primitive . . . 84
5.2 Mark-making primitive . . . 86
5.3 Wrap-up . . . 88

**6 Rendering 3D Polygonal Models** **90**
6.1 The System Architecture . . . 91
6.1.1 3D models . . . 91
6.1.2 Pencil engine . . . 91
6.2 Drawing objects in outline . . . 93
6.3 Rendering objects in tonal contrast . . . 94
6.3.1 Building the tone values chart . . . 94
6.3.2 Placing linear marks . . . 101
6.3.3 Matching the target tone . . . 102
6.3.4 Tone Rendering Results . . . 102
6.4 Drawing steps control . . . 110
6.5 Wrap-up . . . 110

**7 Conclusions** **115**
7.1 Summary . . . 115
7.1.1 Methodology . . . 115
7.1.2 Modeling approach . . . 116
7.2 Extensions and future directions . . . 117

**Bibliography** **120**

# List of Figures


2.1 Roadmap of related work reviewed. . . . . 9
2.2 Notation for diagram of previous works. . . . . 11
2.3 Relationship diagram of previous works on pencil media simulation. . . . . 12
2.4 Relationship diagram of previous works on technical illustration. . . . . 14
2.5 Relationship diagram of previous works on stylized line drawing. . . . . 19
2.6 Relationship diagram of previous works on sketchy drawing. . . . . 21
2.7 Relationship diagram of previous works on post-processing NPR. . . . . 25

3.1 Samples of pencil and paper for the SEM images. . . . . 31
3.2 Distribution of percentage values of lead material for different pencil grades. 32
3.3 Pencil points. . . . . 34
3.4 Pressure distribution coefficients for the pencil. . . . . 35
3.5 Samples of drawing paper. . . . . 36
3.6 Paper grain and its volume. . . . . 37
3.7 SEM image of paper (1). . . . . 38
3.8 SEM image of paper (2). . . . . 38
3.9 SEM image of paper (3). . . . . 39
3.10 SEM image of paper (4). . . . . 39
3.11 Scaling of pencil tip shape. . . . . 40
3.12 Pressure across tip shape . . . . . 41
3.13 Distribution of lead on the grain. . . . . 43
3.14 Grain "biting" lead. . . . . 44
3.15 Volume of grain. . . . . 45
3.16 SEM image of soft pencil on paper (1). . . . . 48
3.17 SEM image of soft pencil on paper (2). . . . . 49
3.18 SEM image of soft pencil on paper (3). . . . . 49
3.19 SEM image of soft pencil on paper (4). . . . . 50
3.20 SEM image of hard pencil on paper (1). . . . . 50
3.21 SEM image of hard pencil on paper (2). . . . . 51
3.22 SEM image of hard pencil on paper (3). . . . . 51
3.23 Test samples of pencil and paper model (1). . . . . 54
3.24 Contour maps of test samples (1). . . . . 55
3.25 Test samples of pencil and paper model (2). . . . . 56
3.26 Contour maps of test samples (2). . . . . 57
3.27 Test samples of pencil and paper model (3). . . . . 58
3.28 Results of pencil and paper model (4). . . . . 59
3.29 Results of pencil and paper model (5). . . . . 60

4.1 SEM samples from blender and eraser. . . . . 62
4.2 Points for blenders/erasers. . . . . 64
4.3 Pressure distribution coefficients for blenders/erasers. . . . . 65
4.4 Pressure distributed on blenders/erasers. . . . . 66
4.5 SEM image of eraser on paper (1). . . . . 67
4.6 SEM image of eraser on paper (2). . . . . 68
4.7 SEM image of eraser (3). . . . . 69
4.8 SEM image of blender on paper (1). . . . . 70
4.9 SEM image of blender on paper (2). . . . . 71

4.10 SEM image of blender (3). . . . . 72
4.11 Swatches of blenders. . . . . 75
4.12 Contour maps of swatches of blenders. . . . . 76
4.13 Swatches and contour maps of eraser. . . . . 77
4.14 Real pencil work with smudging. . . . . 78
4.15 Smudging results (sphere and cup). . . . . 79
4.16 Smudging results (shoe). . . . . 79
4.17 Smudging results (fabric). . . . . 80
4.18 Smudging results (door). . . . . 81
4.19 Smudging results (photograph). . . . . 82

5.1 The pencil stroke primitive. . . . . 85
5.2 Real pencil work mark-making (1). . . . . 87
5.3 Real pencil work with mark-making (2). . . . . 87
5.4 Real pencil work with mark-making (3). . . . . 87
5.5 Real pencil work with mark-making (4). . . . . 88
5.6 The mark-making primitive . . . . . 89

6.1 Architecture of the pencil rendering system. . . . . 92
6.2 Real pencil work with outlines (1). . . . . 94
6.3 Real pencil work with outlines (2). . . . . 95
6.4 Real pencil work with outlines (3). . . . . 96
6.5 Four outline results from our system. . . . . 98
6.6 Result for accented outline from our system. . . . . 99
6.7 Result for outlining from our system. . . . . 100
6.8 Tone value charts generated by the pencil engine. . . . . 101
6.9 Main steps on placing linear marks. . . . . 102
6.10 Four variations of tone value study generated by our system. . . . . 103
6.11 Real pencil work with mass shading. . . . . 105
6.12 Results for mass shading from our system. . . . . 106
6.13 Real pencil work with hatching and feathering shading. . . . . 107
6.14 Result for feathering shading from our system (1). . . . . 107
6.15 Result for feathering shading from our system (2). . . . . 108
6.16 Real pencil work with mass and feathering shading. . . . . 108
6.17 Results of pencil rendering in tonal contrast from our system. . . . . 109
6.18 Real pencil work with drawing steps. . . . . 111
6.19 Results of drawing steps control from our system. . . . . 112
6.20 Examples of a pencil rendering study from our system. . . . . 113

# List of Tables


2.1 Summary of related work . . . . . 7

3.1 Variables for the pencil and paper model. . . . . 33
3.2 Percentage values of lead material for different pencil grades. . . . . 34

4.1 Variables for the blender and eraser model. . . . . 63

6.1 Range values for outlining from the pencil engine. . . . . 97
6.2 Range values for shading from the pencil engine. . . . . 104

# Chapter 1

# Introduction

## 1.1 Non-photorealistic rendering

The display of models using highly realistic illumination models has driven much of the research in computer graphics. Despite much recent progress in efficiency and quality of photorealistic rendering methods, there is one very important open issue remaining: Photorealistic images are not always the best option for representing information in certain application domains (architecture, design, technical and artistic illustration). In response to these limitations on photorealistic rendering methods, several novel approaches, classified as Non-Photorealistic Rendering (NPR), have been developed. The main goal of NPR research is to develop a variety of techniques to attain a pictures' quality with a distinct yet non-photographic "realism" in an attempt to provide alternative display methods for computer-generated images. By providing rendering systems that use these alternative display models users can generate traditional renderings. These systems are not intended to replace artists or illustrators, but rather to provide a tool for users with no training in a particular medium, thus enabling them to produce traditional images.

## 1.2 The research problem

Several approaches in NPR research have been proposed and they can be categorized in two main research directions:

1. Simulation of natural media for drawing (pencil, charcoal, pen-and-ink) or painting (watercolor, oil), including their correspondent rendering tools and primitives (brush, boards, strokes);

2. Rendering methods applied to reference images and/or 3D models directly.

Very few recent works followed the approach of combining both research directions. Winkenbach and Salesin [Wink94, Wink96b, Wink96a] showed that some of these capabilities are achievable by tailoring pen-and-ink medium with 3D NPR rendering techniques which emulates pen-and-ink style. More recently, Curtis et al. [Curt97] showed the same for computer-generated watercolor. These research works cited convincingly as reasons for a new direction in NPR research. The use of any traditional media extends the achievement of characterization, abstraction, invention, and subjective interpretation. Devising models, algorithms and techniques to simulate a particular traditional media and its use in the context of automatic rendering of three-dimensional models is a strong motivating factor behind new research directions in NPR. Many issues need to be addressed, mainly what specific techniques should be evolved and how they might be implemented if they can be implemented at all.

Our research has focused on developing a simulation model for the graphite pencil medium on drawing paper, and implementing the basic rules for achieving traditional graphite pencil illustration styles adapted to the 3D rendering pipeline. We chose the pencil because it is a flexible medium, providing a great variety of styles in terms of line quality, hand gesture, and tone building. It is excellent for preparatory sketches and for finished rendering results. Many people in different contexts such as scientific and technical illustration, architecture, art and design use pencil renderings.

## 1.3 Methodology

After surveying the computer graphics literature we classified existing research works in NPR in the following taxonomy:

1. **Materials:** What media is simulated? This can be drawing media (pencil, pen-and-ink, charcoal) or painting media (oil, watercolor, pastel). What is the rendering primitive? This can be simulation models for board (the drawing/painting surface), brush and strokes.

2. **Subject:** What is the input source for drawing/painting? This can be free composition (i.e. interactive painting systems), direct or post-processing 3D rendering. Direct 3D rendering means that the NPR pipeline access directly the data structures and algorithms coupled to the 3D objects in a scene. Post-processing means that the 3D model is first pre-rendered, and a set of information is stored in buffers to be post-processed by the NPR algorithms.

3. **Process:** What rules are used to generate the image? This can be interactive (user interaction techniques, metaphors, devices...) and/or automatic (rules, algorithms...).

4. **Application:** What is the target public for the system? This determines the rendering style (technical illustration, sketchy artistic drawing, and painterly rendering) based on the application (art, design, architecture, illustration, scientific visualization).

Based on the taxonomy above we have broken the problem of simulating pencil drawing down into four basic parts: (1) simulating the drawing materials (graphite pencil and drawing paper, blenders and kneaded eraser) (2) modeling the drawing primitives (individual pencil strokes and mark-making to create tones and textures) (3) simulating the basic rendering techniques used by artists and illustrators familiar with pencil rendering, and (4) modeling the control of the drawing composition. Each part builds upon the others and is essential to developing the framework for higher-level rendering methods and tools. We then categorized each part into three levels of system design:

1. **Low level: Simulation models**: Drawing materials: low-level simulation models for wood-encased graphite pencil and drawing paper (chap. 3), and for blenders and kneaded eraser (chap. 4).

2. **Medium level: Rendering methods**: (a) Drawing primitives: pencil stroke and mark-making (for tones and textures) (chap. 5) built on top of the drawing materials; (b) Rendering algorithms built on top of the drawing primitives. Algorithms for outlining, shading 3D objects with a look that emulates real pencil drawings (chap. 6).

3. **High level: Drawing composition**: Partial control of the drawing composition through ordering and repeating of drawing steps (chap. 6).

This approach allows that the effectiveness of each technique can be examined independently and in combination. We also selected literature on pencil [Salw25, Gupt33, Ruff69, Lali69, Gupt77, Wats78, Wats83, Lewi84, Borg85, Fran88, Loha93, Pric93, Misa94, Camh97] and drawing [Doug93, Hort94, Team97] to provide guidelines for the development of specific aspects from each of the three system levels.

## 1.4 Contributions

The main contribution of our research is on the modeling and implementation of an integrated framework for non-photorealistic rendering tailoring media simulation, drawing primitives, and 3D rendering techniques correspondent to the graphite pencil media. More specifically this thesis makes the contributions at two levels:

**Concept**

The results from our research showed that graphite pencil is a useful technical and artistic NPR production technique. The development of a pencil and paper renderer contributes to NPR by providing a good model for pencil drawing and by providing an automatic system which 3D models can be rendered in a simple pencil and paper style. The issue of the style of the rendering is beyond the scope of this thesis. Rather the results in this thesis show how the pencil and paper model resembles traditional pencil and paper results. By picking a simple style [Gupt77, Ruff69, Misa94, Wats78] the results show how the basic tools of pencil and paper illustration can be controlled by a computer rendering system.

**Algorithms**

1. *Observational models for wood-encased graphite pencils, drawing paper, stump and tortillon blenders, and kneaded erasers*: Abstraction of essential physical properties and behaviors from real pencil drawing materials. Resulting models are fast and produce quality results.

2. *Drawing primitives and rendering methods*: Visual analogies result from the analysis of types of structural correspondence already developed by artists. The algorithms developed duplicate such visual analogies both independently and in combination.

3. *Tone control for automatic shading of 3D models*:

   Extends the concept of matching the target tone in pen-and-ink using stroke textures [Wink94, Wink96b, Wink96a] to the graphite pencil medium.

## 1.5 Overview

The next chapter presents a review of NPR literature relevant to the research. Chapter 3 describes the pencil and paper model and Chapter 4 describes the blender and eraser model. Chapter 5 describes the pencil stroke and mark-making primitives built on top

of the pencil and paper model. Chapter 6 describes pencil-based outlining and shading methods with results for 3D models. The description of the control of pencil drawing steps from preparatory sketches to finished rendering results is also presented in Chapter 6. In Chapter 7 we conclude with discussions and ideas for future work.

# Chapter 2

# Related Work

This chapter is organized as follows: Section 2.1 gives an overview of the previous related work based on the taxonomy of non-photorealistic rendering (NPR) methods presented on Chapter 1. Section 2.2 provides a categorization of the previous work focusing on the main aspects of our research, and then presents the reviews of each previous work from each of the categories.

## 2.1 General overview

Our work is related to research on automatic NPR of 3D models with none or very little intervention of the user. We use the taxonomy on NPR approaches presented in Chapter 1, and summarize on Table 2.1 the main capabilities of 30 previous work representative to this thesis. An assessment of Table 2.1 is given next.

Appel et al. [Appe79] was the first reported work following the approach of direct 3D NPR methods. In these methods the NPR pipeline directly access the data structures and algorithms coupled to the 3D objects in a scene. Appel et al. improved the wire-frame rendering by providing display models for technical illustration style. Then in 1987 Sasada [Sasa87] improved the shaded renderings by exploring ways of representing 3D models for natural sceneries in a stylized line drawing fashion. In the same year Kamada and Kawai [Kama87] improved the hidden-line treatment by developing methods of rendering 3D models based on technical illustration conventions and in 1990 Dooley and Cohen [Dool90a] continued to explore this approach. In the same year Dooley and Cohen [Dool90b] extended their previous work [Dool90a] by improving the shaded renderings of 3D models again in a technical illustration style. Also in 1990 Saito and Takahashi [Sait90] introduced the idea and methods of post-processing 3D NPR. In these methods the 3D model is first pre-rendered and a set of information is stored in buffers to be post-processed by

| *References* | **Materials** | | **Subject** | | | **Process** | | **Style** | | | |
|---|---|---|---|---|---|---|---|---|---|---|---|
| | Media | Primitives | Direct 3D | Post-proc. | Free | Automatic | Interactive | Technical | Stylized | Sketchy | Painterly |
| [Appe79] | | | √ | | | √ | | √ | | | |
| [Kama87] | | | √ | | | √ | | √ | | | |
| [Sasa87] | | | √ | | | √ | | ~ | √ | | |
| [Bles88] | *charcoal* | √ | | | √ | | √ | | | | |
| [Verm89] | *graphite pencil* | √ | | | √ | | √ | | | | |
| [Dool90a, Dool90b] | | | √ | | | √ | | √ | | | |
| [Sait90] | | | | √ | | √ | | ~ | √ | | |
| [Scho93] | | √ | ~ | √ | ~ | ~ | √ | | ~ | ~ | √ |
| [Leis94] | | | | √ | | √ | | | √ | | |
| [Sait94] | | √ | √ | | | √ | | | √ | | |
| [Stro94] | | √ | √ | | | √ | ~ | | | √ | |
| [Wink94, Wink96b, Wink96a] | *pen-and-ink* | √ | √ | | | √ | ~ | | | √ | |
| [Elbe95b, Elbe95a, Elbe98] | | √ | √ | | | √ | | | √ | | |
| [Hall95] | | √ | √ | | | √ | | ~ | √ | | |
| [Deca96b, Deca96a] | | | | √ | | √ | | | √ | | |
| [Meie96] | | √ | √ | | | √ | | | | | √ |
| [Schl96] | | √ | √ | | | √ | | √ | | | |
| [Curt97] | *watercolor* | √ | | √ | ~ | √ | ~ | | | | √ |
| [Mark97] | | √ | √ | | | √ | | ~ | | √ | |
| [Taka97] | *colored pencil* | | | | √ | | √ | | | | |
| [Gooc98a, Gooc98b] | | | √ | | | √ | ~ | √ | | ~ | |
| [Very99a, Very99b] | | √ | | √ | | √ | | ~ | √ | ~ | ~ |
| This thesis,[Sous99b, Sous99a, Sous99c] | *graphite pencil, paper blender, eraser* | √ | √ | ~ | ~ | √ | ~ | ~ | ~ | √ | |

Table 2.1: Summary of related work according to the taxonomy presented in Chapter 1, Section 1.3. The √ symbol indicates the main emphasis and contributions of the work. The ~ symbol indicates other capabilities of the work.

the NPR algorithms using a set of buffers. We can notice that, during the 90's, the direct 3D NPR approach has been the dominant research direction with contributions on alternative displays models emulating technical illustrations [Schl96, Gooc98a, Gooc98b], stylized line drawings [Sait94, Elbe95b, Elbe95a, Elbe98, Hall95], sketchy drawings [Wink94, Stro94, Wink96b, Wink96a, Mark97], and painterly rendering [Meie96]. Most research on post-processing 3D NPR has been on using and extending the concepts and techniques presented by Saito and Takahashi [Sait90] contributing with displays models for painterly rendering [Scho93, Curt97], stylized line drawing [Leis94, Deca96b, Deca96a], and more recently on texturing in the context of half-toning [Very99a, Very99b].

Notice that the majority of existing NPR works modeled the primitives (brushes, strokes) independently of any particular media. Our work follows an approach not very much explored where 3D NPR techniques are tailored to specific media models. Two particular previous works followed this approach: the works of Winkenbach and Salesin [Wink94, Wink96b, Wink96a] where results were produced from emulating the pen-and-ink illustration style for direct 3D NPR, and the work of Curtis et al. [Curt97] describing a detailed simulation model for watercolor with its painting style for post-processing 3D NPR. Our research has focused on developing a simulation model for the graphite pencil (media and primitives) [Sous99c, Sous99b, Sous99a] (chaps. 3, 4, 5) and using this model in the implementation of the basic rules for achieving traditional pencil illustration styles adapted directly to the 3D rendering pipeline [Sous99a] (chap. 6). The main reason to follow this approach is that it allows the consistent modeling of effects and techniques of a specific media from the low level simulation models until higher-level tools and rendering methods.

Our pencil and paper model [Sous99c] (chap. 3) is based on the graphite, clay, and wax composition of the pencil lead and on the texture and weight of the paper. Our blender and eraser model [Sous99b] (chap. 4) is based on their absorptive and dispersal properties of deposited lead material (graphite, clay, and wax particles) on drawing paper. We also considered most of the effects that are important for a pencil illustrator to master, in particular the order in which pencil materials are used, the pressure applied, the manner in which the pencil is sharpened, and the way the pencil materials are held. Previous work on pencil simulation has addressed few of these issues. Vermeulen and Tanner [Verm89] introduced a simple pencil model as part of an interactive painting system that does not include a model to handle textured paper and other supplementary drawing materials. Takagi and Fujishiro [Taka97] presented a model for paper micro-structure and pigment distribution for colored pencils to be used in digital painting. Bleser et al. [Bles88] presented

a charcoal model as part of an interactive painting system based on a lookup table of pre-designed bit maps from charcoal drawing for each brush. In the commercial realm, some interactive painting systems such as Fractal Design Painter offer pencil, erasers, and blenders models with some interaction with the paper. Even though a number of systems offer "pencil" mode it is difficult to determine what physical model, if any, is being used to simulate the pencil, blenders, and erasers. The models presented on this thesis improve the approximation of graphite pencil renderings on drawing paper.

## 2.2 Classification and reviews

Due to the wide scope of NPR approaches, we need a classification scheme to provide some uniform point of view over the two main aspects of our research: drawing media (pencil) and 3D NPR. We selected and combined specific categories from the taxonomy presented in Chapter 1 resulting in three new categories (see fig. 2.1) with 23 previous related work: **Drawing media** (subsec. 2.2.1) [Bles88, Verm89, Taka97], **direct 3D rendering** (subsec. 2.2.2) [Appe79, Kama87, Sasa87, Dool90a, Dool90b, Stro94, Sait94, Elbe95a, Hall95, Schl96, Wink96a, Meie96, Mark97, Gooc98a], and **post-processing 3D rendering** (subsec. 2.2.3) [Sait90, Scho93, Leis94, Deca96a, Curt97, Very99a].

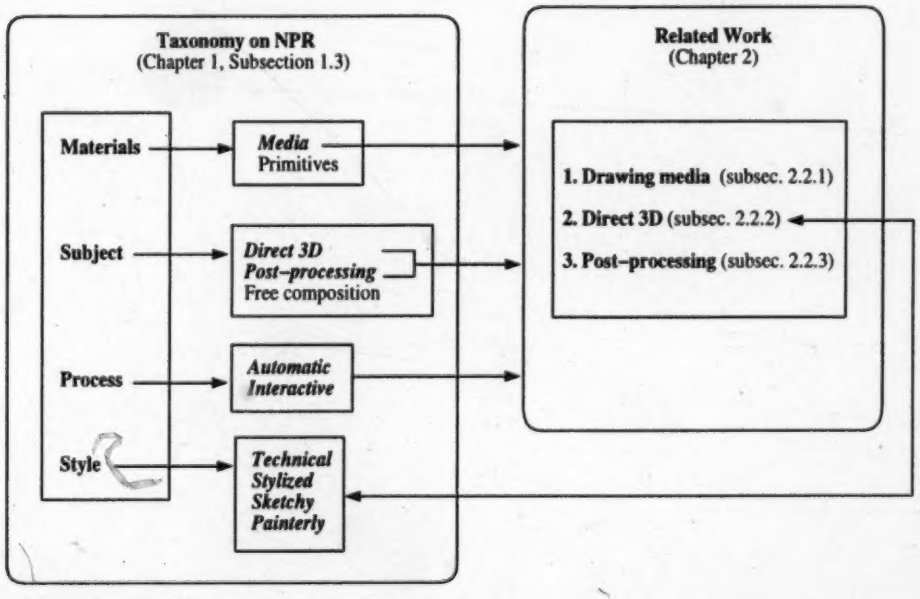


Figure 2.1: Relationship between the taxonomy on NPR methods (chap. 1) and the three new categories of related work reviewed.

Each paper from each of the three categories is briefly reviewed and a list of open research problems (excerpted from the original source) is presented. We illustrate the interrelationships among pieces of previous works based on the open problems reported. We use the diagram notation presented in Figure 2.2 which allows the reader to better visualize how the solutions to the individual problems have evolved over time. For each paper reviewed we also provide an assessment of what has become of the open problems.

### 2.2.1 Category 1: Drawing media

Our pencil model is of the type wood-encased artist-grade graphite pencils. These pencils belong to the family of carbon-based dry drawing media that make black marks or variations of black throughout the black/gray scale. Camhy [Camh97] classifies this kind of media in five categories:

1. Carbon Pencils
2. Charcoal: *Vine, Powdered, Compressed, and Pencils*
3. Graphite: *Powder, Sticks, Crayons, Plastic-Coated Pencils, Paper-Wrapped Pencils, Mechanical Pencils*
4. Wood-encased Graphite Pencils: *School-Grade, Artist-Grade, and Carpenter's Pencils*
5. Graphite for Nonpaper Surfaces

We reviewed previous work in the context of NPR and graphics literature related to the classification above, also including colored pencils. Figure 2.3 illustrates the interrelationship among previous works in this category.

#### (1) PencilSketch — A Pencil-Based Paint System

Vermeulen and Tanner [Verm89] introduced a simple pencil model as part of an interactive painting system which includes:

1. The amount of graphite already on the paper.
2. The hardness of the pencil.
3. The pressure applied to the pencil.
4. The shape of the pencil marks on the paper.

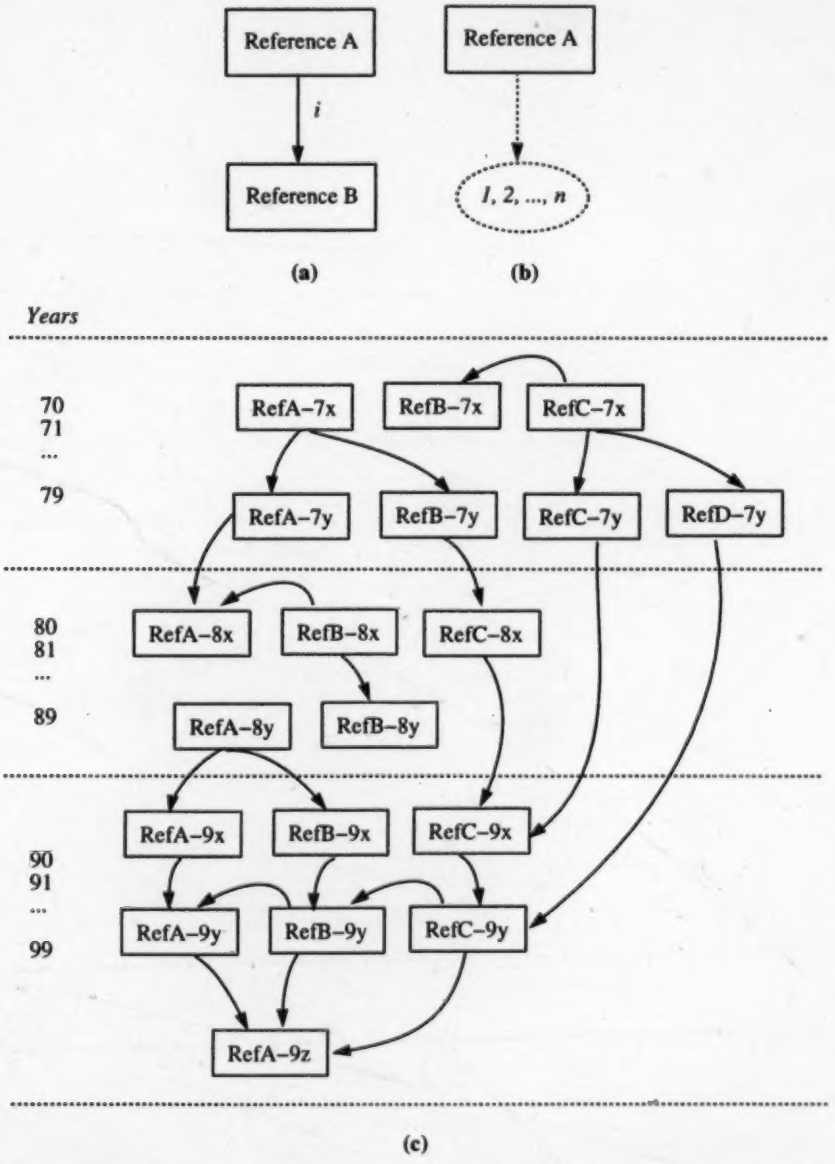


Figure 2.2: Notation for the diagrams describing the interrelationship among previous works. It reads as (a) "open problem *i* from Reference A was addressed by Reference B", (b) "open problems *1, 2, ..., n* from Reference A remain open to further investigations". (c) The diagrams are organized hierarchically based on the chronology of the work reviewed.

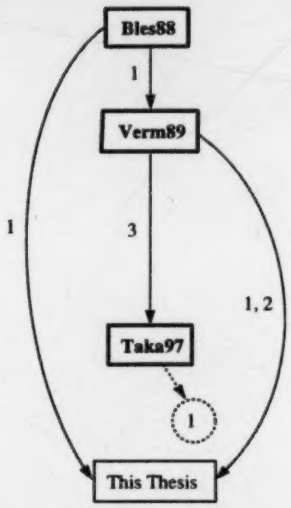


Figure 2.3: Diagram describing the interrelationship among previous works on computer-generated media simulation. See Figure 2.2 for the diagram notation and organization.

5. The tilt of the pencil.

Their model does not process any interaction of the pencil with textured paper.
Open problems:

1. Improve the interaction and improve and extend the underlying conceptual model.
2. Extend the pencil, paper, and eraser models to allow textured paper.
3. Extend the model to colored pencils and paper.

This thesis addresses problem 1 by improving and extending the conceptual model for the pencil system. Our design approach consists of three system levels: materials, rendering methods, and drawing composition (see chap. 1, sec. 1.3 for more details). This thesis also addresses problem 2 contributing with an additional model for blenders (chap. 4). Problem 3 was addressed to some extent by Takagi and Fujishiro [Taka97]. Our model can be also extended to handle colored pencils (chap. 7).

**(2) Charcoal Sketching: Returning Control to the Artist**

Bleser et al. [Bles88] presented a system which allows a user to draw lines in which one small bit map is transferred to the screen using a raster-op for each new x,y position. A matrix of bit maps from charcoal drawing is pre-designed for each brush. The values for

pressure, x tilt, and y tilt are used as indexes in a table lookup to find the correct brush shape with correspondent bit-map.
Open problems:

1. Develop algorithms for creating brushes on the fly.

Vermeulen and Tanner [Verm89] addressed problem 1 by providing a lead function associated with each pencil. This lead function varies in shape and distribution. This thesis also addresses problem 1 by providing a model in which the tip shapes of pencils, blenders, and erasers are modeled and pressure distributed according to the hand gestures modeled (chaps. 3, 4, 5).

**(3) Microscopic Structural Modeling of Colored Pencil Drawings**

Takagi and Fujishiro [Taka97] presented a model for paper 3D microstructure and pigment distribution for colored pencils to be used in digital painting.
Open problems:

1. Redistribution of pigment with water.

Problem 1 has not been addressed. One approach would be to extend our model to colored pencil and combine it with watercolor models [Smal91, Curt97] (see chap. 7).

### 2.2.2 Category 2: Direct 3D rendering methods

In these methods the NPR pipeline directly access the data structures and algorithms coupled to the 3D objects in a scene. We classified the related work according to the rendering style reproduced:

1. **Technical illustrations** by improving wire-frame rendering [Appe79], hidden-line treatment [Kama87, Dool90a], and shaded renderings [Dool90b, Schl96, Gooc98a] (see fig. 2.4),
2. **Stylized line illustrations** [Sasa87, Leis94, Sait94, Hall95, Elbe95a] (see fig. 2.5),
3. **Sketchy drawings** [Stro94, Wink96a, Mark97] (see fig. 2.6),
4. **Painterly styles** [Meie96] (see fig. 2.6).

*Direct 3D rendering: Rendering Style: Technical Illustration*
Figure 2.4 illustrates the interrelationship among previous works in this category.

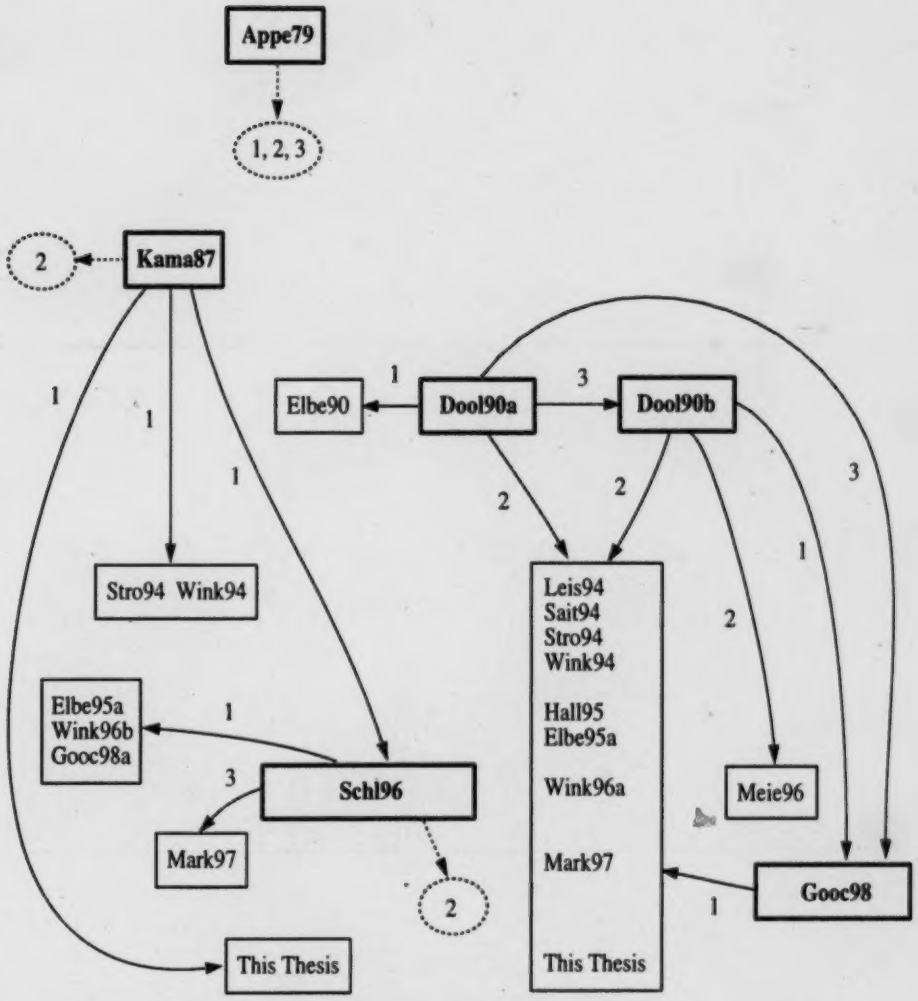


Figure 2.4: Diagram describing the interrelationship among previous works on computer-generated technical illustration direct from 3D models.

**(1) The Haloed Line Effect for Hidden Line Elimination**

Appel et al. [Appe79] presented an algorithm for the haloed line effect which is a common technique in hand drawn technical illustration. This effect assumes the existence of an imaginary region, a halo, surrounding three-dimensional lines that can obscure any lines that pass behind the halo. The input subject to the algorithm is three-dimensional wire frame models. This style may be preferable for depicting structures or finite element networks.
Open problems:

1. Improve the calculation of which lines cross.
2. Explore ways in which the haloed line effect can augment or benefit from the original hidden line techniques.
3. Add additional lines to a scene (patterns, planes) which are not intended to be drawn but which can obscure other lines. This would result in an approximation to complete hidden line elimination.

Problems 1, 2, 3 have not been addressed.

**(2) An Enhanced Treatment of Hidden Lines**

Kamada and Kawai [Kama87] presented a display method where the hidden-lines from three-dimensional objects are not eliminated but displayed in a distinguishable style as commonly used in drafting. The user controls the rules and attributes for determining the line style (full, dashed, dotted, no line) depending on the set of surfaces which hide it.
Open problems:

1. Graphics systems to have a more flexible and user controllable visualization mechanism in order to create pictures for a wide range of user needs.
2. Attribute determination on the basis of some viewing environments. The attributes of lines and surfaces can be determined by using the combination of shielding information as viewed from multiple viewpoints.

Strothotte et al. [Stro94] addressed problem 1 by providing an interactive system that allows the user to better control the drawing composition of the scene in terms of emphasis and points of interest. Winkenbach and Salesin [Wink94] also addressed this problem by allowing the interactive control for the placement of strokes indicating where details should appear

on the surfaces of the objects. Schlechtweg and Strothotte [Schl96] also addressed problem 1 by providing an interactive system that controls the distribution of "drawing resources" allowing different levels of details in the final rendering. This thesis also addresses problem 1 by providing the partial control of drawing steps during the rendering composition (chap. 6). Problem 2 has not been addressed.

**(3) Automatic illustration of 3D geometric models: Lines**

Dooley and Cohen [Dool90a] described a system that automatically generates informative illustrations directly from 3D computer models. The focus is on enlarging the vocabulary of lines, line types and attributes, and their use in technical illustration to convey meaning. Their illustration system allows objects to be assigned importance attributes. These attributes are then used in combination with a set of illustration rules to create the final image. The line attributes take into account the importance of the objects, the line type defined by width, transparency, and style (solid, dashed, invisible), and the way that objects obscure each other.

Open problems:

1. Determining a full set of hidden line segments from complex assemblies of free-form objects.
2. Other types of line style, such as sketchy lines.
3. Intelligent use of surface shading techniques such as ray tracing or radiosity in combination with line drawings.

Problem 1 was addressed by Elber and Cohen [Elbe90] by describing a technique that extracts the visible curves for a given scene without the need to approximate the surface by polygons. Problem 2 was addressed by a number of researchers [Sait94, Stro94, Wink94, Hall95, Elbe95a, Wink96b, Mark97] and also addressed on this thesis (chaps. 4, 5, 6). Problem 3 was addressed by Gooch et al. [Gooc98b] by presenting a shading model tailored to imitate colored technical drawings which is also used in combination with line drawings. Dooley and Cohen [Dool90b] also addressed problem 3 by using ray-tracing and line drawing (see next paper (4) below).

**(4) Automatic illustration of 3D geometric models: Surfaces**

Dooley and Cohen [Dool90b] describe an extension to their previous system [Dool90a] for automating the illustration of geometric models based on traditional hand illustration meth-

ods. The focus is on how surfaces are displayed and then composited with line illustrations. Lines are passed through a hidden line detection routine. Surfaces are ray traced to gather visibility information including a list of hidden surfaces. The collected visibility data is then used to map the model geometry to drawable primitives. The line attributes are color, width, transparency and style (solid, dashed, dotted, invisible). Surfaces are addressed with a screen space based pattern, producing a "hatching" appearance.
Open problems:

1. The use of color to increase the power of the illustration paradigm in an integrated way.

2. Other types of line style, such as sketchy lines, and surface types, such as painterly quality.

Problem 1 corresponds to open problem 3 from Dooley and Cohen [Dool90a] and problem 2 corresponds to open problem 1 also from Dooley and Cohen [Dool90a]. Meier [Meie96] also addressed problem 2 by providing a system that automatically places painterly marks on 3D models.

**(5) Rendering Line-Drawings with Limited Resources**

Schlechtweg and Strothotte [Schl96] presented a system which is based on a line-renderer and which enables a user to interact with the drawing created. Their concept is to measure the use of "drawing resources" (the set of contour and hatching lines) for each object in a scene. Based on these measures, the system controls the level of detail, and with it the level of abstraction contained in the line drawing. The measures used include the overall line count, overall line length, average line length, object visibility, line width, and line brightness.
Open problems:

1. Examine the use of splines and free form surfaces

2. Study a new method of interaction to enter the hatching or reduction parameters, using the pointing device as a kind of eraser, removing more and more detail when moving over a surface.

3. Develop very effective ways to do the rendering in near real-time as reaction to the interactions.

Problem 1 was addressed by some researchers [Gooc98a, Elbe95a, Wink96b]. Problem 2 has not been addressed. Problem 3 was addressed by Markosian et al. [Mark97] by optimizing silhouette detection.

**(6) Interactive Non-Photorealistic Technical Illustration**

Gooch [Gooc98a] explored lighting, shading, and line illustration conventions used by technical illustrators. These conventions are implemented in a modeling system to create a new method of displaying and viewing complex NURBS models. In particular, silhouettes and edge lines are drawn in a manner similar to pen-and-ink drawings, and a shading algorithm is used that is similar to ink-wash or airbrush renderings for areas inside the silhouettes. This shading has a low intensity variation so that the black silhouettes remain visually distinct, and it has a cool-to-warm hue transition to help accent surface orientation. Applying these illustration methods produces images that are closer to human-drawn illustrations than is provided by traditional computer graphics approaches.
Open problems:

1. Incorporating other illustration techniques such as automatic layout, different line styles, cut-aways, exploded views, and object transparency.

2. Exploring a nonlinear shading model or a perceptually uniform gradation from cool to warm may tap into more shape information.

3. Scientifically analyzing whether or not the techniques presented here provides more shape information than traditional approaches in computer graphics may lead to more effective methods for conveying the important geometric properties of 3D models.

The incorporation of different line styles (part of problem 1) has been addressed before by a number of reserachers [Sait94, Stro94, Wink94, Hall95, Elbe95a, Wink96b, Mark97] and continued to be addressed on this thesis. Other issues from problem 1 have not been addressed. Problem 2 has not been addressed. The main idea of problem 3 was addressed before by Schumann et al. [Schu96] where an empirical study was performed with architects who compared the output of a sketch-renderer for producing NPR line drawings with standard output of CAD systems. Their results showed that the different kinds of renditions actually have a very different effect on viewers.

*Direct 3D rendering: Rendering Style: Stylized Line Illustrations*

Figure 2.5 illustrates the interrelationship among previous works in this category.

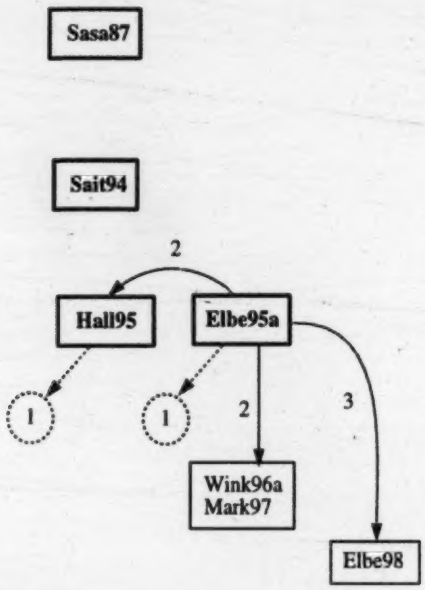


Figure 2.5: Diagram describing the interrelationship among previous works on computer-generated stylized line drawing direct from 3D models.

### (7) Drawing natural scenery by computer graphics

Sasada [Sasa87] analyzed hand-drawings of natural sceneries (mountains, trees, water) and developed algorithms that model the phenomena governing those drawings. These algorithms operate over 3D meshes and surface models (for mountains and waters). For trees, shape pattern generation was used.

No open problems reported.

### (8) Real-time Previewing for Volume Visualization

Saito [Sait94] proposed a new approach for volume visualization with the aim of the real-time previewing of 3D scalar fields. Instead of voxels, hierarchically sampled points are used to store scalar values. Each sampled point has a priority value, and the sets of points that have higher priority than any particular level are evenly distributed in 3D. In the rendering step, points are selected by certain criteria using priority level, scalar value, and the gradient magnitude. Each selected point is drawn as a simple primitive such as line segment(s) or polygons with up to four vertices.

No open problems reported.

**(9) Comic-strip Rendering**

Hall [Hall95] proposed a method that simulates the shading and shadowing of a regular, planar grid on the surface of an object. This grid generates a crosshatch shading effect. The thickness and spacing of the grid lines are adjusted according to the lighting information at a specific point on the object. Additionally, each model can be rendered in a different style.
Open problems:

1. Develop algorithms to yield images with non-regular patterns.

Problem 1 has not been addressed by explicitly extending the author's approach. However, non-regular patterns for shading and texturing were addressed by some researchers [Stro94, Wink94, Elbe95a, Wink96b] and also addressed on this thesis.

**(10) Line art rendering via a coverage of isoparametric curves**

Elber [Elbe95a] presents a model for free-form surface coverage using a set of isoparametric curves, which exploits a simple lighting model to control the density of the coverage.
Open problems:

1. A more advanced lighting model can improve the quality of the result.
2. New methods to achieve highly aesthetic line-art renderings of synthetic scenes.
3. Efficient ways to create a parameterization independent coverage.

Problem 1 has not been addressed. Problem 2 has been addressed in [Wink96a, Mark97] and also on this thesis. Problem 3 was addressed by Elber [Elbe98].

*Direct 3D rendering: Rendering Style: Sketchy/Artistic Drawing*

Figure 2.6 illustrates the interrelationship among previous works in this category.

**(11) How to Render Frames and Influence People**

Strothotte et al. [Stro94] presented the design and implementation of a system for rendering sketches that are similar to drawings done by hand. The user manipulates parameters defining how lines are drawn and how shadows are used. The system also automatically accentuates or suppresses details over different parts of the image by changing the line rendering

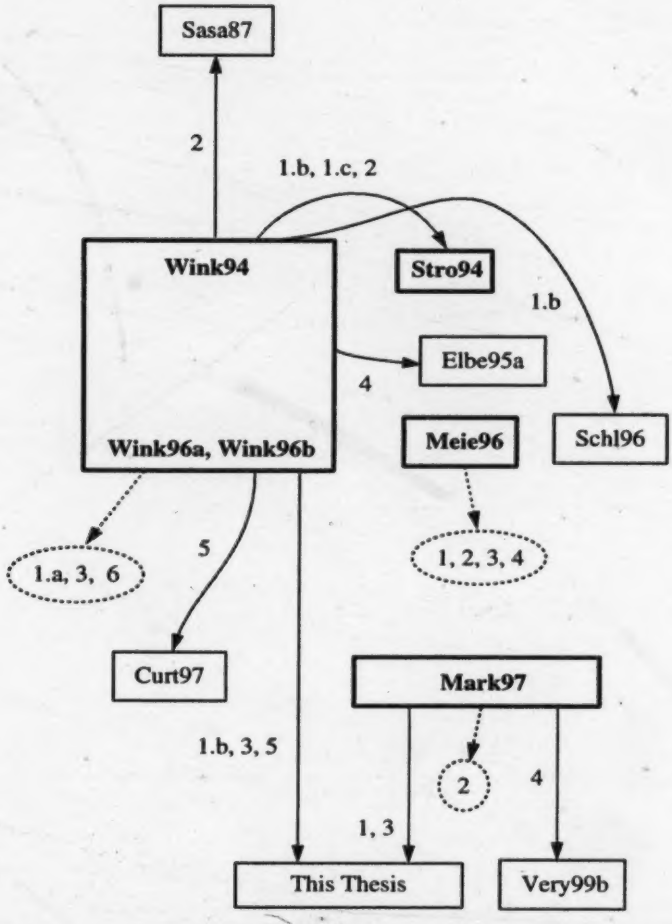


Figure 2.6: Diagram describing the interrelationship among previous works on computer-generated sketchy drawing and painterly rendering direct from 3D models.

styles. Finally the authors also present line rendering methods to represent movements of objects and rendering of natural forms based on L-systems.
No open problems reported.

**(12) Computer Generated Pen-and-Ink Illustration**

Winkenbach [Wink96a] described the principles of pen-and-ink illustration showing how a great number of them can be implemented as part of an automated rendering system. The most important points presented are the following:

1. Software architecture for pen-and-ink rendering, showing how the traditional graphics pipeline must be modified to support pen-and-ink rendering.
2. Prioritized stroke textures, providing a framework for creating textures from pen-and-ink strokes. It also provides a methodology to build procedural versions of these textures, taking into account the resolution of the target device and the size of the image into account.
3. Stroke textures on flat-shaded polygonal models.
4. Stroke textures on parametric surfaces, providing a mathematical framework and algorithms allowing stroke textures to be mapped onto parametric free-form surfaces.
5. Planar map algorithms, showing how to build planar maps from 3D geometric data and their use for stroke clipping and outlining.

Open problems:

1. Further development to design a truly effective and flexible illustration system:
   (a) Illustration effects such as exploded views, cut-aways, and peel-back views.
   (b) High-level interactive tools that give the user enough flexibility to compose a good illustration.
   (c) Very high-level controls to adjust parameters such as emphasis, indication, or lighting.
2. Render natural forms such as trees, grass, water, and human figures.
3. Automate and improve the creation of stroke textures.

4. Generalize the free-form hatching algorithm to handle a broader class of curved surfaces.

5. Devise algorithms and techniques to handle other styles of illustration (watercolor, pencil drawing, air brushing, etc.)

6. Consider computer-generated imagery as a style of its own and find new and effective ways of conveying visual information that do not necessarily mimic traditional illustration forms.

Problem 1.a has not been addressed. Problems 1.b and 1.c deal with drawing composition issues. Strothotte et al. [Stro94] and Schlechtweg and Strothotte [Schl96] addressed it (see open problem 1 from Kamada and Kawai [Kama87]). This thesis also addresses problem 1.b by providing the partial control of drawing steps during the rendering composition (chap. 6). Sasada [Sasa87] addressed problem 2 to some extent by presenting results from renderings of mountains, trees, and water. Strothotte et al. [Stro94] also addressed problem 2 to some extent with some line drawing results for L-systems. This thesis addresses problem 3 to some extent by introducing the mark-making primitive that extends the concept of stroke textures for pen-and-ink to graphite pencil. Problem 4 has been addressed by Elber [Elbe95b, Elbe98]. Problem 5 was addressed by Curtis et al. [Curt97] by presenting a detailed simulation model for watercolor. This thesis also addresses problem 5 by presenting models for graphite pencil drawing materials. Problem 6 has not been addressed. Schofield [Scho93] also presented conceptual aspects and points of views about problem 6.

**(13) Real-time Non-photorealistic Rendering**

Markosian et al. [Mark97] presented a non-photorealistic rendering technique based on the idea that a great deal of information can be effectively conveyed by very few strokes. They demonstrate the use of three main techniques (probabilistic identification of silhouette edges, inter-frame coherence of silhouette edges, and fast visibility determination using improvements and simplification in Appel's hidden-line algorithm) to support a variety of rendering styles. These include a spare line-rendering style, a variety of sketchy hand-drawn styles, and a technique for adding shading strokes to basic visible-line renderings.
Open problems:

1. Generalize the handling of shading strokes to support arbitrary lighting conditions and to better control the density of strokes in screen space to match a target gray value.

2. Enhance the shaded stroke renderings by the addition of cast shadows.

3. Explore different rendering styles.

4. Use of additional information in model definitions which can be used to produce non-photorealistic renderings which reflect information about a model beyond basic geometric attributes, or which target particular esthetic effects.

This thesis addresses problem 1 by describing a method to match the target tone with the mark-making shading primitive and tone value charts (chaps. 5, 6). Problem 2 has not been addressed. Problem 3 has been addressed before by a number of researchers [Sait94, Stro94, Wink94, Hall95, Elbe95a, Wink96b] and is also addressed in this thesis by modeling traditional graphite pencil rendering styles (chap. 6). Problem 4 has been addressed by a number of researchers [Sait90, Scho93, Deca96b, Curt97, Very99b].

*Direct 3D rendering: Rendering Style: Painterly Rendering*

Figure 2.6 illustrates the interrelationship among previous works in this category.

**(14) Painterly Rendering for Animation**

Meier [Meie96] presented a technique for rendering animations in a painterly style. It combines two rendering methods: (1) the use of particles to define locations in the 3D object geometry where brush strokes will be rendered and (2) the use of reference pictures to define 2D brush stroke attributes (color, size, and orientation). Her algorithm solves two major problems in rendering animations in a painterly style: (1) coherence over time without exhibiting random frame-by-frame changes and (2) the stick of brush strokes to the animating surfaces and not the viewplane, which eliminates the "shower door" effect.

Open problems:

1. Use the method to render surfaces that are difficult to model (e.g. trees) and render using traditional geometry and texture maps.

2. Automate brush stroke size based on the screen surface addressed, and then changes the size smoothly as the object changes size using multi-resolution techniques.

3. Use a better particle placement method that covers both the geometric surface and screen space more evenly.

4. Implement longer, deformable brushes that can follow curves on a surface.

Problems 1, 2, 3, and 4 have not been addressed. Hertzmann [Hert98] presented a technique for painting with long, curved brushed strokes, aligned to normals of image gradients. One possible direction to address problem 4 is to investigate the extension of Hertzmann's technique to 3D models.

### 2.2.3 Category 3: Post-processing 3D rendering methods

Post-processing means that the 3D model is first pre-rendered and a set of information is stored in buffers to be post-processed by the NPR algorithms. Although this thesis is based on direct 3D NPR methods we decided to review 5 representative previous works on post-processing 3D NPR mainly to provide a uniform view of 3D NPR. Also the combination of both direct and post-processing 3D NPR techniques is a potential direction to further investigation. Figure 2.7 illustrates the interrelationship among previous works in this category.

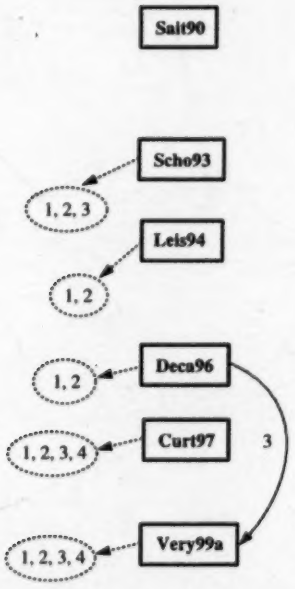


Figure 2.7: Diagram describing the interrelationship among previous works on NPR post-processed from 3D models.

#### (1) Comprehensible Rendering of 3-D Shapes

Saito and Takahashi [Sait90] presented a technique that preserve geometric properties in a per-pixel basis from pre-rendered 3D models in G-buffers which are then post-processed

using combinations of 2D image enhancement techniques: drawing discontinuities, contour lines, and curved hatching.
No open problems reported.

**(2) Non-Photorealistic Rendering: A Critical Examination and Proposed System**

Schofield [Scho93] presented a framework for non-photorealistic rendering systems and describes the design and implementation of a system based on the G-buffer approach. His dissertation covers three main technical issues:

1. The mark synthesizer, which is an engine for generating a wide variety of efficient, parametised painterly marks.
2. The enriched pixel scene description (EPixel), which follows the G-buffer approach, by storing a set of geometrical and other information for each pixel from pre-rendered scenes. Several rendering techniques using the EPixel buffers are described.
3. The sketcher trees, which provides the basis for a framework to facilitate the authorship of rendering styles in ways that are intuitive, flexible, and extensible. These trees embodies algorithms that are configured by the user, and at each node a set of unique instructions and operations guide the action and technique of drawing. At the bottom of the tree a graphic element (mark, texture, dot, and effect) is applied to the image.

These models were then combined into a prototype system called Piranesi, which allows a semi-automatic non-photorealistic rendering approach.
Open problems:

1. Combine Digital Photogrammetry with Un-lighting techniques to generate EPixel images from photographs.
2. An intuitive interface that allows the authoring and tweaking of Sketchers in ways that artists and designers will understand has yet to be built.
3. An important phase in the investigation will be the monitoring of the systems ability and limitations in a proper design environment.

Problems 1, 2 have not been addressed. Problem 3 has been addressed in a different context by Schumann et al. [Schu96] (see open problem 3 from Gooch [Gooc98a]).

**(3) Computer generated copper plates**

Leister [Leis94] described a method to generate copper plates used for presenting technical facts and for book illustrations. The method ray traces the objects and post-processes the results with image processing operators in order to determine some of the optical properties of copper plates. The algorithm processes hatches, edges, and second order rays.
Open problems:

1. How to use the technique for computer animation.
2. Investigate the problems occurring in motion blur and interference.

Problems 1 and 2 have not been addressed.

**(4) Cartoon-Looking Rendering of 3D-Scenes**

Decaudin [Deca96b] presented a rendering algorithm which produces images having the appearance of a traditional cartoon from a 3D description of the scene (a static or an animated scene). The 3D scene is rendered with techniques allowing to:

- Outline the profiles and edges of objects in back.
- Color uniformly the patches.
- Render shadows (self-shadows and projected shadows) due to light sources.

Open problems:

1. Treat transparent objects
2. Control the thickness of the features of contour independent of anti-aliasing
3. Vary this thickness of the lines according to the curve of surface.

Problems 1 and 2 have not been addressed. Problem 3 has been addressed by Winkenbach and Salesin [Wink96b], Elber [Elbe95a] and Veryovka [Very99a].

**(5) Computer-Generated Watercolor**

Curtis et al. [Curt97] characterize the most important effects of watercolor and show how they can be simulated automatically. Their watercolor model uses a cellular automaton to simulate fluid flow and pigment dispersion, including a sophisticated paper model, a

complex shallow water simulation, and a faithful rendering and optical compositing of pigmented layers based on the Kubelka-Munk model. They demonstrate how their simulation model can be used in an interactive paint system, as a method for automatic image "watercolorization", and as a mechanism for non-photorealistic rendering of three-dimensional scenes.

Open problems:

1. Other effects: spattering, drybrush technique, integrate watercolor with other media.
2. Automatic rendering: specify wet areas so that hard edges are placed properly; color separation algorithm to calculate the optimal palette of pigments to use for various regions of the image; automatic recognition and generation of textures using drybrush, spattering, scraping, and other techniques.
3. Generalization: develop a model that could integrate backruns and wet-in-wet flow, parameterized by wetness.
4. Animation issues: develop a system that takes into account the issue of coherency over time and allows the user to control these artifacts.

Problems 1, 2, 3, and 4 have not been addressed. Meier [Meie96] has addressed problem 4 in the context of general painterly rendering without considering any specific painting media.

**(6) Texture Control in Digital Halftoning**

Veryovka [Very99a] presented a new approach to expressive display of images by controlling the appearance of texture in halftoned images. His methods are based on previous halftoning algorithms (ordered dither and error diffusion) and they explore the ability of the ordered dither algorithm to define halftoning texture through the arrangement of threshold values in its dither matrix. A user may introduce a variety of artistic effects in the image. Examples include embossing an image with a texture or text; approximation of traditional art styles and rendering techniques — pencil drawing, carving, oil brush painting. Veryovka's method also includes techniques that allow us to map texture features to enhance representation of image gradient, 3-D scene information and subjective user defined information [Very99b].

Open problems:

1. Control the individual placement of graphics primitives.

2. The control of texture scale and direction is limited to piece-wise constant parameters. Continuous changes of these texture features must be correlated and require additional investigation.

3. Use of optimization based halftoning techniques to enhance the approximation of image features and avoid strong artificial texturing.

4. Develop additional image quality metrics taking into account many known properties of the human visual system including contrast sensitivity function, texture orientation and viewing conditions.

Problems 1, 2, 3, and 4 have not been addressed.

## 2.3 Wrap-up

In this chapter we reviewed representative sources from the NPR literature as follows: The main capabilities of 30 previous related work to this thesis were summarized and assessed according to the taxonomy of NPR methods introduced in Chapter 1. These works were then further categorized focusing on the two main aspects of this thesis (drawing media and 3D NPR), resulting in three new categories and 23 previous works. We briefly review each work from each of the three categories listing their open problems reported. Finally we illustrate and assess the interrelationships among papers from each category.

# Chapter 3

# Pencil and Paper Model

This chapter presents a pencil and paper model that produce realistic looking pencil marks, textures, and tones. Our model is based on an observation of how lead pencils interact with drawing paper. Our model considers parameters such as the particle composition of the lead, the texture of the paper, the position and shape of the pencil point, and the pressure applied to the pencil. We demonstrate the capabilities of our approach with a variety of images and compare them to digitized pencil drawings. The resulting values of the parameters were found by careful use of the system until the satisfactory results were achieved.

The organization of this chapter is as follows. Section 3.1 describes the observational approach taken to build our model. Section 3.2 presents in detail the pencil model and Section 3.3 presents the paper model. The interaction between the two models is described in Section 3.4. Section 3.5 presents results from our models on different paper textures, various pencil swatches (tone samples), and on tone rendering methods.

## 3.1 The observational approach

Our approach is based on an observational model of how real graphite pencils interact with drawing paper. The goal was to capture the essential physical properties and behaviors observed to produce quality pencil marks at interactive rates. Our intention was not to develop a highly physically accurate model, which would lead to a computationally expensive simulation. All parameters described are important to achieve good pencil simulation results. The observations were performed by producing a great variety of pencil swatches, strokes, and marks over different types of drawing papers, and magnifying them by using the Hitachi S-2700 scanning electron microscope (SEM) from the Department of Chemical and Materials Engineering at the University of Alberta. These images were used to aid in the

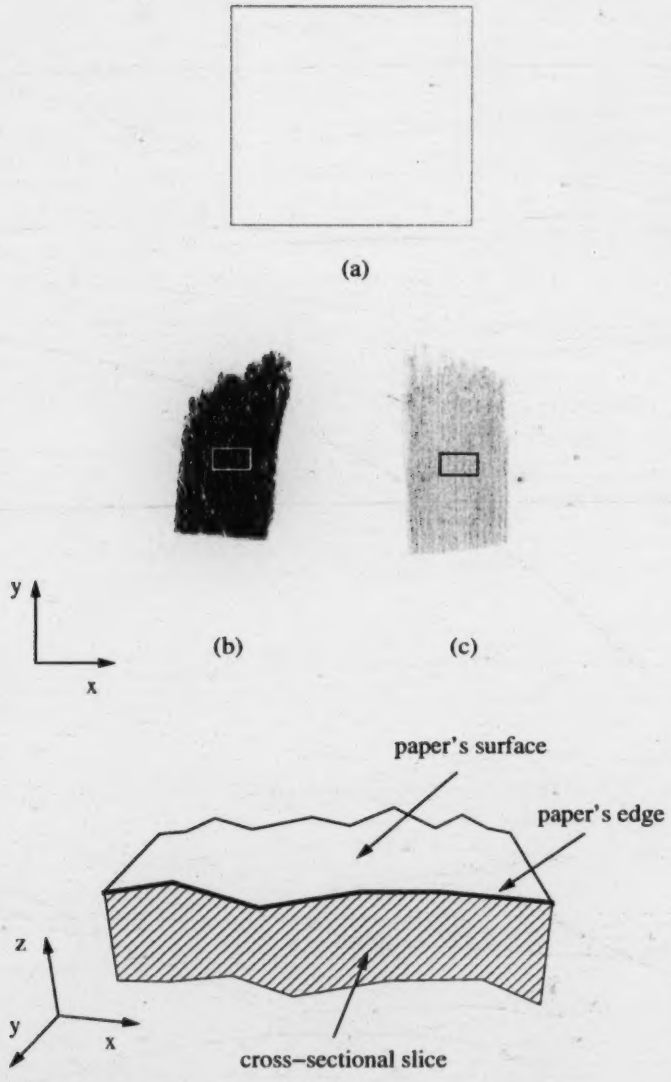


Figure 3.1: Samples of 15mm in diameter (rectangular area within samples in (a), (b), (c)) used to generate the SEM results: (a) medium weight, moderate tooth drawing paper (SEM images in figs. 3.7, 3.8, 3.9, 3.10), (b) soft pencil applied on paper in (a) (figs. 3.16, 3.17, 3.18, 3.19), (c) hard-pencil applied on paper in (a) (figs. 3.20, 3.21, 3.22). The bottom of the figure illustrates the viewing position for the cross-sectional views of the samples used for the SEM images (figs. 3.9, 3.10, 3.18, 3.19, 3.22).

development of the observational models for pencils and papers. Aerial and cross-sectional views from real pencil drawing samples (fig. 3.1) were generated by the SEM at 10kv accelerating voltage, with different magnifications, and with scale resolution in microns (one micron equals to approximately one millionth of a meter in length).

## 3.2 Pencil model

Our pencil model is from the category of wood-encased artist-grade graphite pencils [Camh97]. It has two main aspects: the degree of hardness and softness and the kinds of sharpened points. They are described in the next subsections. A list of variables used throughout this section is given in Table 3.1.

### 3.2.1 Hard and soft pencils

Every pencil contains a writing core (or "lead") which is made from a mixture of graphite, wax, and clay, the latter of which is the binding agent. The hardness of the lead depends on the percentage amount of graphite and clay. The more graphite it contains the softer and the thicker it is. Pencil hardness is graded in degrees $P_d$. Usually nineteen degrees are used ranging from 9H to 8B. Wax is included for lubrication. Table 3.2 presents the percentage values of graphite, clay, and wax particles for the nineteen grades of pencil. Figure 3.2 illustrates the linear distribution of the lead material content for the entire range of pencil grades. The thickness for a particular lead degree can be also approximated by linearly interpolating between the thickness of the hardest lead (2 *mm* for 9H) and the thickness of the softest lead (4 *mm* for 8B).

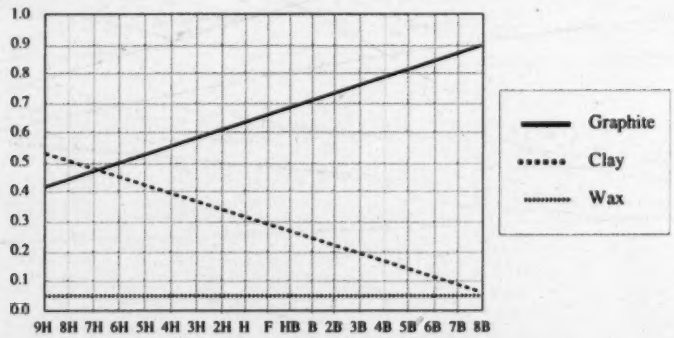


Figure 3.2: Linear distribution percentage of graphite, clay, and wax for nineteen degrees of pencil leads based on information received from pencil manufacturers.

| | |
|---|---|
| **Pencil model** (sec. 3.2) | |
| $P_d$ | Pencil degree of hardness. |
| $G_p, C_p, W_p$ | Percentages of graphite, clay, and wax particles. |
| $T_s$ | Tip shape. |
| $P_c$ | Pressure distribution coefficients. |
| **Paper model** (sec. 3.3) | |
| $w$ | Paper weight. |
| $F_s$ | Total amount of lead material to fill the surface of the grain. |
| $F_v$ | Total amount of lead material to fill the volume of the grain. |
| $V_g$ | Grain porous volume. |
| $T_v$ | Lead threshold volume. |
| *Variables at paper(x,y) indexed by k:* | |
| $L_k$ | Lead threshold volume. |
| $D_k$ | Percentage of lead material distributed. |
| **Pencil and paper interaction** (sec. 3.4) | |
| $p$ | Pressure applied to the pencil. |
| $p'_c, p'_{c_i}$ | Pencil pressure at the pressure distribution coefficients $P_c$. |
| $(xs, ys, ps)$ | Interpolated coordinates and pressure at the tip shape $T_s$. |
| $P_a$ | Averaged pencil pressure. |
| $D_l$ | Depth of lead into the grain. |
| $B_v$ | Volume of lead bitten by the grain. |
| $h_m$ | Medium grain height. |
| $M$ | Percentage of extra lead material. |
| *Variables at paper(x,y) indexed by k:* | |
| $B_k$ | Volume of lead bitten. |
| $E_k$ | Amount of paper damaged. |
| $(G_k, C_k, W_k)$ | Amount of graphite, clay, and wax deposited. |
| $T_k$ | Total amount of lead material deposited. |
| $A_k$ | Amount of graphite deposited. |
| $F_t$ | Maximum amount of lead material. |
| $I_k$ | Reflected intensity of lead material. |

Table 3.1: List of variables used for the pencil and paper model.

| Pencil Number | Graphite | Clay | Wax |
|---|---|---|---|
| 9H | 0.41 | 0.53 | 0.05 |
| 8H | 0.44 | 0.50 | 0.05 |
| 7H | 0.47 | 0.47 | 0.05 |
| 6H | 0.50 | 0.45 | 0.05 |
| 5H | 0.52 | 0.42 | 0.05 |
| 4H | 0.55 | 0.39 | 0.05 |
| 3H | 0.58 | 0.36 | 0.05 |
| 2H | 0.60 | 0.34 | 0.05 |
| H | 0.63 | 0.31 | 0.05 |
| F | 0.66 | 0.28 | 0.05 |
| HB | 0.68 | 0.26 | 0.05 |
| B | 0.71 | 0.23 | 0.05 |
| 2B | 0.74 | 0.20 | 0.05 |
| 3B | 0.76 | 0.18 | 0.05 |
| 4B | 0.79 | 0.15 | 0.05 |
| 5B | 0.82 | 0.12 | 0.05 |
| 6B | 0.84 | 0.10 | 0.05 |
| 7B | 0.87 | 0.73 | 0.05 |
| 8B | 0.90 | 0.04 | 0.05 |

Table 3.2: Percentage values of graphite, clay, and wax particles for the entire range of pencil grades based on information received from pencil manufacturers.

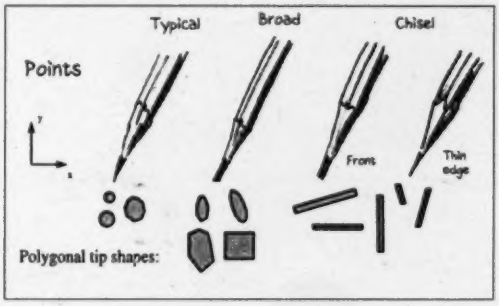


Figure 3.3: Different kinds of canonical points [Gupt77, pp. 22] and their polygonal tip shapes.

### 3.2.2 Pencil points

Sharpening a pencil in different ways changes the shape of the contact surface between the pencil and the paper. The pencil responds rapidly to almost any demand. Sharply pointed, it gives a line as fine and clean-cut as that of the pen; bluntly pointed, it can be used much like the brush. A pencil point is defined by tip shape and pressure distribution coefficients over the point's surface.

#### Tip shape

The tip shape is defined as a polygonal outline based on the shape of three canonical types of sharpened pencil points (typical, broad, and chiseled) [Gupt77, pp. 22] (see fig. 3.3).

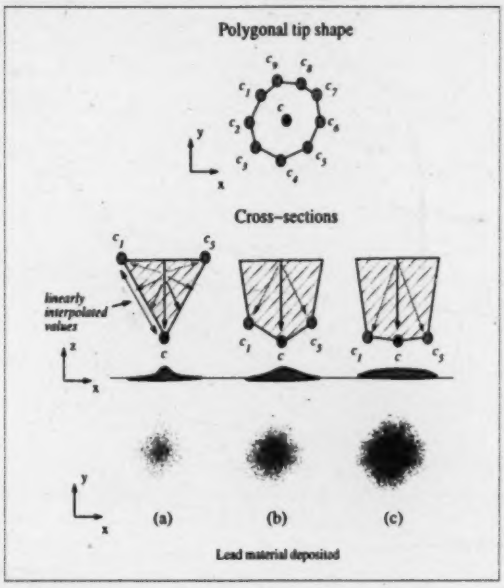


Figure 3.4: Different values of pressure distribution coefficients $(c, c_i), i \in [1, 9]$ across the polygonal shape result in different distribution of lead material over the paper's surface. The results for lead material deposited are for $c = 1.0$ and the same $c_i$ values (0.2 for (a), 0.5 for (b), and 0.9 for (c)) for all vertices in the polygonal tip shape.

A pencil tip shape is defined as $T_s = \{(x_i, y_i), s : 3 \leq i \leq n\}$, where $(x_i, y_i)$ is one the $n$ vertices of the polygon and $s$ is the scale factor of the polygon used to account for the thickness of the lead.

**Pressure distribution coefficients**

Pressure distribution coefficients are values between 0 and 1 representing the percentage of the pencil's point surface that, on average, makes contact with the paper. This value is used to locally scale the pressure being applied to the pencil. The pressure distribution coefficients are defined as $P_c = (c, x, y), (c_i, xi, y_i) : 1 \leq i \leq n\}$ where $c$ is the value of the main pressure distribution coefficient whose location $(x, y)$ can be anywhere within the polygon defining the tip shape (default location is at the center of the polygon), and $c_i$ is the value of the pressure distribution coefficient at vertex $(x_i, y_i)$ from the polygonal tip shape. Different values can be assigned to $c$ and to each $c_i$. The closer they are to 1.0, the more surface is in contact with the paper. The closer they are to 0.0, the less surface is in contact with the paper. The values between $c$ and $c_i$ are computed by linear interpolation, thus defining the overall shape of the pencil's tip (see fig. 3.4).

## 3.3 Paper model

Good pencils are essential, but the quality of a pencil drawing also depends on the paper used. Pencil illustrators pay as much attention to their choice of paper as to the choice of pencils. Papers are made in a great variety of weights and textures. The thickness of drawing paper is determined by its weight: the heavier the paper, the thicker it is. The weight of drawing paper $w$ is measured in terms of grams per square inch (*gsi*), ranging from 48 *gsi* to 300 *gsi*. Paper textures for pencil work (categorized as smooth, semi-rough and rough) have a "tooth", which is a slight roughness forming peaks and valleys that enables lead material to adhere to the paper. To represent the clusters of those peaks and valleys from real papers (see SEM images on figs. 3.7 and 3.8) we model the paper texture as a height field $0 \leq h \leq 1$, with $0 \leq w \leq 1$. Many of our papers are procedurally generated as reported by Curtis et al. [Curt97]. Another way of generating the paper textures is to extract the height field from a digitized paper sample. Figure 3.5 illustrate some of the digital samples of the papers' surfaces used in our model. A list of variables used throughout this section is given in Table 3.1.

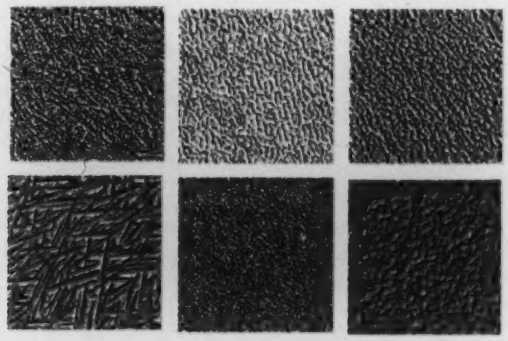

Figure 3.5: Examples of paper samples used in our model.

### 3.3.1 Paper grain

The smallest element of the paper's roughness is the grain. A grain is defined by four paper heights $h_k$, $k \in [1,4]$, where $h_1$ is at paper location $(x,y)$ and its three neighbors $h_2$ at $(x,y+1)$, $h_3$ at $(x+1,y+1)$, and $h_4$ at $(x+1,y)$ (fig. 3.6(a)). In our model each pixel corresponds to a paper location $(x,y)$ with specific variables (indexed by $k$) associated with it (see tab. 3.1).

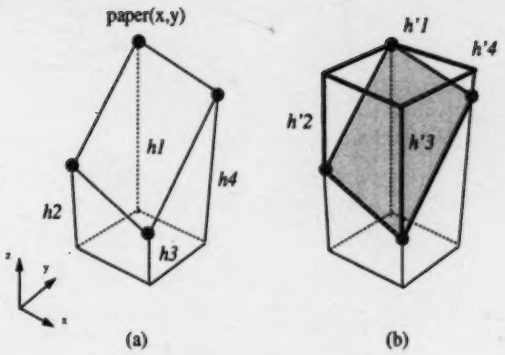


Figure 3.6: (a) a paper grain formed by four heights $h_k$ with $h_{max} = h_1$, (b) the volume above the grain $V_g$ (thicker black lines) to be filled with lead material.

## 3.4 Pencil and paper interaction

Pencil strokes are left on paper through friction between the lead and the paper. The paper grains react to the hardness of the pencil and to the pressure exerted upon it. For example, a soft pencil with a medium pressure can make an even dark tone (figs. 3.1(a), 3.16). The same pencil with reduced pressure makes a light tone with a grainy effect because the lead skids over the topmost fibers of the paper. A hard pencil with firm pressure makes a light smooth tone, destroying the graininess of the paper texture (figs. 3.1(b), 3.20).

In our system, for each time the pencil passes over the paper, the following steps are necessary to model the interaction process:

1. Evaluate the polygonal tip shape of the pencil's point (subsec. 3.4.1).
2. Distribute pressure applied to the pencil across the tip shape (subsec. 3.4.2).
3. Compute the paper porous volume (subsec. 3.4.3).
4. Process the grain biting the lead (subsec. 3.4.4).
5. Compute damage caused by the lead to the paper's grains (subsec. 3.4.5).

Finally we compute the reflected intensity of lead material (subsec. 3.4.6). The interaction process from each step and the illumination model evaluation are explained next. A list of variables used throughout this section is given in Table 3.1.

Figure 3.7: Aerial view x50 of paper sample from Figure 3.1(a). Paper roughness is resulting from the clustering of paper fibers forming peaks and valleys across the paper surface.

Figure 3.8: Aerial view x200 of paper sample from Figure 3.1(a). Refer to the caption in Figure 3.5.

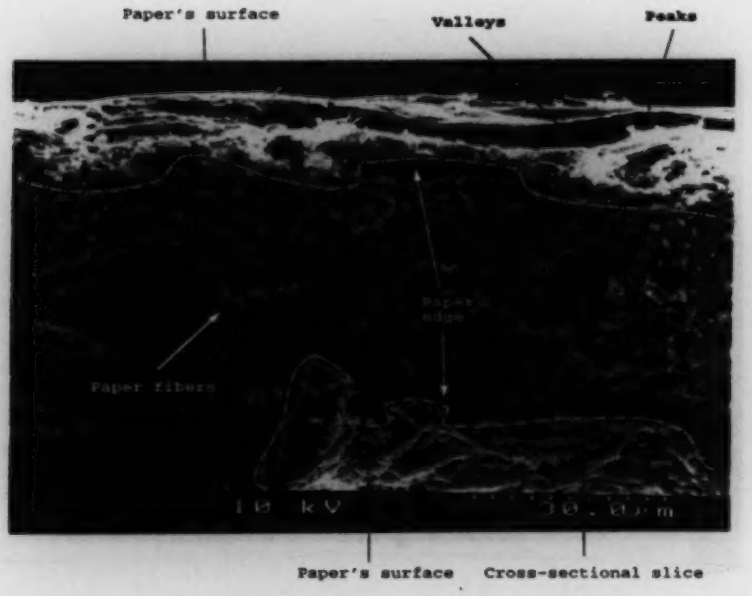


Figure 3.9: Cross-sectional view x1000 of paper sample from Figure 3.1(a). Refer to the caption in Figure 3.5.

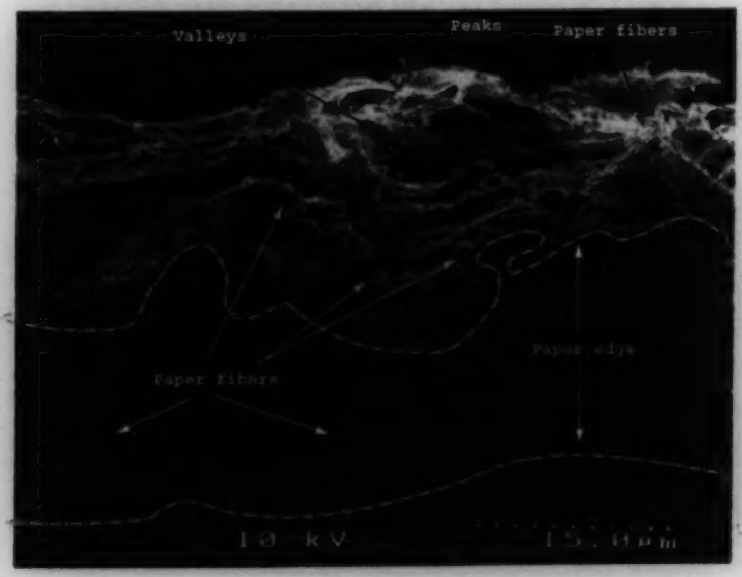


Figure 3.10: Cross-sectional view x2000 of paper sample from Figure 3.1(a). Refer to the caption in Figure 3.5.

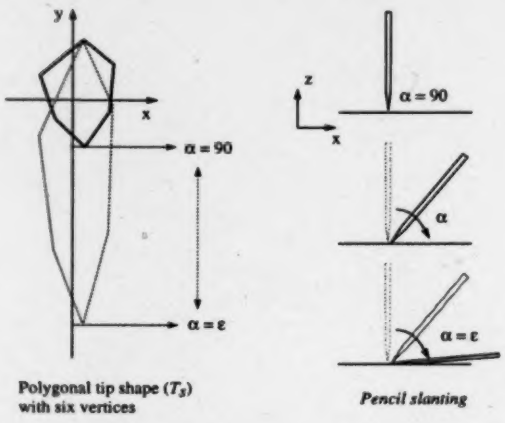


Figure 3.11: Scaling of the canonical tip shape of the pencil point (thicker black lines). The new shape (dotted lines) is dependent on the slanting angle $\alpha$ of the pencil.

### 3.4.1 Polygonal tip shape evaluation

The canonical polygonal tip shape for any selected pencil's point (fig. 3.3) is scaled according to the angle $\alpha$ defined by slanting the pencil. The more the pencil is slanted, the larger the tip is. The resulting scaled tip shape resembles the overall topology of the canonical shape (fig. 3.11). Next the point shape is rotated by $\beta$ degrees based on the movements of the wrist and the whole arm. Finally pressure distribution coefficients (fig. 3.4) are assigned to the scaled polygonal shape.

### 3.4.2 Pressure distribution

The pressure value applied to the pencil $p \in [0, 1]$ is distributed across the polygonal tip shape. This process takes into account the pressure distribution coefficients of the pencil's tip with the paper's surface (subsec. 3.2.2). Two steps are necessary (see fig. 3.12):

1. The pressure values at the pressure distribution coefficients are evaluated as:

$$\begin{aligned} p'_c &\leftarrow p \times c \\ p'_{c_i} &\leftarrow p \times c_i \end{aligned} \tag{3.1}$$

2. The pressure across the polygonal tip shape is computed by scan converting two lines at a time for each triangle from the polygonal tip shape, resulting in four points: the current height $h$ at $(xs, ys)$ and its three neighbors $(xs+1, ys)$, $(xs+1, ys+1)$, and $(xs, ys+1)$, each with the correspondent pressure value $ps$. These four points define

the paper's grain that bites the lead (see fig. 3.6(a)). The four pressure values *ps* from the grain are averaged resulting in the pressure value $P_a$ which is used to evaluate the lead interacting with the paper's grain.

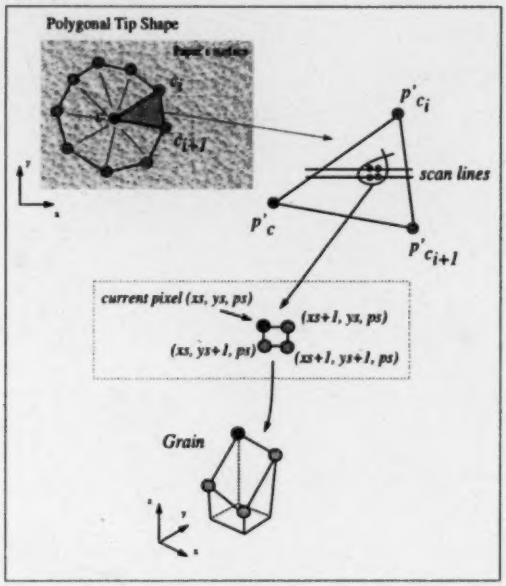


Figure 3.12: The pressure distribution process across the polygonal tip shape from the pencil's point.

### 3.4.3 Paper porous volume

The third processing step of the lead interacting with the paper is the computation of the lead threshold volume $T_v$ for the grain, which is the maximum amount of lead material (graphite, clay, and wax particles) that can be deposited in the grain's volume $V_g$ (fig. 3.6(b)). Two cases may occur:

1. If all the grain heights $h_k$ are equal then $T_v$ is equal to $F_s = 500$ *lpu* (lead particle units), which is the maximum amount of lead material necessary to fill the flat surface of the grain. Basically only a little bit of lead gets deposited forming a thin layer.

2. If at least one of the grain heights $h_k$ is different then the volume above the grain at $(x, y)$ is defined by the bilinear patch whose heights are defined by

$$h'_k \leftarrow h_{max} - h_k \tag{3.2}$$

where $h_{max}$ is the maximum height of the paper grain (see fig. 3.6). For convenience we have defined all of our grains over the unit square. Thus the volume above the grain is

$$V_g \leftarrow \frac{1}{4} \times h'_1 + \frac{1}{4} \times h'_2 + \frac{1}{4} \times h'_4 + \frac{1}{4} \times h'_3 \tag{3.3}$$

and $T_v$ is given by:

$$T_v \leftarrow V_g \times F_v \tag{3.4}$$

where $F_v$ is the maximum amount of lead material necessary to completely fill the grain's volume. In this case $F_v \in [1000, 3000]$ *lpu*. Basically in this case more lead is deposited on unwearied areas of the paper than of the top of flatter areas.

The values in *lpu* are based on our observations in which for a particular paper there is a maximum absorption rate of lead and that this can be changed according to the paper. We found that the values presented give satisfactory results for the threes kinds of paper textures modeled (smooth, semi-rough, rough).

**Lead volume distribution**

Now we need to proportionally distribute $T_v$ among the paper locations at $h_k$ in the grain. Each of the four $k$ locations has a variable $L_k$ which is the local lead threshold volume for $k$. We observed that the higher the height $h_k$ is, the greater the percentage of lead material that will stick to it (see fig. 3.13). For each pencil pass $L_k$ is initialized to 0.0. The distribution is computed as follows:

$$L_k \leftarrow L_k + D_k \times T_v \tag{3.5}$$

$L_k$ is accumulative because it takes into account other neighbor grains sharing the same $h_k$. $D_k \in [0,1]$ is the percentage of lead material distributed at $h_k$ (see fig. 3.13):

$$D_k \leftarrow \frac{h_k}{S_h} \tag{3.6}$$

where $S_h \leftarrow \sum_{i=1}^{4} h_i$. If $S_h = 0.0$ then $D1 \leftarrow D_2 \leftarrow D_3 \leftarrow D_4 \leftarrow 0.25$. This means that all heights $h_k$ from the paper grain receive the same percentage of lead material.

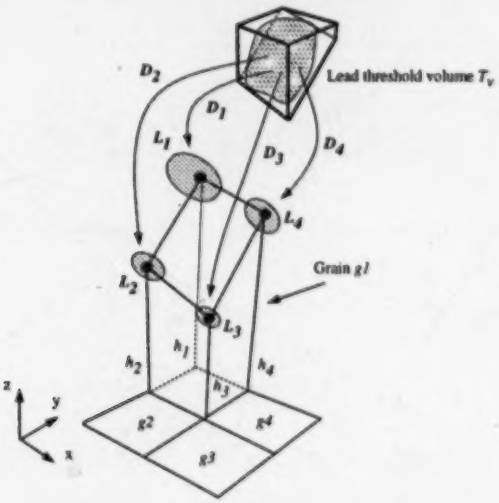


Figure 3.13: Proportional distribution of lead material among the grain's heights. In the example $D_1 > D_4 > D_2 > D_3$ and $D_1 + D_2 + D_3 + D_4 = 1.0$. Also $h_3$ is shared by the four grains $g1, g2, g3, g4$. This means that $h_3$ accumulates lead material $L_k$ bitten by the four grains (see eq. 3.5).

### 3.4.4 How much lead material is "bitten"

The amount of lead removed by the paper's grain is computed in five steps:

(a) compute the depth of lead into the grain,

(b) compute the volume bitten,

(c) scale it according to the current lead degree,

(d) distribute it among the grain's heights,

(e) compute the amount of lead deposited.

**Step 1: Depth of lead in the grain**

The lead penetrates a certain amount into the heights $h_k$ of the paper grain. This is computed as follows:

$$D_l \leftarrow h_{max} - (h_{max} \times P_a) \tag{3.7}$$

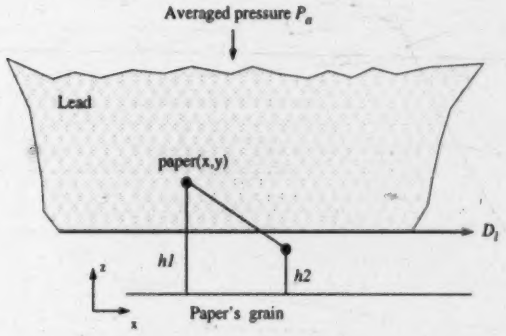


Figure 3.14: The heights of the paper's grain above the $D_l$ line "bite" the lead.

If $D_l < h_{min}$ then $D_l = h_{min}$ where $h_{min}$ is the minimum height $h_k$ of the paper grain. $D_l$ is used to evaluate the amount of lead material bitten by the paper's grain (see fig. 3.14).

**Step 2: Volume bitten**

Lead material "bitten" by the paper's grain remains among the paper's surface fibers (see figs. 3.16 - 3.19).

Our model now computes the volume of lead bitten $B_v$ by the grain. The following two cases may occur:

(a) All heights $h_k$ are equal or above $D_l$ meaning that the whole grain bites the lead. In this case we have:

$$B_v \leftarrow T_v \tag{3.8}$$

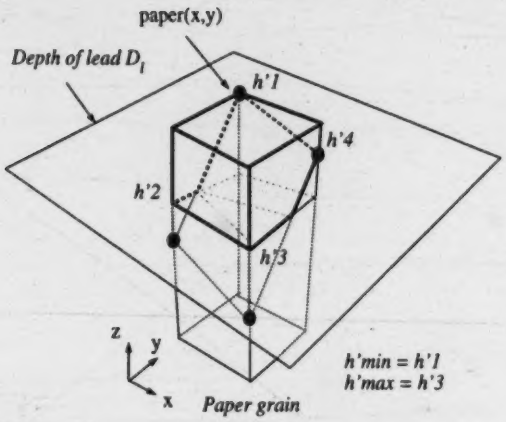


Figure 3.15: Refer to fig. 3.6. Grain's volume (thicker black lines) that bites the lead when the depth plane is above from at least one of the grain heights $h'_k$.

(b) At least one height $h_k$ from the grain is bellow $D_l$ (see figs. 3.14 and 3.15). In this case we use a linear approximation to the volume defined by the intersection of the clipping plane defined by $D_l$ and the bilinear surface defined by the grain's heights (fig. 3.15). $B_v$ is thus approximated by:

$$B_v \leftarrow T_v \times h_m \tag{3.9}$$

with

$$h_m \leftarrow \frac{(h'_{max} - D_l)}{(h'_{max} - h'_{min})} \tag{3.10}$$

where $h'_{min}$ and $h'_{max}$ are the minimum and maximum heights $h'_k$ of the grain (eq. 3.2, figs. 3.6(b) and 3.15).

**Step 3: Volume adjustment**

We observed that less lead is bitten from hard leads than from softer leads (see figs. 3.16 and 3.20). Hence we need to adjust the volume of lead bitten $B_v$ as follows:

$$B_v \leftarrow B_v \times ba(P_d) \tag{3.11}$$

where $ba(P_d)$ is the bite adjustment function which returns a scaling factor ($0 \leq ba \leq 1$), given the degree of the pencil being used $P_d$ (tab. 3.1). The closer $ba$ is to 1.0 (very soft lead), the closer the lead material is to the computed bitten volume $B_v$. The closer $ba$ is to 0.0 (very hard lead), the less the bitten lead material is.

**Step 4: Volume distribution**

We need to proportionally distribute the grain's bitten volume $B_v$ among the grain heights $h_k$. As in the lead volume distribution (subsec. 3.4.3) we observed that the higher the grain height is, the greater the percentage of lead material that will stick to it (fig. 3.13). This distribution is given by:

$$B_k \leftarrow B_v \times D_k \tag{3.12}$$

**Paper grain is full**

At each grain height $h_k$, if the total amount of lead material deposited $T_k$ is greater or equal to the lead threshold volume $L_k$, then the paper grain is completely filled with lead material. Hence it is important to progressively reduce the amount of extra lead that can be deposited. Our approach is to scale the bite volume $B_k$ as follows:

$$B_k \leftarrow B_k \times M^p \tag{3.13}$$

Where $p$ is the pressure applied to the pencil. This accounts for a decreasing ability to leave lead on a paper that is fully saturated. In our experience we have found that values $0.97 \leq M \leq 0.99$ yield realistic results.

**Step 5: How much lead material is deposited**

The amount of lead deposited at $h_k$ is given by $(G_p, C_p, W_p) \times B_k$. The total amount of graphite, clay, and wax particles ($Gk$, $Ck$ and $Wk$ respectively) deposited after each pass of the pencil over the paper surface at $h_k$ is computed as:

$$\begin{aligned} G_k &\leftarrow G_k + G_p \times B_k \\ C_k &\leftarrow C_k + C_p \times B_k \\ W_k &\leftarrow W_k + W_p \times B_k \end{aligned} \tag{3.14}$$

Finally, the total amount of lead material deposited at $h_k$ is given by

$$T_k \leftarrow G_k + C_k + W_k \tag{3.15}$$

### 3.4.5 Paper damage computation

Paper grains are flattened due to the pressure $P_a$ and hardness of the lead, which is determined by its degree $P_d$. We observed that harder leads damage the paper grains more than softer leads (see figs. 3.16 - 3.22). For every grain's height $h_k$ that bites the lead, the amount of paper damaged $E_k$ is computed as follows:

$$E_k \leftarrow D_l \times da(P_d) \times w \tag{3.16}$$

where $da(P_d)$ (damage adjustment) is a function returning a scaling factor ($0 \leq da \leq 1$), given the pencil degree $P_d$ used. When $da$ is close to 1.0 there is a large amount of paper damaged which can be similar to the value of $D_l$. The closer $da$ is to 1.0 (very hard lead), the more paper is damaged. The closer $da$ is to 0.0 (very soft lead), the less paper is damaged. The closer $w$ is to 0.0 (very heavy paper) the more resistant the paper is to the lead. This means that less paper is damaged. The grain's height $h_k$ is then adjusted as follows:

$$h_k \leftarrow h_k - E_k \tag{3.17}$$

When $h_k$ is equal to 0.0 the grain has been totally flattened.

### 3.4.6 Intensity value of deposited lead material

Finally we compute the reflected intensity of lead material $I_k$ deposited at paper location $h_k$. We assume that graphite particles are black and clay and wax particles are optically neutral components. The reflected intensity depends on the amount of graphite present at $h_k$ which is computed as follows:

$$A_k \leftarrow \frac{G_k}{F_t} \tag{3.18}$$

where $F_t \leftarrow F_s + F_v$ is the maximum amount of lead material necessary to completely cover the paper's flat surface ($F_s$, subsec. 3.4.3) and to completely fill the grain's volume ($F_v$, subsec. 3.4.3). The reflected intensity $I_k \in [0, 1]$ is then given by:

$$I_k \leftarrow 1.0 - A_k \tag{3.19}$$

Figure 3.16: Aerial view x50 of soft pencil sample from Figure 3.1(b). Lead material is adhered to the paper fibers filling its valleys and covering its peaks. Compare with Figure 3.7 and notice how the paper fibers are now barely visible due to the covering of the paper with lead material.

## 3.5 Results

### 3.5.1 Lead material distribution and tone blending

The bottom row of Figure 3.23 illustrate results from our model by using different textures of drawing papers and testing the effects of lead material over them. In addition we present in the same figure scans of real pencil work to compare with results from our model. The paper texture of Figure 3.23 with 4B pencil was computed from a digitized sample. The paper texture of Figure 3.23 with 6B and 6H pencils was procedurally generated.

It is important to illustrate the effects of layers of soft lead material over layers of hard lead material, and vice-versa. In this manner we build areas of tone that are used to describe forms and light. In Figure 3.25(a) a soft pencil is first rubbed over the paper in one direction and then rubbing a hard pencil over the top at an angle

Figure 3.17: Aerial view x200 of soft pencil sample from Figure 3.1(b). Refer to the caption in Figure 3.16.

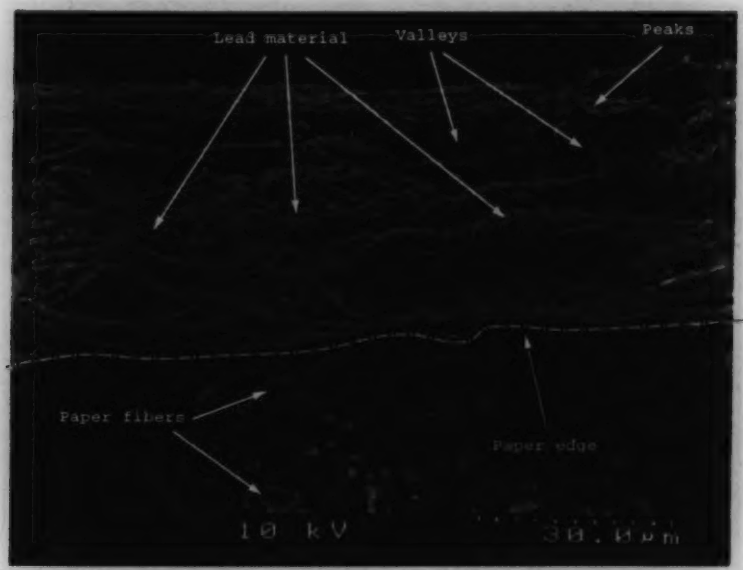


Figure 3.18: Cross-sectional view x1000 of soft pencil sample from Figure 3.1(b). Lead material is adhered to the paper fibers filling its valleys and covering its peaks. Compare with Figure 3.9 and notice how lead material (with a "cloudy" aspect) covers the paper roughness.

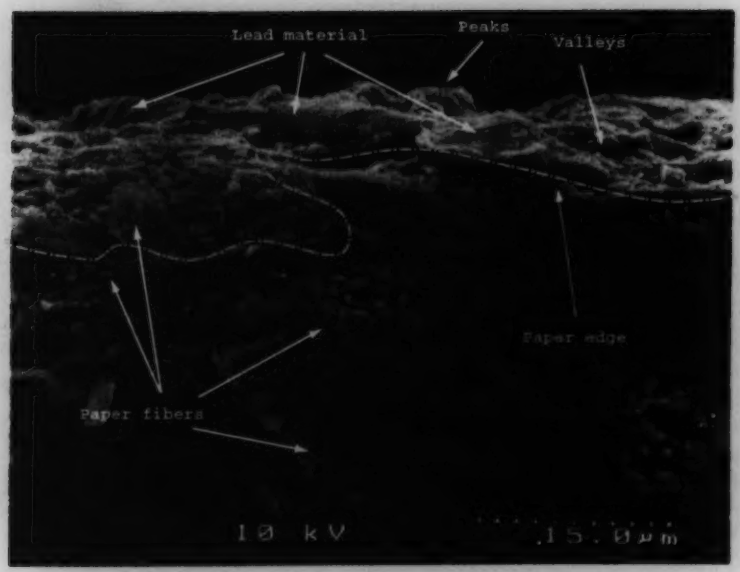


Figure 3.19: Cross-sectional view x2000 of soft pencil sample from Figure 3.1(b). Refer to the caption in Figure 3.18.

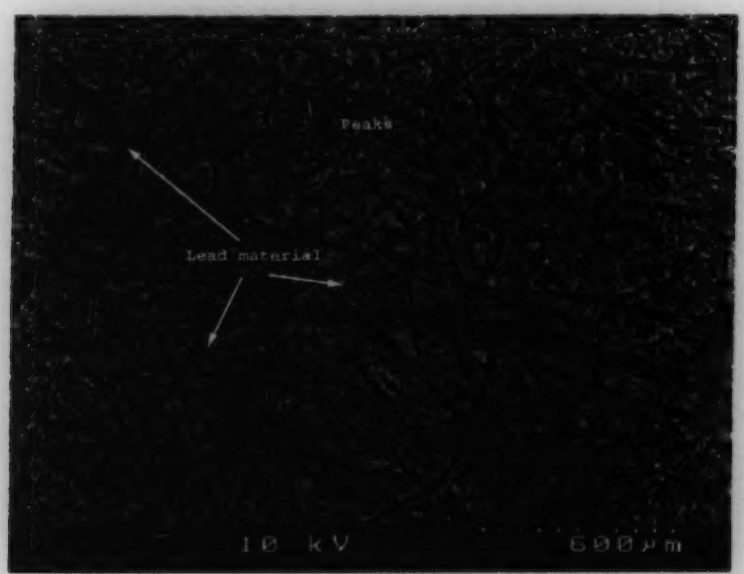


Figure 3.20: Aerial view x50 of hard pencil sample from Figure 3.1(c). The black lines with varying thickness are the effects of the pencil point destroying the paper fibers. Compare with Figure 3.5 and notice the clustering of paper fibers before and after the pencil rubbing. Notice that less lead material has been deposited in comparison with Figure 3.16.

Figure 3.21: Aerial view x200 of hard pencil sample from Figure 3.1(c). Refer to the caption in Figure 3.20.

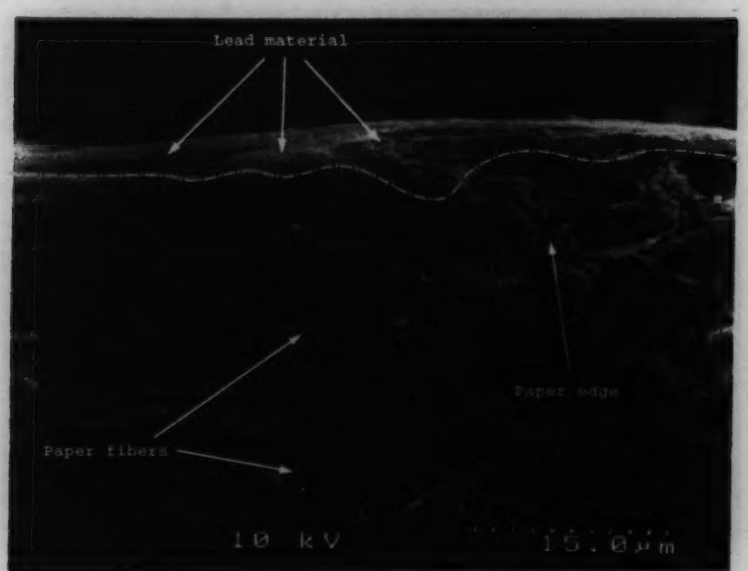


Figure 3.22: Cross-sectional view x2000 of hard pencil sample from Figure 3.1(c). Compare with Figure 3.8 and notice that the peaks and valleys from the paper grains have been totally flattened.

to the first. The result is that the intersection area between the two layers of lead material gets darker. In Figure 3.25(b) we do the opposite, a layer of a soft lead on top of a layer of a hard lead. This illustrates how full grains can be slightly altered by successive passes but the effect is minimal. Compare results from our model with scans of real pencil swatches presented in the top row of Figure 3.25.

**Evaluation**

All the results were generated on an OCTANE$^{TM}$ Power Desktop[2] and printed at 200*dpi* on a 600 *dpi* HP LaserJet 5Si MX printer. Real samples were scanned at 150 *dpi*. The computational cost of this stage is due mainly to the evaluation of the pencil and paper interaction model at each pixel (2.009919e-05 sec.). The response time was satisfactory at interactive rates. The images from the results show that our simulation model produces similar results to the strokes and swatches generated with real graphite pencils over drawing papers. Our simulation model qualitatively captures many of the effects observed in real pencil work. In addition, contour maps were generated for both the real and simulated sample results for every intensity value less than or equal to the median intensity value. The evaluation criteria is that the distribution of contour lines from the real samples should be *approximately* the same as for the simulated samples. Based on this criteria our model makes a satisfactory distribution of lead material across the drawing paper (see figs. 3.23, 3.24 and figs. 3.25, 3.26).

### 3.5.2 Paper damage

Figure 3.27 illustrates the effects of paper damage after rubbing a pencils over it. A canonical broad pencil shape is used. Our approach was to first rub a hard pencil and then a soft one to reveal the paper grains. The upper row of Figure 3.27 illustrates no damage to the paper and the bottom row illustrates damage to the paper.

### 3.5.3 Alternative drawing surfaces

Interesting effects can be achieved by properly selecting the paper texture for pencil drawing. Our next set of results illustrates this. We start with the *frottage* ("rubbing") technique which is the process of reproducing a raised or impressed image or texture by placing a piece of paper over it and making a rubbing with the lead [Camh97,

[2]All rendering is done in software.

pp. 120-124]. Figure 3.28 illustrates coin rubbing using hard and soft pencils. We generate the textures from digitized samples. The intensity values $i$ at each pixel $(x, y)$ on the reference images define the height field $h$ of the paper's surface (sec. 3.3) where $h_{(x,y)} = i_{(x,y)}$. For each paper location $(x, y)$ (correspondent to the reference image pixel location $(x, y)$) the pencil and paper model is evaluated. The intensity $i_{(x,y)}$ is used to adjust the pressure $p$ applied to a single pencil resulting in the correct amount of lead material deposited at paper $(x, y)$. The pressure $p$ applied to the pencil is the only parameter that changes at this stage, and it is given by $p = 1.0 - i_{(x,y)}$. This means that in order to achieve a darker intensity more pressure is required. This approach is based on traditional pencil rendering methods to create tone values [Lewi84]. If the user provides additional pressure $pa$ then the final pressure value $p$ is scaled as $p = p \times pa$. We also apply the rubbing technique using a 4B pencil using a photograph as a reference image for the paper's surface (fig. 3.29).

## 3.6 Wrap-up

We have presented an observational model of graphite pencil and drawing paper. The model for interaction between the pencil and paper took into account the composition of the lead pencil and the texture and weight of the paper. Assuming that clay and wax are optically neutral elements we also presented an observational illumination model for pencil lead. Additional parameters included the pencil point and pressure. We have illustrated the results of our pencil and paper model by duplicating pencil swatches and by generating similar images using different pencil and paper textures.

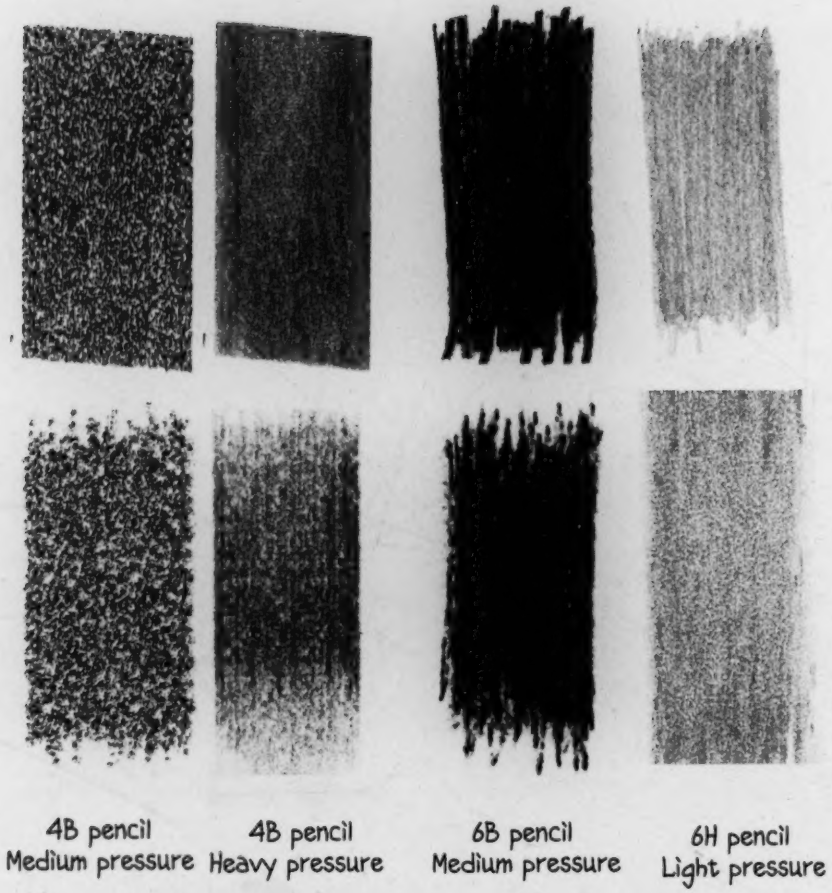


Figure 3.23: Our simulation model applied over drawing paper (bottom row). Compare results with real pencil work (top row). Notice that our simulation results have a good approximation to the gray level intensity due to a well distributed amount of lead material across the paper's surface. The damage to the paper grain is also satisfactory as the perceived roughness of the paper's surface from both the real and simulated models is approximately the same.

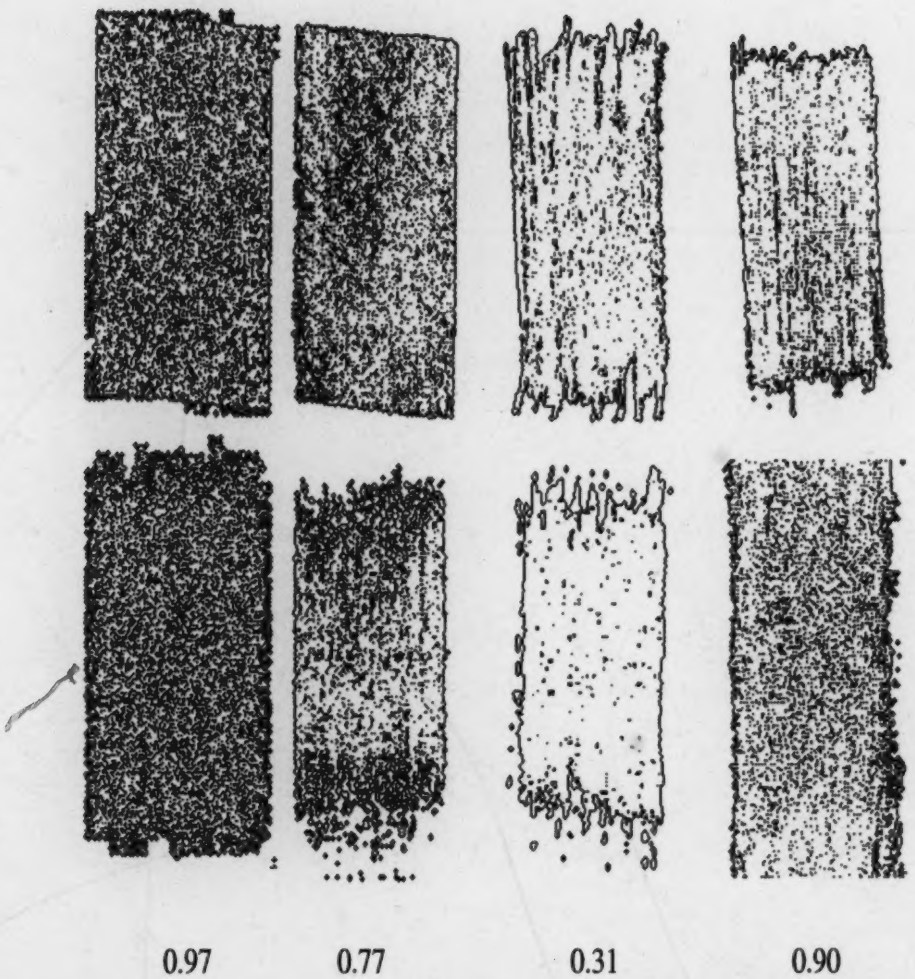


Figure 3.24: Contour maps for the results from Figure 3.23. Values represent the threshold median intensity value. Top row is from real pencil and bottom row from our pencil and paper model. This is an alternative way of visualizing the distribution of lead material across the paper's surface. The evaluation criteria is that the distribution of contour lines from the real samples should be *approximately* the same as for the simulated samples. Based on this criteria our model makes a satisfactory distribution of lead material across the drawing.

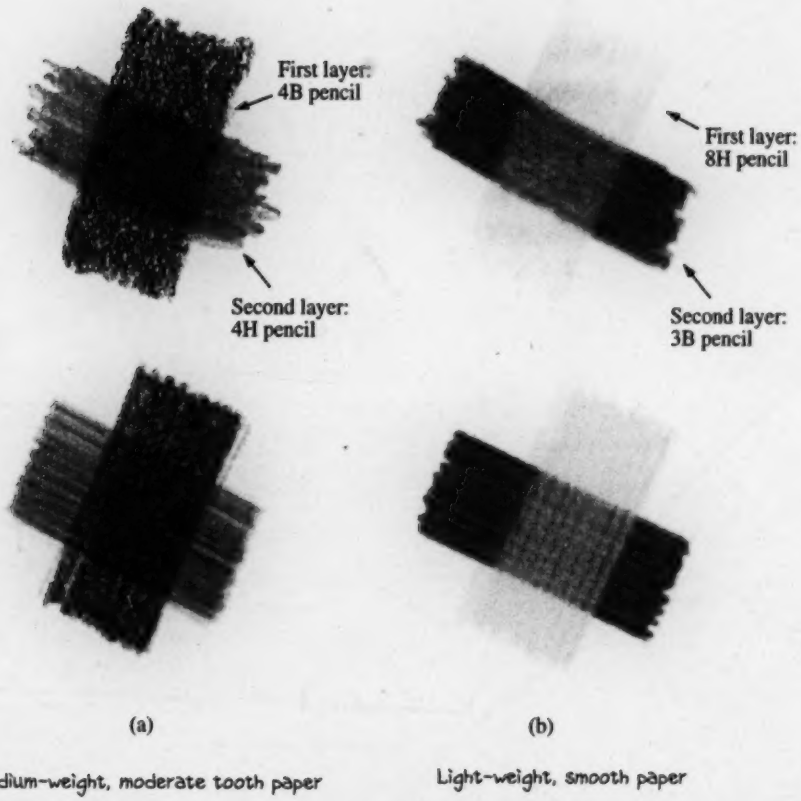


Figure 3.25: Real (top row) and simulated (bottom row) examples of pencil swatches illustrating the blending effects from layering lead material over drawing paper. Note that our simulation results have a good approximation to the gray level intensity due to the blending of lead material from different pencil grades (intersection area of the two layers of swatches). Pencils were slanted by $\alpha = 45.0$ degrees, sharpened with a broad point. Simulated results were generated automatically by the mark-making primitive (chap. 5) taking about 30 *sec.* for each layer of lead material. (1) first layer: light pressure, rubbing a few times; second layer: light pressure, rubbing a few times with pencil a little bit slanted. (2) first layer: light pressure, rubbing a few times, pencil a bit slanted; second layer: light pressure, rubbing a few times.

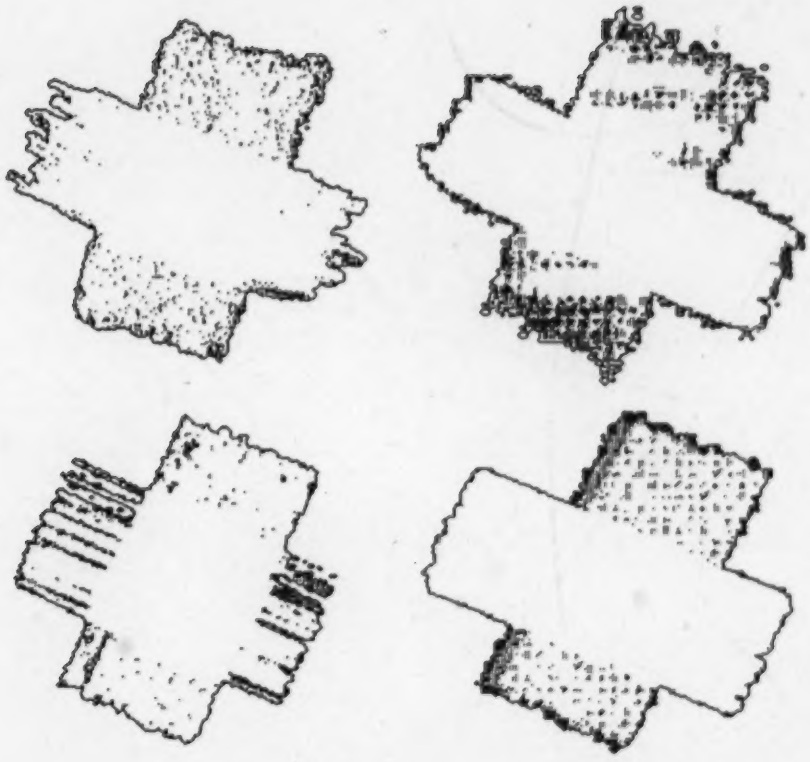


Figure 3.26: Contour maps for the results from Figure 3.25. Values represent the threshold median intensity value. Top row is from real pencil and bottom row from our pencil and paper model. Note that the distribution of contour lines in the intersection area of the two layers of swatches is equal for both the real and simulated results. This means that our model has a good approximation of the distribution and blending of lead material from two different pencil grades.

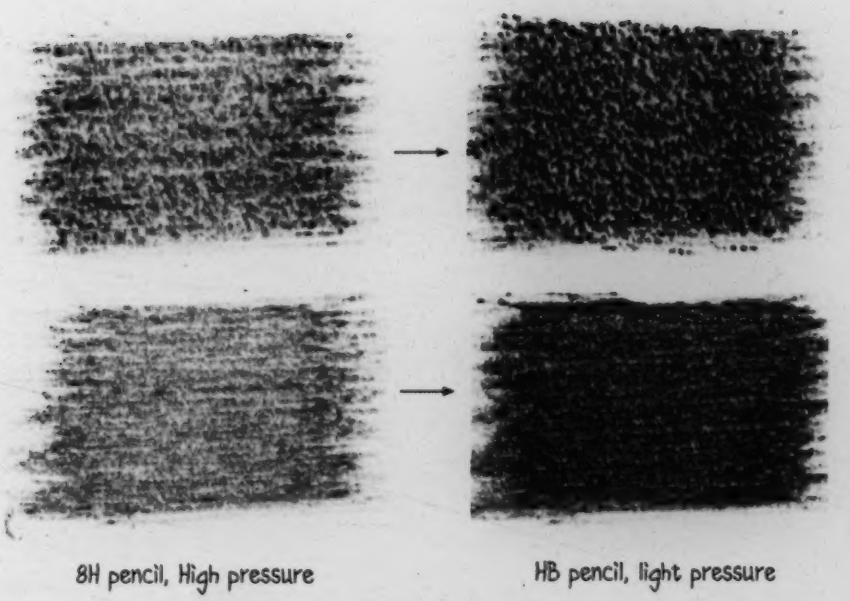


Figure 3.27: Our simulation model without paper damage (top row) and with paper damage (bottom row). On the top row the pencil is first applied (left) and after a while (right) notice that the amount of deposited lead material increases clearly revealing the paper grain. On the bottom row the pencil is first applied (left) and after a while (right) notice that the amount of deposited lead material increases but the paper grain are almost completely damaged.

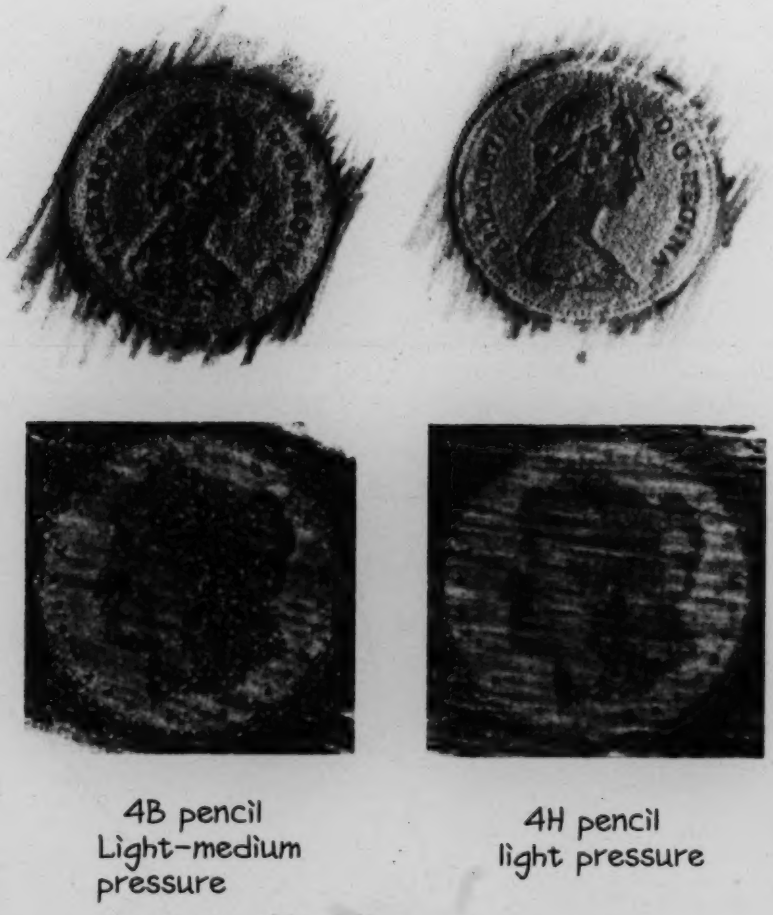


Figure 3.28: Pencil rubbing technique [Camh97, pp. 120-124] using our simulation model (bottom row). Compare behavior of lead deposit with real pencil work (top row).

(a) (b)

Figure 3.29: (a) High contrast photograph of Patricia (resolution of 279x388 pixels). (b) Automatic rendering using 6H pencil (2.18 sec.) followed by interactive rendering (pencil point from the pencil and paper model adapted to an interactive illustration system) with strokes interactively applied using medium-soft pencils applied with light pressure (15 sec.).

# Chapter 4

# Blender and Eraser Model

In this chapter we present a blender and eraser model [Sous99b] that extends our graphite pencil and paper model (chap. 3). This blender and eraser model enhances the rendering results producing realistic looking graphite pencil tones and textures. Our model is based on observations on the absorptive and dispersal properties of blenders and erasers interacting with lead material deposited over drawing paper. The parameters of our model are the particle composition of the lead over the paper, the texture of the paper, the position and shape of the blender and eraser, and the pressure applied to them. We demonstrate the capabilities of our approach with a variety of pencil swatches and compare them to digitized pencil drawings. We also present automatic and interactive image-based rendering results implementing traditional graphite pencil tone rendering methods. The methods presented in this chapter are analogous to that of Chapter 3.

This chapter is organized as follows. In Section 4.2 we present the blender and eraser model. In Section 4.3 we describe in detail the modeling of the processes involved when blenders and erasers interact with lead material and paper. In Section 4.4 we show results from our models on different paper textures, various pencil swatches, and on tone rendering methods.

## 4.1 The observational approach

Like the pencil and paper model our approach is based on an observational model of how real blenders and erasers interact with lead material already deposited on drawing paper. The goal was to capture the essential physical properties and behaviors observed in order to produce quality blenders and erasers marks at interactive rates.

Our intention was not to develop a highly physically accurate model, which would result in a computationally expensive simulation. Aerial and cross-sectional views from real blenders and erasers samples (fig. 4.1) were generated by the SEM at 10kv accelerating voltage, with different magnifications, and with scale resolution in microns.

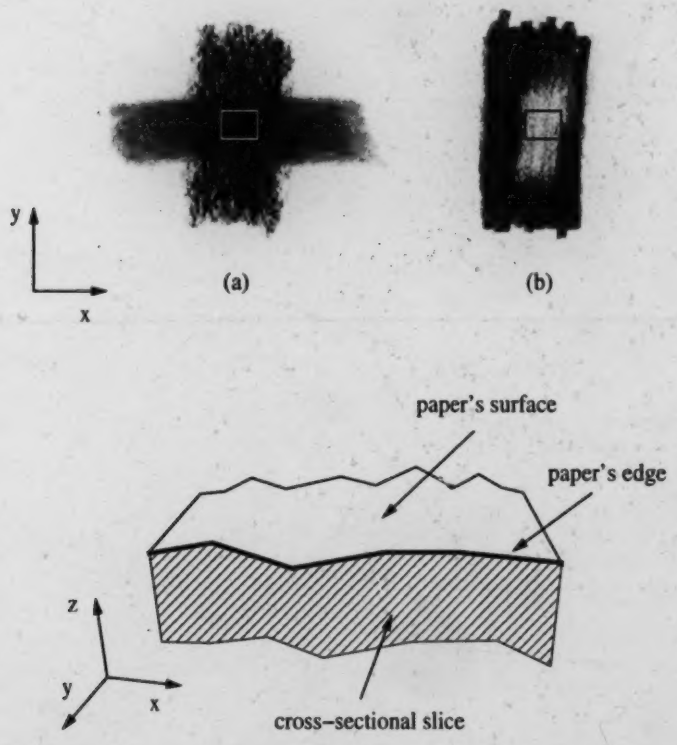


Figure 4.1: Samples of 15mm in diameter (rectangular area within samples in (a), (b)) used to generate the SEM results: (a) stump blender (figs. 4.8, 4.9, 4.10), (b) kneaded eraser (figs. 4.5, 4.6, 4.7). The bottom of the figure illustrates the viewing position for the cross-sectional views of the samples used for the SEM images (figs. 4.7, 4.10).

## 4.2 Model description

A blender is any tool that can be used to soften edges or to make a smooth transition between tone values. We modeled two kinds of blenders:

(a) Tortillon, which is a cylinder, made of paper rolled into a long, tapered point at one end for blending tiny areas and fine lines.

(b) Stump, which is not as thin and pointy as a tortillon. Made of compressed paper, felt, or chamois, a stump can have up to a half-inch diameter.

Erasers remove surface particles to lighten a drawing. We modeled the kneaded eraser which is one of the most effective erasers made for graphite pencil. It can be used to lighten tones leaving white areas that have been covered, and it does not leave eraser dust behind. Kneaded erasers come in rectangular blocks. A piece of it is cut or torn off and kneaded between thumb and fingers until it becomes soft and pliable. It can be modeled into any shape (fig. 4.2).

A list of variables used throughout this section is given in Table 4.1.

| **Blender and Eraser model** (sec. 4.2) | |
|---|---|
| $T_s$ | Tip shape. |
| $P_c$ | Pressure distribution coefficients. |
| **Blender/Eraser interaction with lead and paper** (sec. 4.3) | |
| $p$ | Pressure applied to the blender/eraser. |
| $p'_c, p'_{c_i}$ | Blender/eraser pressure at the pressure distribution coefficients $P_c$. |
| $(xs, ys, ps)$ | Interpolated coordinates and pressure at the tip shape $T_s$. |
| $lmr$ | Amount of lead removed from paper. |
| $lm_{(x,y)}$ | Lead material deposited on paper(x,y). |
| $plr$ | Percentage of lead material removed. |
| $lm_{(xb,yb)}$ | Lead material deposited on the blender buffer (xb,yb). |
| $t$ | Absorption/storage capacity of lead material in the blender. |

Table 4.1: List of variables used for the blender and eraser model.

### 4.2.1 Tip shapes

The tip shapes for blenders and kneaded erasers are defined as a polygonal outline based on the shape of canonical types of points (fig. 4.2). This approach is similar to the modeling of pencil points (see chap. 3, subsec. 3.2.2). A blender/eraser tip is defined as $T_s = \{(x_i, y_i), s : 3 \leq i \leq n\}$, where $(x_i, y_i)$ is one the $n$ vertices of the polygon and $s$ is the scale factor of the polygon used to account for the width of the blender/eraser.

### 4.2.2 Pressure distribution coefficients

Pressure distribution coefficients are values between 0 and 1 representing the percentage of the blender's and eraser's point surface that, on average, makes con-

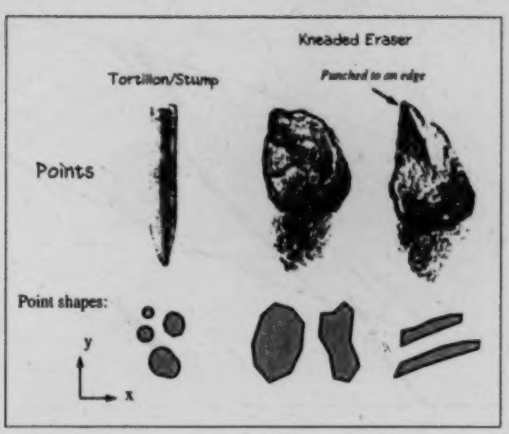


Figure 4.2: Different kinds of canonical points for blenders/erasers and their polygonal shapes modeling the surface area in contact with the paper.

tact with the paper. This value is used to locally scale the pressure being applied to the blender/eraser. The pressure distribution coefficients are defined as $P_c = (c, x, y), (c_i, xi, y_i) : 1 \leq i \leq n\}$ where $c$ is the value of the main pressure distribution coefficient whose location $(x, y)$ can be anywhere within the polygon defining the tip shape (default location is at the center of the polygon), and $c_i$ is the value of the pressure distribution coefficient at vertex $(x_i, y_i)$ from the polygonal tip shape. Different values can be assigned to $c$ and to each $c_i$. The closer they are to 1.0, the more surface is in contact with the paper. The closer they are to 0.0, the less surface is in contact with the paper. The values between $c$ and $c_i$ are computed by linear interpolation, thus defining the overall shape of the blender/eraser tip (see fig. 4.3).

## 4.3 Blender and erasers interacting with lead and paper

By flattening out a kneaded eraser, placing it firmly over an area, and then pulling quickly, lead material will be lifted away without rubbing the paper surface. As the kneaded eraser rubs the paper's surface lead material is removed sticking completely to the eraser's point. No lead material is deposited back on the paper (figs. 4.5, 4.6, 4.7).

We modeled this interaction process in three main steps:

(a) Evaluate the polygonal shape of the eraser's point (subsecs. 4.3.1 and 4.3.2).

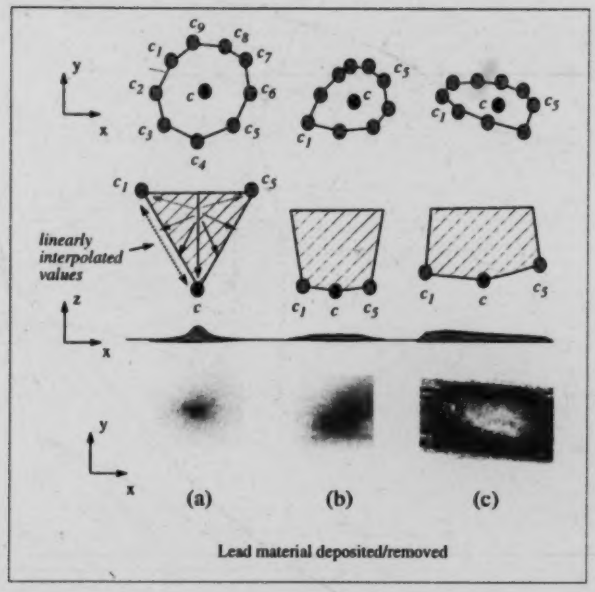


Figure 4.3: Examples of the $xy$ polygonal shape, cross-sectional views, and results using our model for (a) tortillon and (b) stump blenders, and (c) kneaded eraser. Different values of pressure distribution coefficients ($c$ and $c_i$) across the polygonal shape result in different deposit and removal of lead material over the paper's surface. The results for lead material blended are for $c = 1.0$ and the same $c_i$ value for all vertices in the polygonal shape ((a) 0.2 for the tortillon, (b) 0.5 for the stump). The result for lead material erased (c) has $c = 1.0$ and $c_i$ values with slight variations between 0.7 and 0.9.

(b) Distribute pressure applied to the eraser across its point (subsec. 4.3.3).

(c) Process the removal of lead material (subsec. 4.3.4).

Blending changes the texture of an image. When a graphite pencil is drawn across a surface, it leaves particles on top of the paper fibers. The empty valleys result in a textured look to a line or an area of tone. Blending pushes the lead into the surface so that the paper's low grains become filled. This results in tones that seem smoother, more intense, and deeper in value. As the blender rubs the paper's surface, lead material is removed sticking to the blender's point, and a certain amount of lead material is then deposited back on the paper (figs. 4.8, 4.9, 4.10). The third step for blenders involves both the removal and the deposit of lead material.

The interaction process for each step for blenders and kneaded erasers are explained next.

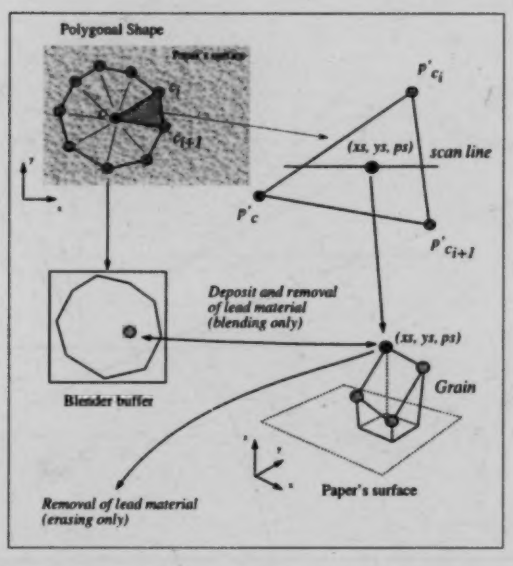


Figure 4.4: The pressure distribution process across the polygonal shape from the blender's and eraser's point.

### 4.3.1 Polygonal shape evaluation

The canonical polygonal shape for any selected blender's and eraser's point (fig. 4.2) is scaled according to the pressure applied over it. Next the point shape is rotated by $\beta$ degrees based on the movements of the wrist and the whole arm. Finally pressure distribution coefficients (subsec. 4.2.2) are assigned to the scaled polygonal shape.

### 4.3.2 Blender buffer

Every blender has a buffer associated with it. This buffer keeps track of the current amount of lead material deposited and removed due to interaction with the paper (subsec. 4.3.4). Kneaded erasers do not need this buffer because they only remove lead. The buffer is defined as an array of pixels with the same resolution as of the current evaluated polygonal shape defining the blender (fig. 4.4). At each location $(xb, yb)$ on the buffer we store and remove lead material $lm_{(xb,yb)}$. For the first polygonal shape every buffer location $(xb, yb)$ is initialized to 0. If the polygonal shape changes then only the size of the buffer is adjusted, preserving the information about lead material that has already been deposited and removed.

Figure 4.5: Aerial view x50 of kneaded eraser from Figure 4.1(b). Notice the reduction of lead material from the paper. Compare with Figure 3.5 and notice that paper fibers are also more visible, revealing a similar roughness structure to the paper in Figure 3.5 (chap. 3). Black lines with varying thickness are due to paper fibers damaged by the eraser.

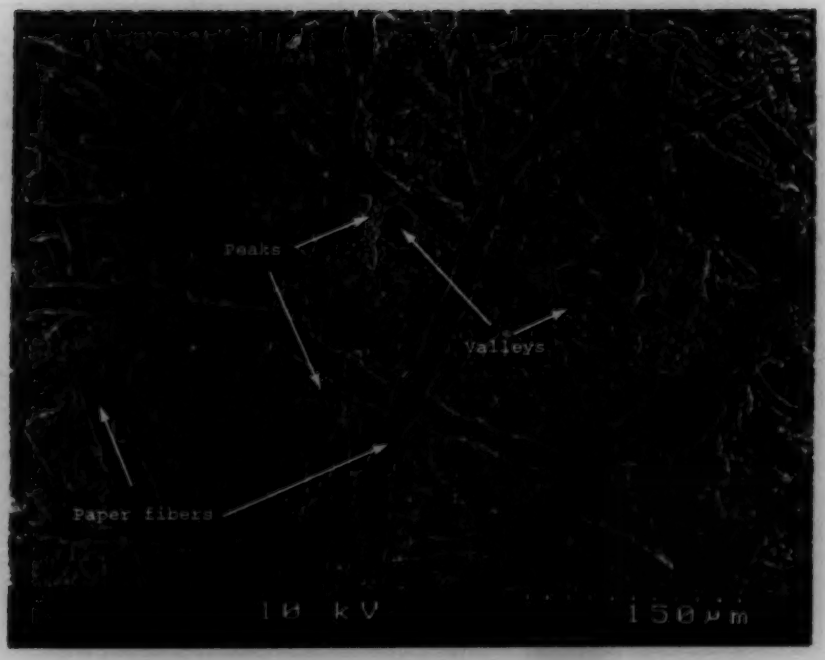


Figure 4.6: Aerial view x200 of kneaded eraser from Figure 4.1(b). Refer to the caption in Figure 4.5.

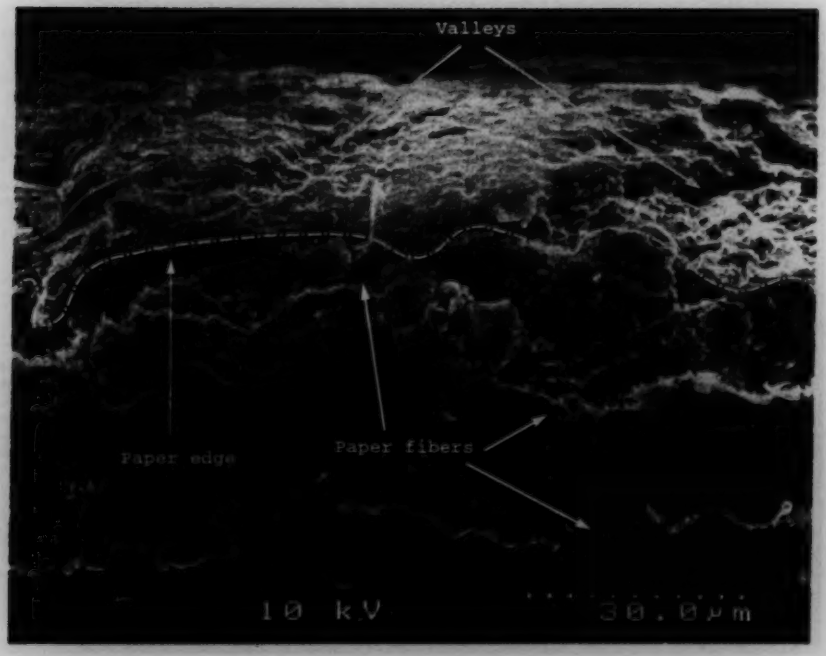


Figure 4.7: Cross-sectional view x1000 of kneaded eraser sample from Figure 4.1(b). Compare with Figures 3.7 and 3.18 and notice how lead material has been progressively removed revealing a similar structure to the original paper roughness.

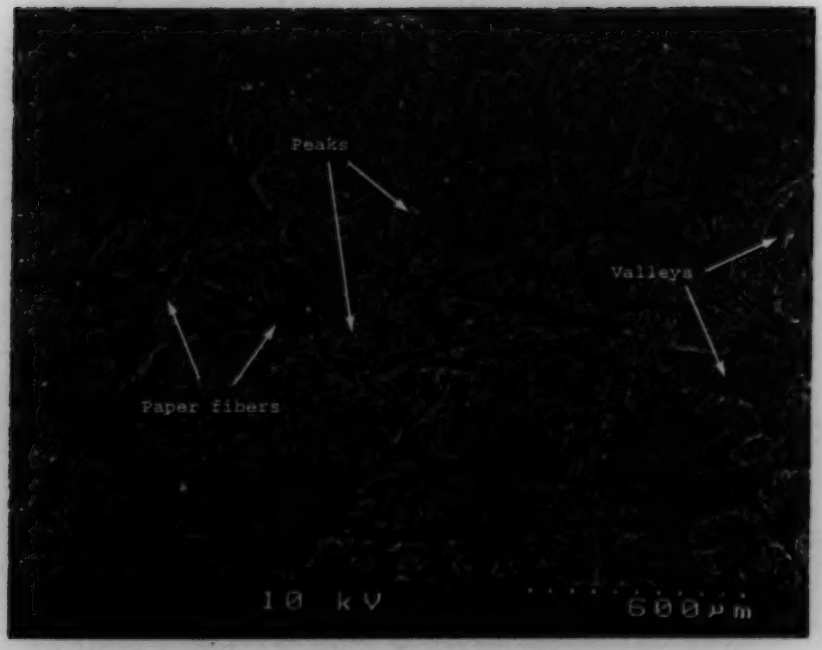


Figure 4.8: Aerial view x50 of blender sample from Figure 4.1(a). The blending process creates large areas with a uniform distribution of lead material deposited on them. These areas have similar shapes and are regularly distributed across the paper surface. Compare with Figures 3.5 and 3.16 to better visualize the before and after effects of blending. Black lines are paper fibers damaged by the blender.

Figure 4.9: Aerial view x200 of blender sample from Figure 4.1(a). Refer to the caption in Figure 4.8.

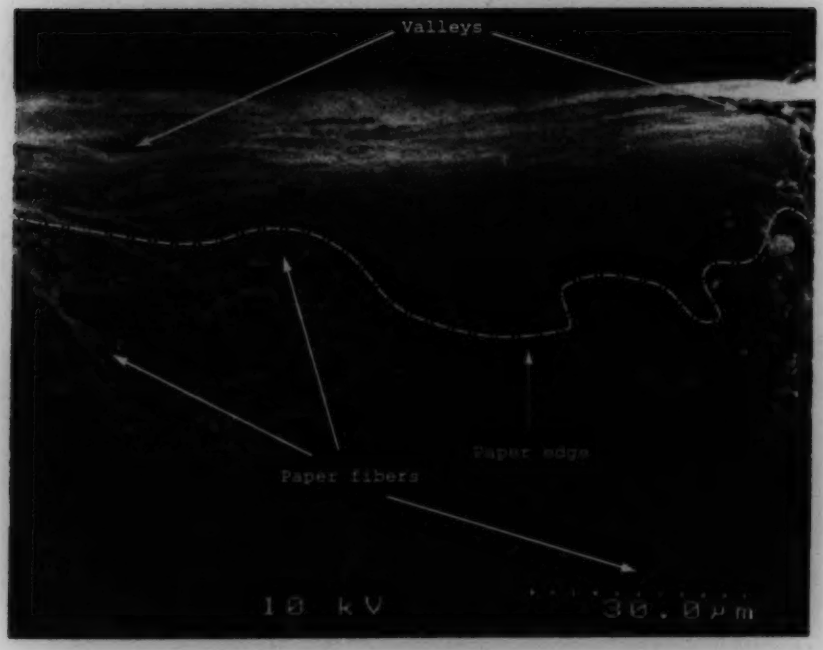


Figure 4.10: Cross-sectional view x1000 of blender sample from Figure 4.1(b). Compare with Figure 3.18 and notice how lead material has been uniformly distributed across the paper surface, covering its peaks and valleys.

### 4.3.3 Pressure distribution

The pressure value applied to the blender/eraser $p$ ($0 \leq p \leq 1$) is distributed across the polygonal shape defining the blender's and eraser's point. This process takes into account the pressure distribution coefficients of the blender's and eraser's point with the paper's surface (subsec. 4.2.2). Two steps are necessary (fig. 4.4):

(a) The pressure values $p'$ at the pressure distribution coefficients are evaluated as:

$$\begin{aligned} p'_c &\leftarrow p \times c \\ p'_{c_i} &\leftarrow p \times c_i \end{aligned} \tag{4.1}$$

(b) The pressure across the polygonal shape is computed by scan converting one line at a time for each triangle from the polygonal shape, resulting in the location $(xs, ys)$ with the correspondent pressure value $ps$.

### 4.3.4 Deposit and removal of lead material

The transfer of lead material from paper to blender and from blender to paper is computed as follows:

*From paper to blender*

(a) A certain amount of lead material $lmr$ is removed from paper $(x, y)$:

$$lmr \leftarrow lm_{(xs,ys)} \times (ps \times plr), plr = 0.7, \tag{4.2}$$

where $plr$ is the percentage of lead material removed.

(b) The amount of lead material on the paper is reduced:

$$lm_{(xs,ys)} \leftarrow lm_{(xs,ys)} - lmr \tag{4.3}$$

(c) Lead material $lmr$ removed from the paper is deposited on the blender buffer $(xb, yb)$:

$$lm_{(xb,yb)} \leftarrow lm_{(xb,yb)} + lmr \tag{4.4}$$

*From blender to paper*

(a) A certain amount of lead material is removed from blender $(xb, yb)$:

$$lmr \leftarrow lm_{(xb,yb)} \times (ps \times plr), plr = 0.5 \tag{4.5}$$

(b) The amount of lead material on the blender is reduced:

$$lm_{(xb,yb)} \leftarrow lm_{(xb,yb)} - (lmr \times t) \tag{4.6}$$

where $t$ $(0 \leq t \leq 1)$ models the absorption/storage capacity of lead material in the blender. The closer $t$ is to 0 the greater the absorption/storage capacity of the blender. We defined $t = 0.2$ for tortillons and $t = 0.5$ for stumps.

(c) Lead material $lmr$ is deposited on the paper $(xs, ys)$:

$$lm_{(xs,ys)} \leftarrow lm_{(xs,ys)} + (lmr \times t) \tag{4.7}$$

We have found that the values for $plr(0.7, 0.5)$ and $t(0.2, 0.5)$ give credible results. They are based on our observations on the absorption and dispersion behavior of blenders and erasers over deposited lead material. For a kneaded eraser only steps 1 and 2 from *paper to blender* are necessary.

## 4.4 Results

### 4.4.1 Blender and eraser swatches

This first set of results illustrates the effects of blending (fig. 4.11) and erasing (fig. 4.13) pencil swatches over medium-weight, semi-rough paper's surfaces. To evaluate the blender and eraser model we chose representative swatches of real pencil drawings and used our system to duplicate the effect. This is the same approach used for the first set of results for the pencil and paper model (chap. 3, subsec. 3.5.1). We adapted our models (pencil and paper, blender and eraser) to an interactive illustration system using digital samples for the paper's texture. Our evaluation is thus conducted by observing how close to the original swatches are the computer-generated ones. Besides this we used a thresholded contour display that bestowed us some further insights into the distribution of the graphite. This is the same evaluation approach used for the first set of results for the pencil and paper model (chap. 3, subsec. 3.5.1). All the results were generated on an OCTANE$^{TM}$ Power Desktop[2] and printed at 200*dpi* on a 600 *dpi* HP LaserJet 5Si MX printer. Real samples were scanned at 150 *dpi*. The response time was satisfactory at interactive rates. The images from the results show that our simulation model produces similar results to the

[2] All rendering is done in software.

strokes and swatches generated with real blenders and kneaded eraser over lead material on drawing papers. This means that our model makes a satisfactory dispersion and absorption of lead material across the drawing paper (see figs. 4.12 and 4.13).

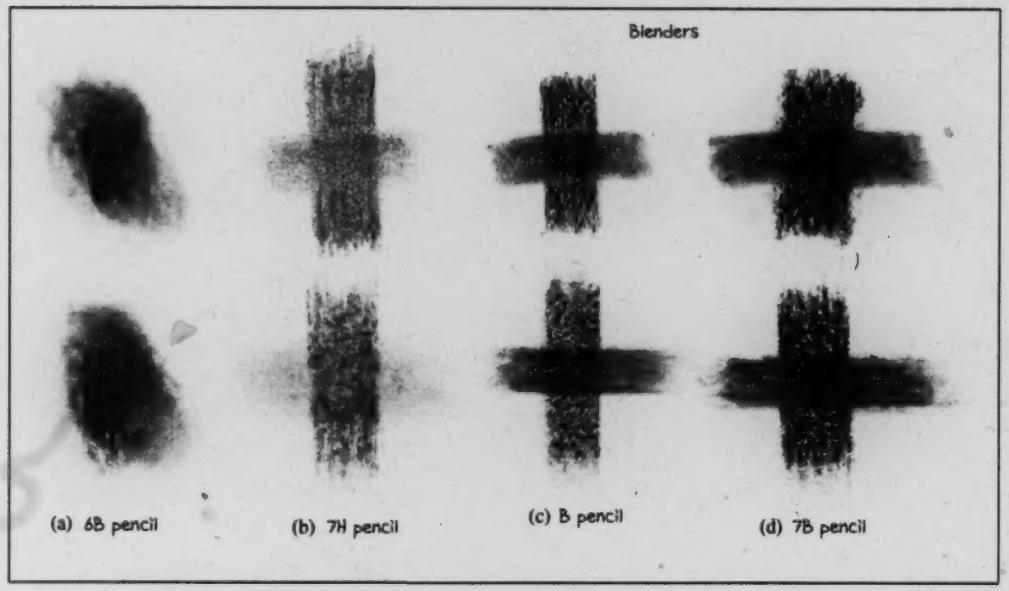


Figure 4.11: The bottom row shows results from our blender model applied over the pencil and paper model. Compare results in the blended area with real pencil work (top row). For blenders: (a) a 6B pencil was rubbed firmly and then a tortillon was rubbed over it with circular gestures and medium to low pressure (20 sec.); (b), (c), and (d): pencil strokes were rubbed vertically and then stumps were rubbed horizontally (15 - 25 sec.).

### 4.4.2 Tone rendering using smudge

The second set of results illustrates results for tone rendering using a method called smudging. The images were generated using methods for blenders and kneaded erasers recommended by review of pencil literature and contact with artists and illustrators [Camh97, Wats78, Lewi84, Pric93]. Blenders and kneaded eraser are excellent for this rendering method, used for illustrating soft subject matter and shadows. Three rendering stages are necessary:

(a) The tone values in the subject are rendered by using one pencil hardness (degree).

(b) Certain portions of the drawing are smudged using blenders.

(c) A kneaded eraser is then used to lighten the areas where there are highlights.

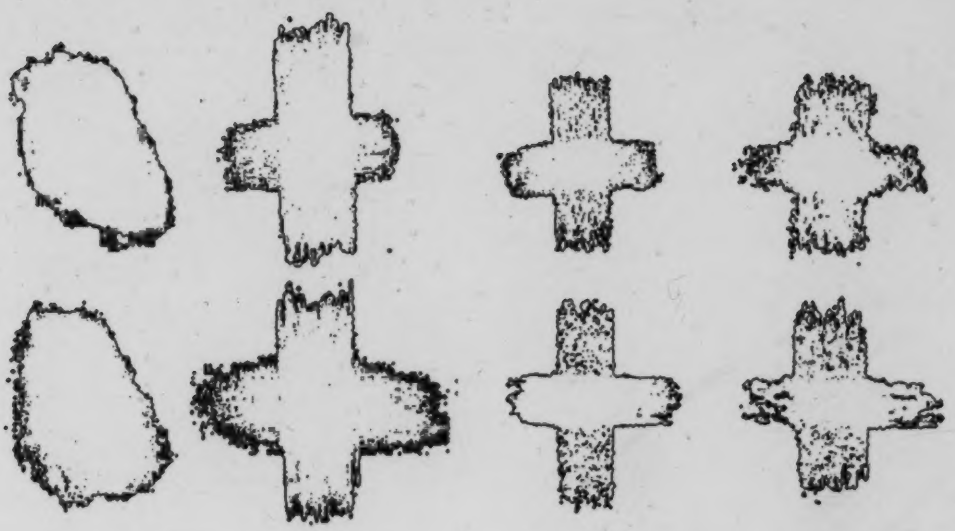

(a) 0.97 (b) 0.96 (c) 0.78 (d) 0.58

Figure 4.12: The bottom row shows contour maps within the intensity value for the results from our blender model shown in Figure 4.11. Note that the distribution of contour lines is approximately the same between the real and simulated results. This means that our model has a good approximation of the distribution of lead material after the blending process.

Figure 4.14 illustrates a real pencil work using blenders and kneaded erasers.

We demonstrate several image-based rendering results for smudging using the models presented. We use reference images of one real pencil drawing (fig. 4.15, (*sphere*)), four real pen-and-ink illustrations (figs. 4.15, (*cup*), 4.16, 4.17, and 4.18), and one photograph (fig. 4.19). The intensity values $i$ at each pixel $(x, y)$ on the reference images define the height field $h$ of the paper's surface where $h_{(x,y)} = i_{(x,y)}$.

Our goal was to create a pencil rendered version for each of the reference images. The rendering pipeline consists of two stages:

*First rendering stage*

This first stage is done automatically by our system (part (b) from figs. 4.15 to 4.19) by scan-converting the reference image (paper texture). For each paper location $(x, y)$ (correspondent to the reference image pixel location $(x, y)$ in the scan line) the pencil and paper model is evaluated (chap. 3, sec. 3.4).

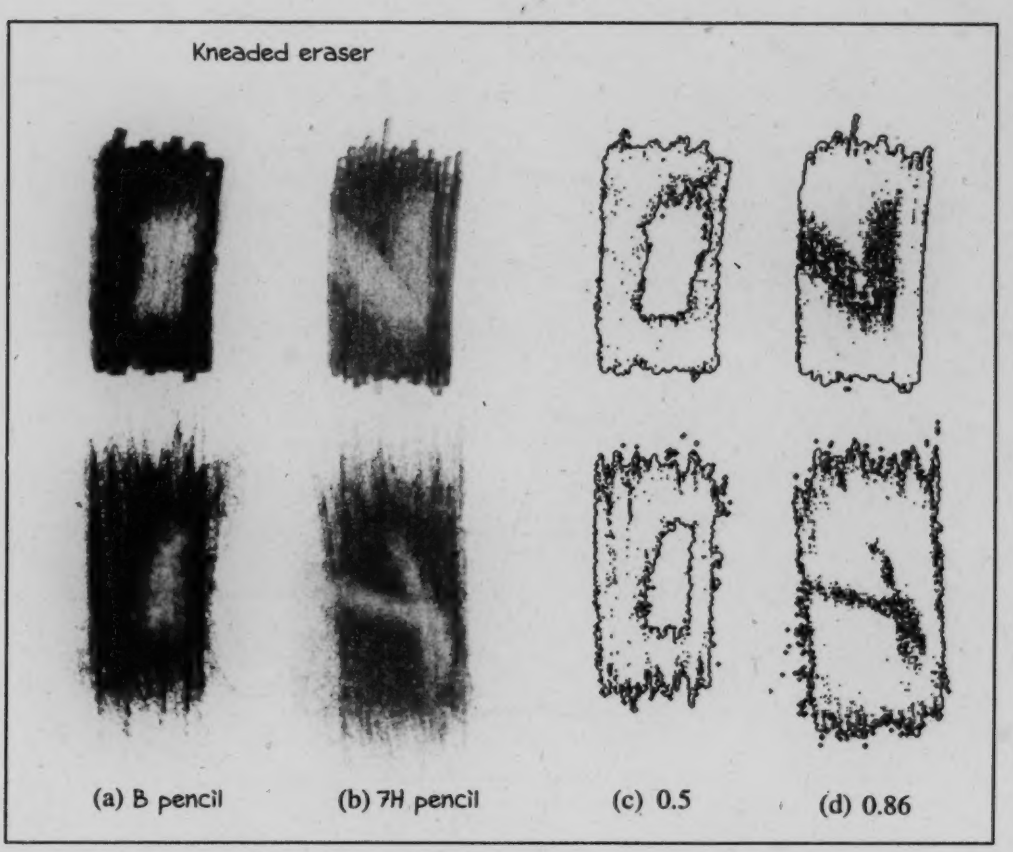


Figure 4.13: The bottom row (a), (b) shows results from our kneaded eraser model applied over the pencil and paper model. Compare results in the erased area with real pencil work (top row); (c) (d) illustrate the contour maps for (a), (b) respectively. Note that the distribution of contour lines is approximately the same between the real and simulated results. This means that our model has a good approximation of the absorption of lead material after the erasing process.

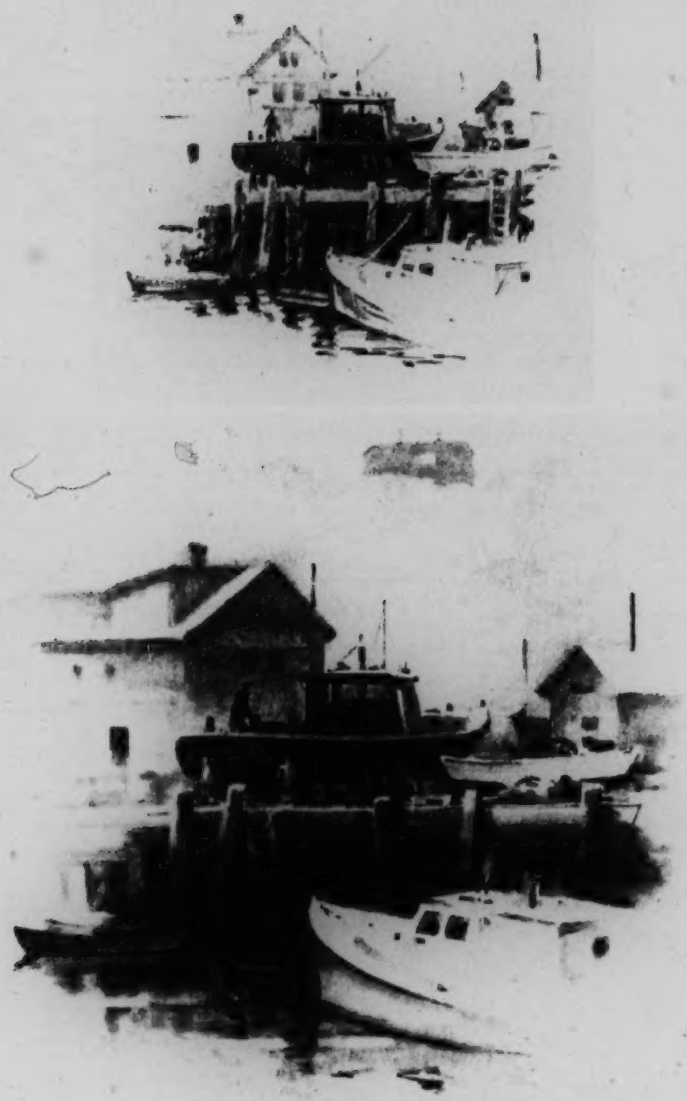

Figure 4.14: Example of real pencil work using the smudging effects [Lewi84]. The drawing in the top row was done with pencils alone. The drawing in the bottom row was smudged.

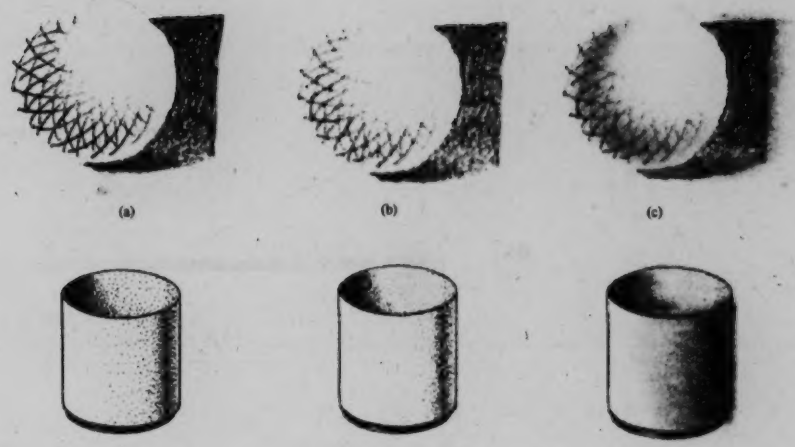


Figure 4.15: (a) Real pencil drawing of a sphere (resolution of 283x218 pixels) rendered using a very soft pencil and cross-hatching to convey tone values (top row); cup rendered in pen-and-ink (resolution of 240x282 pixels) using ink dots (bottom row). Next stages using our simulation models: (b) Automatic rendering using 2B pencil (1.24 sec. for the sphere and 1.36 sec. for the cup). (c) Smudging the crosshatched lines on the sphere (30 sec.) and the ink dots on the cup (25 sec.) creating a better effect on the tone. Shadow is also smudged around the sphere to make it softer. Notice the excess of graphite, which spreads as we smudge the drawing. Kneaded eraser enhances highlight and clears some portions of the shadows (8 sec. for the sphere and 10 sec. for the cup)

Figure 4.16: (a) Real pen-and-ink illustration of a shoe (resolution of 402x345 pixels) rendered using a few simple tones that create the illusion of form and depth. (b) Automatic rendering using 3B pencil (2.79 sec.). (c) Smudging the lines (30 sec.) and then applying the kneaded eraser on top and inside the shoe enhancing its tonal contrast (12 sec.).

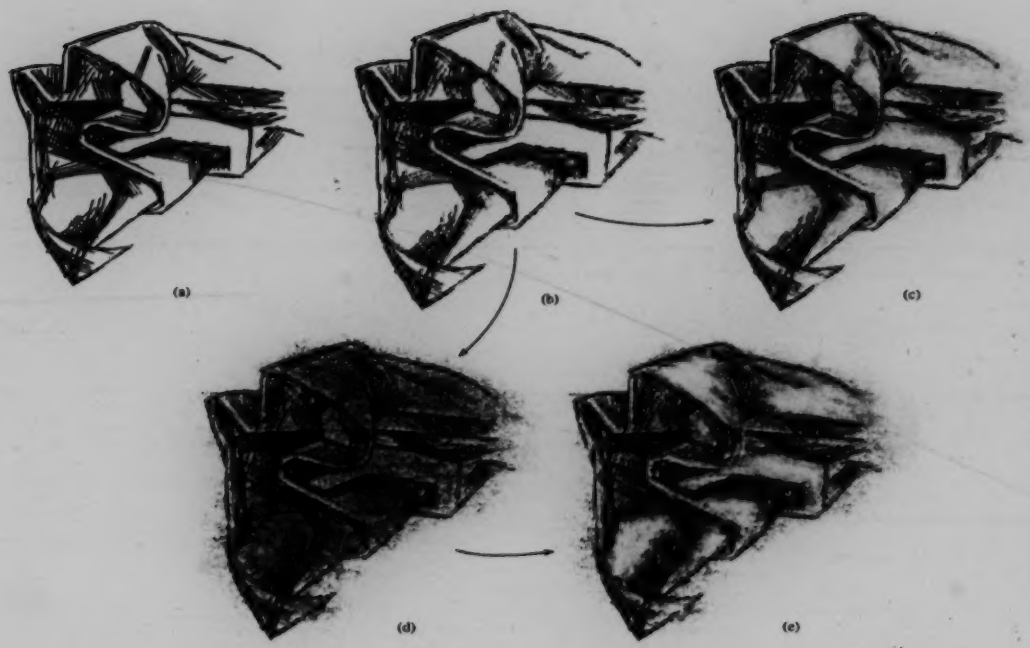


Figure 4.17: (a) Real pen-and-ink illustration of fabric (resolution of 323x382 pixels) accentuating folds by drawing them crisply. (b) Automatic rendering using 4B pencil (2.48 sec.). (c) Smudging and erasing certain parts (40 sec.). (d) Smudging the entire drawing from (b) in a relatively flat-tone (30 sec.) and then (e) using the kneaded eraser to set up areas of highlights (25 sec.) [Pric93, Mayw98].

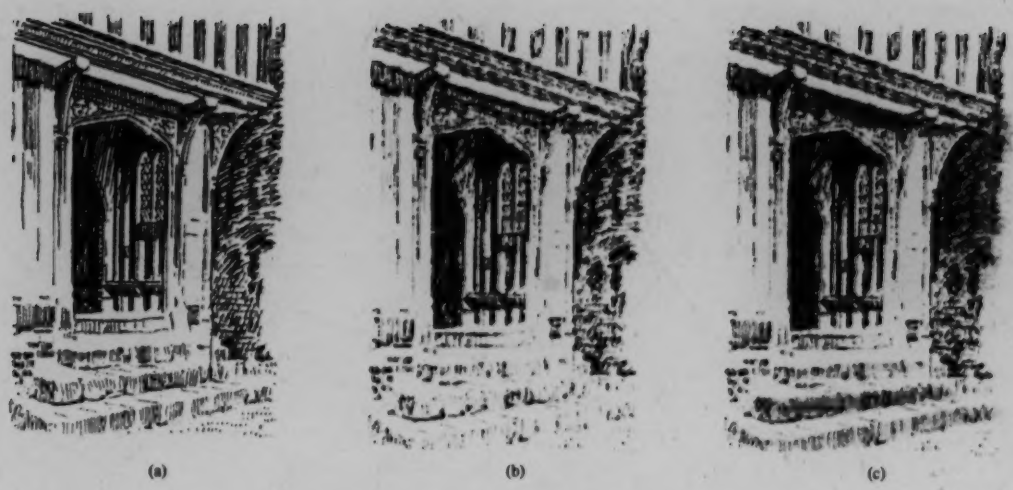

(a) (b) (c)

Figure 4.18: (a) Real pen-and-ink rendering on tracing paper (resolution of 320x408 pixels). (b) Automatic rendering using 6B pencil (2.63 sec.). (c) Smudging most of the shadow lines and the tone strokes for the bushes (35 sec.).

The computational cost of this stage is due mainly to the evaluation of the pencil point from the pencil and paper model at each pixel on the reference image. The total cost = Number of pixels on the image × Pencil and paper interaction process (chap. 3, sec. 3.4) evaluated at each pixel on the polygonal shape for the pencil point. For the results presented in this paper we use a pencil point with size equal to one pixel. The response time was satisfactory at interactive rates (see figures' captions).

For each pixel at paper $(x, y)$ from the scan line, the intensity $i_{(x,y)}$ is used to adjust the pressure $p$ applied to a single pencil resulting in the correct amount of lead material deposited at paper $(x, y)$. The pressure $p$ applied to the pencil is the only parameter that changes at this stage, and it is given by $p = 1.0 - i_{(x,y)}$. This means that in order to achieve a darker intensity more pressure is required. This approach is based on traditional pencil rendering methods to create tone values [Lewi84].

If the user provides additional pressure $pa$ then the final pressure value $p$ is scaled as $p = p \times pa$. This is the case for Figure 4.19 where pencil strokes using our model were interactively defined over the photograph after the automatic evaluation of the pencil and paper model during the scan-conversion of the reference image (paper texture). In this case the only parameter changed was the pressure applied to the pencil.

(a)

(b) (c)

Figure 4.19: (a) High contrast photograph of Patricia (resolution of 279x388 pixels). (b) Automatic rendering using 6H pencil (2.18 sec.) (first stage, subsec. 4.4.2) followed by interactive rendering (pencil point from the pencil and paper model adapted to an interactive illustration system) with strokes interactively applied using medium-soft pencils applied with light pressure (15 sec.). (c) Smudging the darker tones, the background plane of the photograph, and lightly smudging the shadows and some of the face lines (40 sec.). Kneaded eraser lightly applied to emphasize the highlights (30 sec.).

*Second rendering stage*

For this stage we adapt the blender and eraser model to an interactive illustration system. The user interactively controls the blenders and the kneaded eraser to compose the final image (part (c) from figs. 4.15, 4.16, 4.18, 4.19, and parts (c, d, e) from fig. 4.17). The response time was satisfactory at interactive rates (see figures' captions). For each paper location $(x, y)$ (correspondent to the reference image pixel location $(x, y)$) the blender and eraser model is evaluated, with $c$ from the blender's and eraser's point located at $(x, y)$ (subsec. 4.2.2, fig. 4.4). The pressure distribution coefficients ($c$ and $c_i$) have values equal to 1.0. For the results in this chapter we use blender and eraser polygonal shapes with resolutions of 1 - 10 pixels. Like in the first stage, the pressure $p$ applied to blenders/erasers is also adjusted according to $i_{(x,y)}$. In this case $pi_{(x,y)} = i_{(x,y)}$, this means that in order to achieve a lighter intensity more pressure is required.

## 4.5 Wrap-up

We have presented an observational model of blenders and kneaded eraser to be used with the graphite pencil and drawing paper model presented in Chapter 3. The model for interaction between blenders and erasers with lead and paper took into account parameters such as the particle composition of the lead over the paper, the texture of the paper, the position and shape of the blender and eraser, and the pressure applied to them. We have illustrated the results of our blender and eraser model by duplicating pencil swatches and by generating images. The images were generated using methods for blenders and kneaded erasers recommended by review of pencil literature and contact with artists and illustrators.

# Chapter 5

# Drawing Primitives

One of the advantages of the graphite pencil is that it responds rapidly to almost any demand. Sharply pointed, it gives a line as fine and clean-cut as that of the pen; bluntly pointed, it can be used much like the brush. It will make strokes sufficiently light and delicate, or bold and vigorous, to suit the most exacting technician, or tones so smooth that no trace of line can be found. It is responsive to the slightest variation of pressure or direction, allowing the artist to produce almost any type of individual stroke or, in the case of tone, to create uniform areas of grade at will from light to dark or vice versa. In this chapter we present the models for the pencil stroke primitive and the mark-making primitive to create areas of tones and textures [Sous99a]. Both primitives are built on top of the pencil and paper model presented in Chapter 3. The evaluation of the higher level modules of the system presented in this chapter was done less rigorously. We simply tried to make images in the same style as those found in the pencil literature.

## 5.1 Pencil stroke primitive

When using pencils, different types of strokes are produced depending on the pencil's hardness, its point, and how it is applied to the paper. Also there are many ways of handling the pencil and various effects over the stroke can be achieved [Gupt77, pp. 24-25], [Camh97, pp. 39-42], [Team97].

We define a pencil stroke $S$ consisting of a number of line segments, a path, and a character function. The path $P(t) : [0,1] \rightarrow R^2$ results from using a curve to approximate the line segments (fig. 5.1, top row). Different approximation functions can be applied. We use Bezier curves and B-Splines.

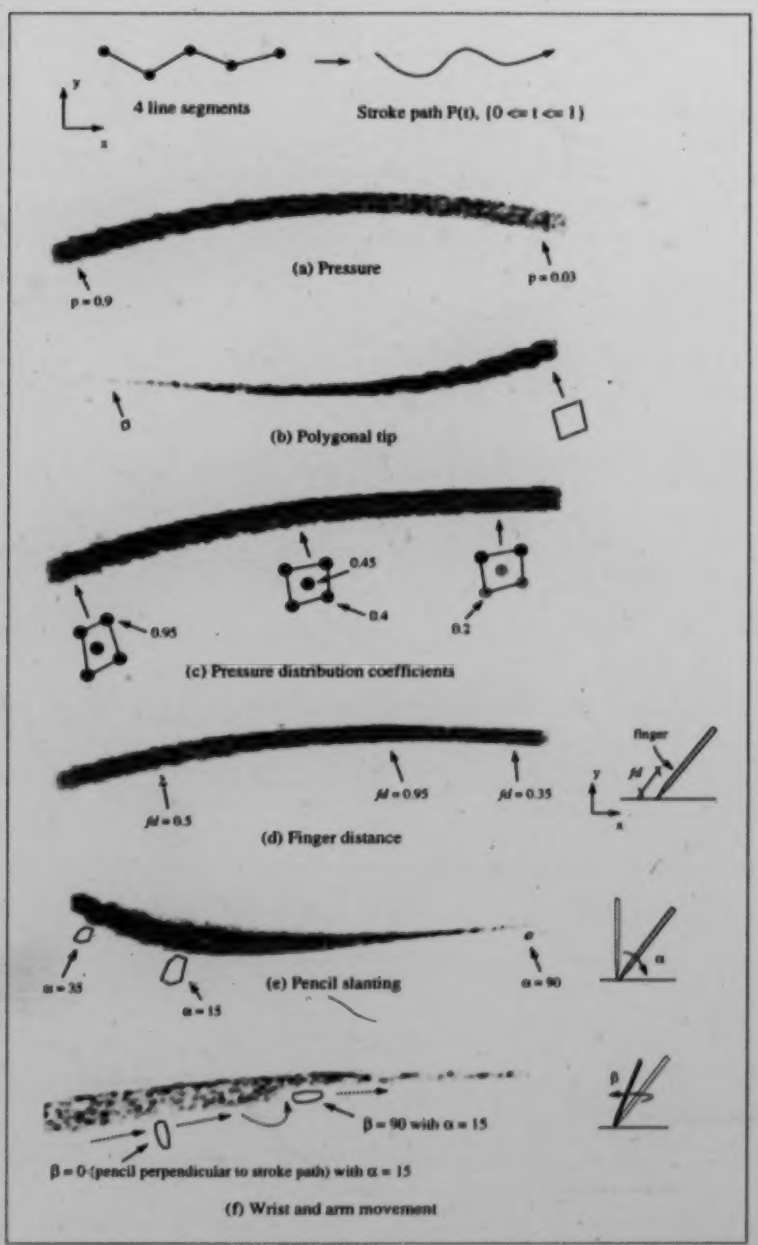


Figure 5.1: Example of a path for a pencil stroke (top row) and variation of six parameters from the character function $C(t)$ defining the pencil stroke primitive (sec. 5.1), rubbed with soft leads over a rough, medium-weight paper.

The character function varies stroke parameters at particular scalar distances $t$ along the path. We extend the character function, $C(t) = (C_w(t), C_p(t))$ (waviness and pressure parameters respectively), defined by Winkenbach and Salesin for a pen-and-ink stroke [Wink94] to include parameters that relate to the factors that influence a real pencil stroke. Each of the seven character parameters are pressure $C_p(t)$, point shape $C_{ps}(t)$, pressure distribution coefficients $C_{pdc}(t)$, waviness $C_w(t)$, finger distance $C_{fd}(t)$, pencil slanting $C_\alpha(t)$, and wrist/arm movements $C_\beta(t)$. Figure 5.1 shows a series of closeups of individual pencil strokes generated with our model. They illustrate various effects (varying pressure, angle, etc) from the character function $C(t)$ of the stroke primitive. The strokes are rendered by scan-converting copies of the pencil tip polygon modified by the character function $C(t)$ placed at each pixel location along the path defined by the base curve with the waviness function added. Waviness functions simulate the hand movements by randomly modulating the curve defining the path. Previous researchers have reported using this approach [Scho93, Sali94, Wink94, Stro94, Mark97]. We apply periodic waviness functions with random noise and turbulence to each pair of coordinates $(x, y)$ at scalar distances $t$ along the stroke's path. Each stroke parameter from the character function $C(t)$ has a specific range of values that gives satisfactory results for outlining (chap. 6, tab. 6.1) and shading (chap. 6, tab. 6.2). Random noise and turbulence are also applied to these values to enhance the effects of hand gestures.

## 5.2 Mark-making primitive

The mark-making primitive models a collection of strokes parallel to each other in a specific direction. It can be done in a formal, structured way or in a loose, "scribbled" way (sic.), according to the drawing style and approach. The main purpose of this primitive is to create areas of tone and texture [Hort94]. Figures 5.2 - 5.5 illustrate examples of real pencil work in mark-making.

In our model, the mark-making $M$ consists of a path $P(t) : [0, 1] \rightarrow R^2$ and a character function $C(t)$. The path $P(t)$ consists of one or more line segments. The character functions $C(t)$ varies its parameters along the path as a function of $t$. Figure 5.6 illustrates the parameters and results from our model of three basic kinds of mark-making techniques [Hort94]:

(a) Hatching, where each stroke $S \in [0, 1]$ along the path has a specific length

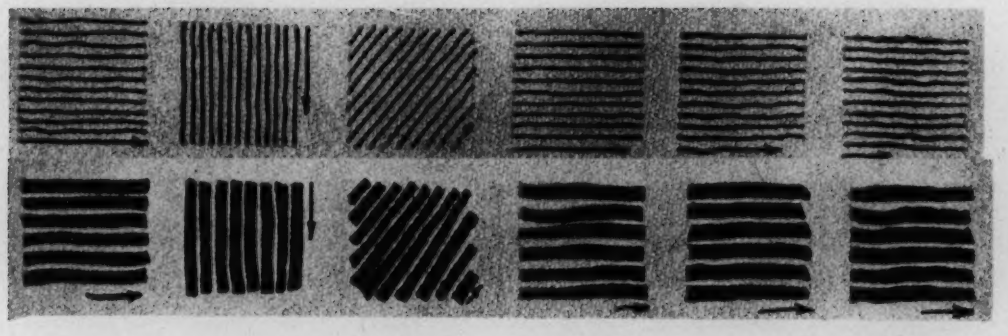

Figure 5.2: Examples of mark-making in real pencil work using sharp points (top row) and broader points (bottom row) [Gupt77]. The marks were slowly drawn with uniform and unequal pressure.

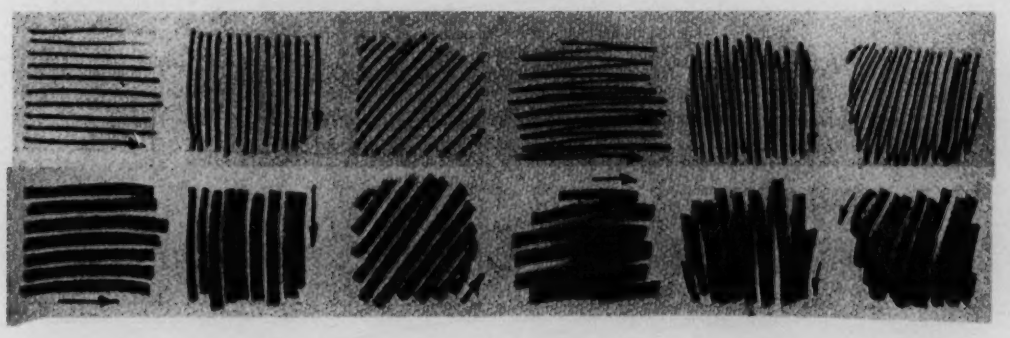

Figure 5.3: Examples of mark-making in real pencil work using sharp points (top row) and broader points (bottom row) [Gupt77]. The marks were quickly drawn in one direction and back and forth.

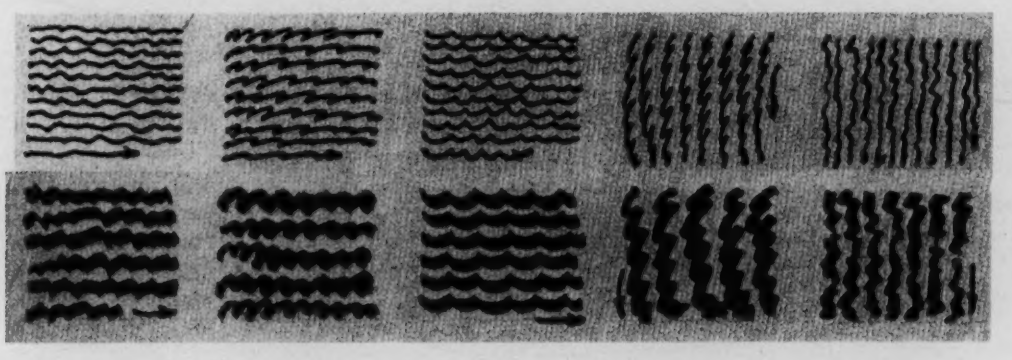

Figure 5.4: Examples of mark-making in real pencil work using sharp points (top row) and broader points (bottom row) [Gupt77]. The marks were produced with irregular strokes drawn using uniform and varied pressure.

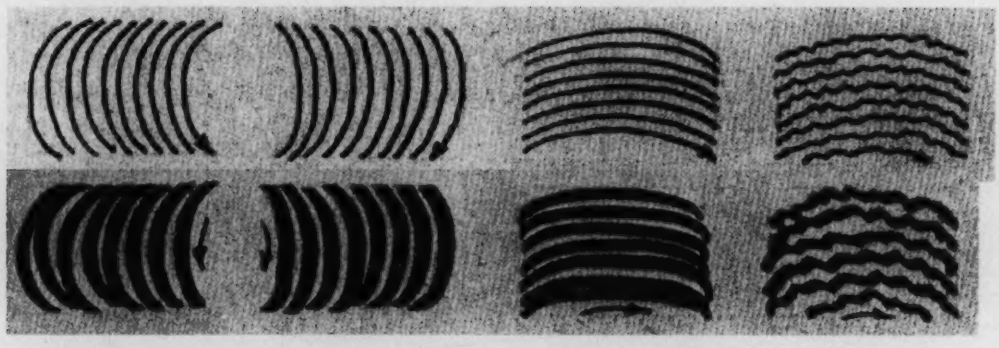

Figure 5.5: Examples of mark-making in real pencil work using sharp points (top row) and broader points (bottom row) [Gupt77]. The marks were produced with curved strokes.

$l \in [0,1]$ and angle $\theta$. The parameter $d \in [0,1]$ determines the distance between pair of strokes.

(b) Zigzag or back-and-forth has the hatching parameters where each pair of strokes $S1$ and $S2$ along the path has a scalar distance $t1 \in [0,1]$ and $t2 \in [0,1]$ respectively which determines the connection point to the third stroke $S3$.

(c) Feathering, which is a different style of zigzagging. It has the zigzag parameters where each pair of strokes $S1$ and $S2$ along the path has a scalar distance $a \in [0,1]$ and $b \in [0,1]$ respectively. Another point $c \in [0,1]$ between $a$ and $b$ defines the breaking point of the stroke $S3$.

Each parameter from the character function $C(t)$ has a specific range of values that gives satisfactory results for shading (chap. 6). Random noise and turbulence are also applied to these values to enhance the effects of hand gestures in pencil mark-making.

## 5.3 Wrap-up

We have presented two pencil drawing primitives (stroke and mark-making) built on top of the pencil and paper model. The primitives are modeled considering the factors that influence real pencil stroke and mark-making methods.

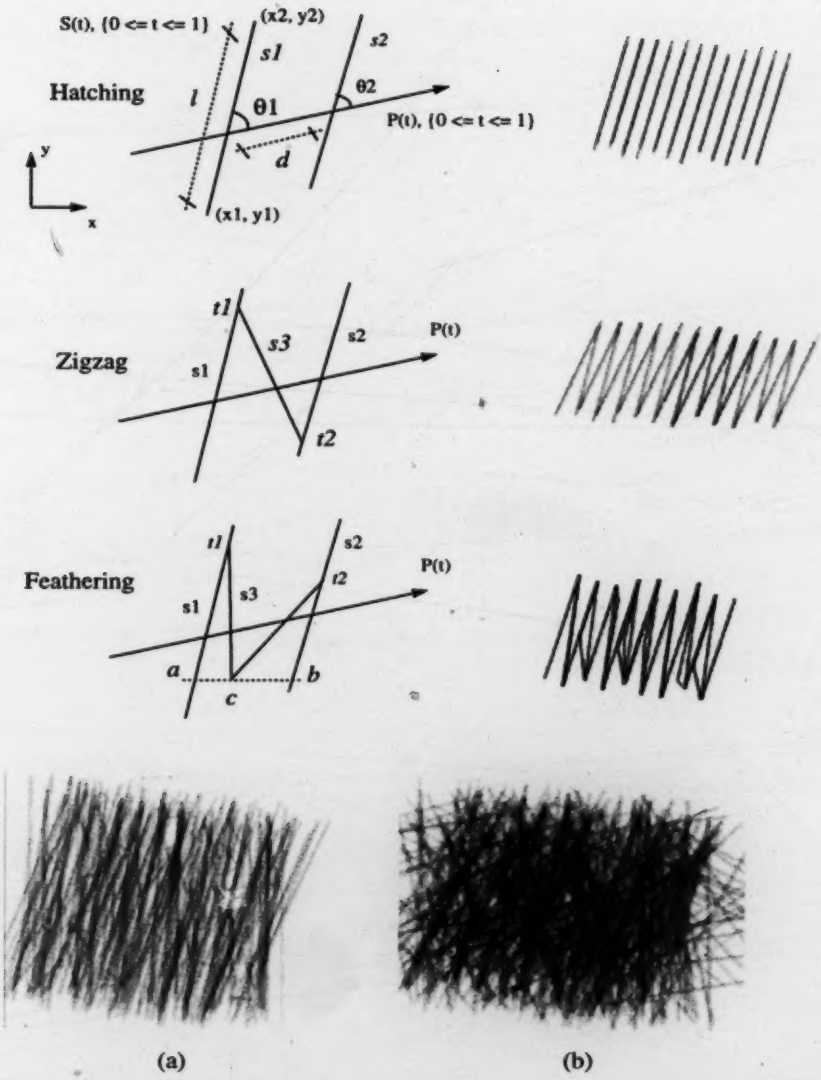


Figure 5.6: The mark-making primitive is used to build up tones and textures. This figure illustrates three variations of the mark-making primitive with results from our model. The two images (a) and (b) at the lower part of the figure start with one layer zigzagging and feathering in one direction over the path $P(t)$ with a medium soft pencil. Another layer of the primitive was laid at different angles variations ($-10 \leq \theta \leq 10$) for (a) and ($-45 \leq \theta \leq 45$) for (b).

# Chapter 6

# Rendering 3D Polygonal Models

In this chapter we present non-photorealistic rendering methods that simulate the basic rendering techniques used by artists and illustrators familiar with graphite pencil rendering. The methods are based on traditional pencil illustration techniques recommended by review of pencil literature [Salw25, Gupt77, Lewi84, Fran88, Pric93, Doug93, Hort94, Misa94, Camh97, Team97]. We implemented rendering techniques for automatic outlining and shading of 3D polygonal models. These techniques are built on top of an observational model of graphite pencil and drawing paper (chap. 3), and on the mark-making and stroke primitives (chap. 5). We also describe the partial control of the drawing composition through ordering and repeating of drawing steps from preparatory sketches to finished rendering results. The evaluation of the higher level modules of the system presented in this chapter was done less rigorously. We simply tried to make images in the same style as those found in the pencil literature.

The chapter is organized into four parts:

(a) The architecture of the pencil rendering system (sec. 6.1).

(b) Pencil-based outlining methods and results for 3D models (sec. 6.2).

(c) Description of what is necessary to build tone using graphite pencils and how we modeled the processes involved. We also present results for the fundamental methods for rendering 3D objects in pencil tonal contrast (sec. 6.3).

(d) Description of the control of pencil drawing steps from preparatory sketches to finished rendering results (sec. 6.4).

## 6.1 The System Architecture

The next sections describe the modeling and implementation of the basic traditional pencil rendering techniques for outlining and shading using the pencil stroke and mark-making primitives, and the pencil and paper model. Figure 6.1 illustrates the basic architecture of our pencil rendering system.

### 6.1.1 3D models

Our pencil engine is built on the 3D modeling and rendering system presented in Glaeser [Glae94]. The 3D models were generated using the modeling language from the same reference. Our system currently works just for polygonal models. The inputs are the visible edges, faces, and shadows. The lightness values for edges, faces, and shadows are evaluated using the Phong illumination model with flat shading, either as a pre-computation step, yielding a reference gray-scale image, or directly as the pencil strokes are generated. Most of the processing described in this paper assume that we have 3D information as well as the visible polygons and edges projected in the normalized coordinate space. The geometric models have not been pre-processed in any way to make rendering easier. The main goal is to apply our pencil engine to simple flat polygonal models emulating traditional graphite pencil renderings in different ways to match the target tone. Strokes are applied to each individual face of the models. The individual faces are not merged to enabling covering an area with large strokes. This problem remains open to further investigation.

### 6.1.2 Pencil engine

Our pencil engine is organized in three main subsystems: (1) materials (pencil, paper), (2) primitives (stroke, mark-making), and (3) rendering methods (outline, shading, tone value chart). Outline methods (sec. 6.2) use the pencil stroke primitive. Each stroke primitive is procedurally generated by functions written in a C-based interpreted language. These functions get as input parameter values for the stroke primitive within the range given in Table 6.1. Shading methods (sec. 6.3) use the pencil mark-making primitive which also uses the stroke primitive. Each mark-making primitive is also procedurally generated. These functions get as input parameter values for the mark-making primitive within the range given in Table 6.2. A tone value chart (subsec. 6.3.1) controls the number of pencil passes (layers) applied to the

mark-making primitive, the pressure applied to each stroke, and the lead hardness of a particular pencil. This results in matching the target tone of the 3D model (subsec. 6.3.3). At present the user interface consists of a control panel presenting the range of values for the pencil engine parameters (see tabs. 6.1 and 6.2). While the system is automatically rendering the model, the user has the option of modifying the parameter values for the stroke and mark-making primitives during run-time while receiving feedback in real-time, thus guiding the rendering process. We envision the use of our system in combination with 3D modeling/rendering systems allowing the user to intuitively control the essential pencil rendering parameters such as specification of drawing materials, outlining and shading methods, and specification of drawing steps. The system would then automatically render the 3D models emulating traditional graphite pencil illustrations.

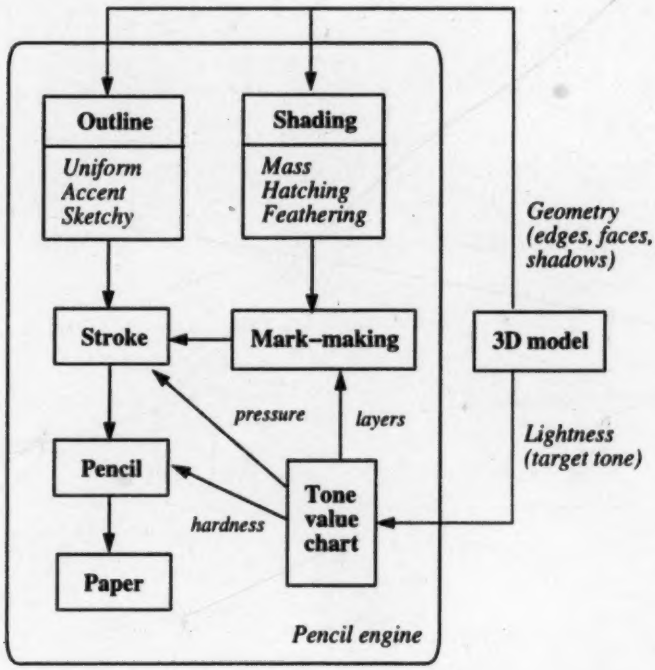


Figure 6.1: Architecture of our pencil rendering system.

## 6.2 Drawing objects in outline

The simplest and most direct type of rendering is that of outlining or shape description. Salwey [Salw25] states that

> Pencil lines for outlining are usually a convention considered as depicting the boundaries between different tone values.

He also states that

> as the work becomes more advanced and approaches what may be termed "highly finished work," the hard line, unless it is specially retained and accentuated for decorative effect, should gradually be eliminated. At the same time realism must not be carried to such an extent that the characteristics of the pencil rendering technique or the manner in which the drawing has been rendered is lost.

Figures 6.2, 6.3 and 6.4 illustrate examples of real pencil work in outline. In our system, outline pencil strokes are drawn for each visible edge $e(t)$ from every visible face and shadow of the model. Figures 6.5, 6.6, 6.7, 6.19, and 6.20(a) illustrate outlines of 3D models generated by our system. These results use default parameters which are given in Table 6.1. We have implemented three classes of traditional pencil-based outlines [Gupt77, Pric93, Doug93]:

(a) **Uniform or flat**: This method uses lines with a fixed degree of thickness and pressure for the whole drawing (figs. 6.2 and 6.5(a), 6.19). It is good for illustration but it lacks sensitivity [Pric93].

(b) **Accented**: The pressure applied to the pencil is adjusted to lighten and darken the line giving more character and expressiveness to the outline [Gupt77] (figs. 6.2 and 6.4). The accented effect can be achieved by using the "sine wave" pressure function presented by Winkenbach and Salesin [Wink94] (see tab. 6.1, waviness function $w4$) or by adjusting the pressure of the pencil according to the interpolated lightness values $ei(t)$ along the edge with the function $p(t) = 1.0 - ei(t)$. This means that in order to achieve a darker intensity more pressure is required (figs. 6.5(b) and 6.6).

(c) **Sketchy**: The lines are drawn with quick and spontaneous strokes until the user is satisfied that the shape is adequately represented (figs. 6.2, 6.3, 6.4, 6.5(c)(d),

6.7, 6.20(a)). It emphasizes the vitality of the drawing marks themselves, making the drawing more subjective, because the focus is balanced between representation (what is drawn) and characterization (how it is drawn) [Doug93].

Figure 6.2: Examples of outlines in real pencil work [Gupt77]. From left to right: uniform, accented, and sketchy outlines.

## 6.3 Rendering objects in tonal contrast

Drawing media differ in the techniques used to achieve shading that matches the target tone of the subject. In pen-and-ink the approach is to alternate the lines with the white of the paper itself. Each kind of line, depending on its proximity and thickness, can produce planes having different values and textures. This approach was implemented by Winkenbach and Salesin using prioritized stroke textures for the pen-and-ink renderer [Wink94]. Graphite pencils on the other hand can produce gradations of values between black and white. This section describes the processes involved.

### 6.3.1 Building the tone values chart

In pencil drawing, values between black and white are usually organized into a tone value chart with three basic tones (light, mid and dark), or ten values, the lightest value being the white of the paper [Gupt77, Lewi84, Pric93, Team97].

We define a tone value chart as an array $tvc_i$, $\{3 \leq i \leq 11\}$. Although we are not limited to this tone value range we decided to use it to be consistent with the

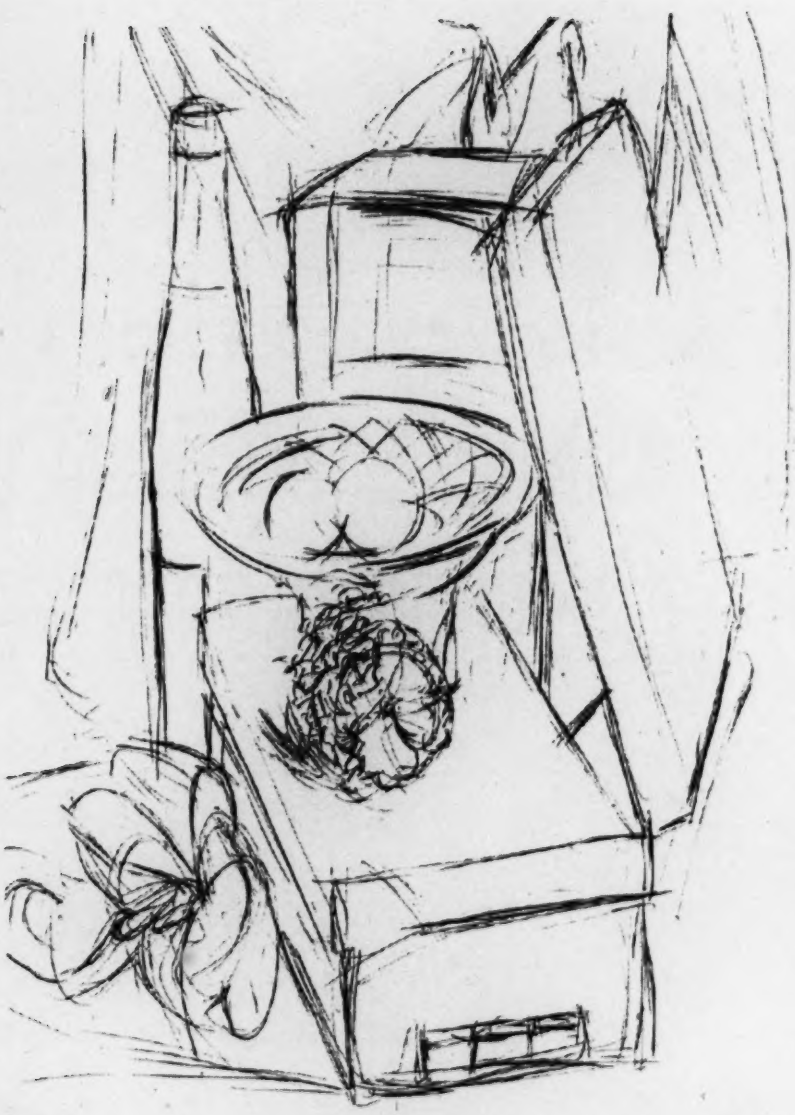

Figure 6.3: Example of sketchy outline in real pencil work [Doug93].

Figure 6.4: Example of accented/sketchy outline in real pencil work [Doug93].

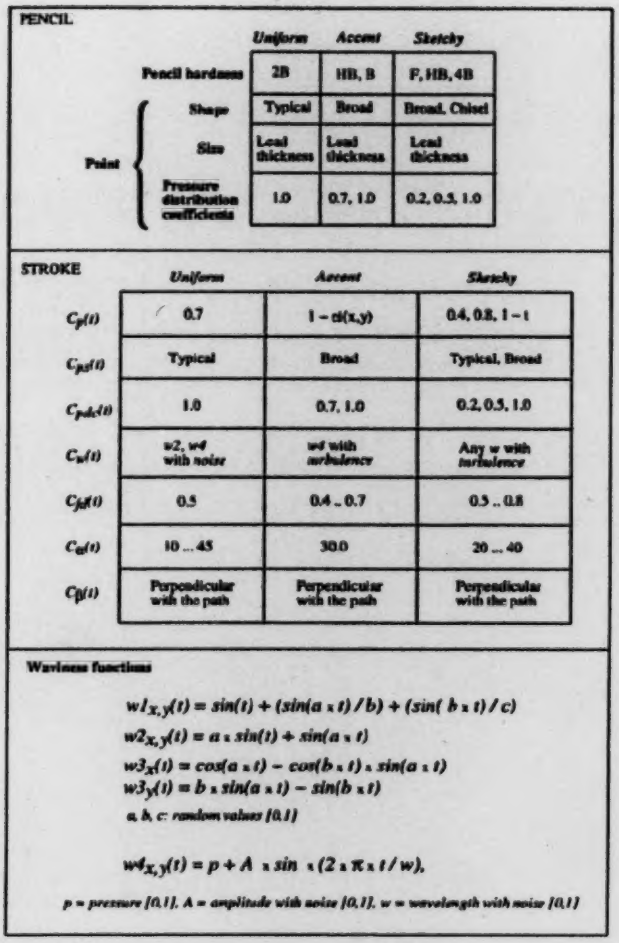


Table 6.1: Default range values for the outlining parameters.

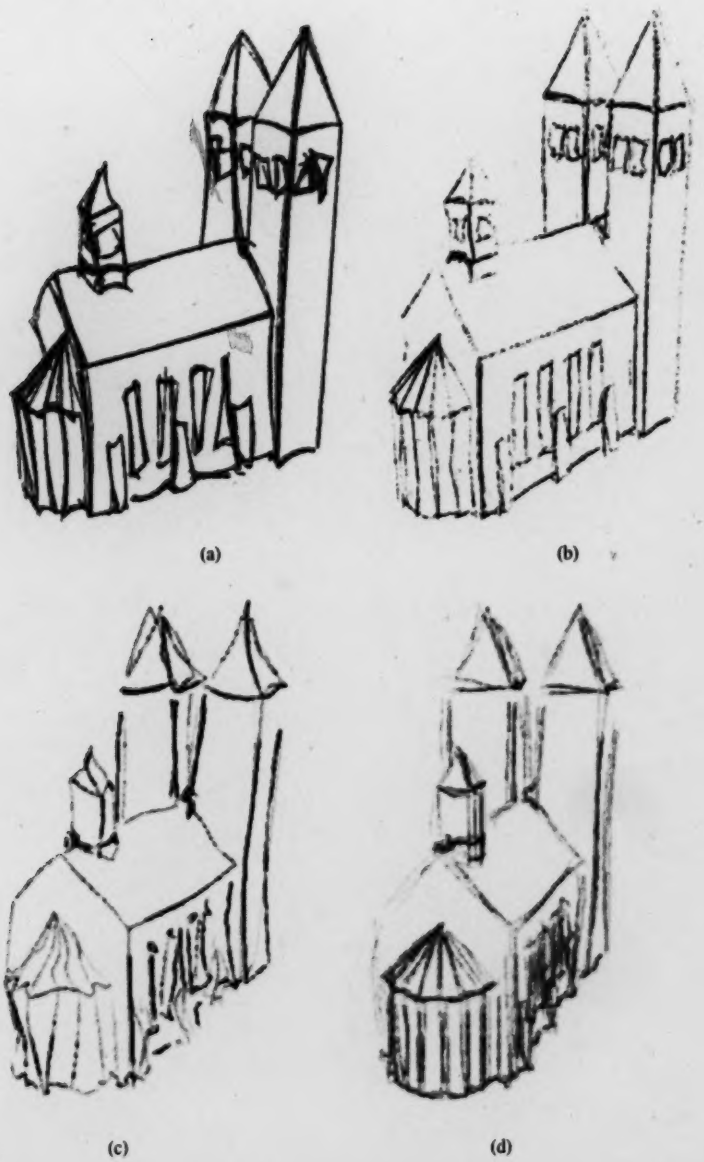


Figure 6.5: Outline results over semi-rough paper of 3D model of a church (298 edges, 100 faces) from our system: (a) uniform with 2B pencil (10 sec.), (b) accent with 3B pencil (7 sec.), (c) sketchy with H and B pencils (10 sec.), and (d) less sketchy with 2H and HB pencils (9 sec.).

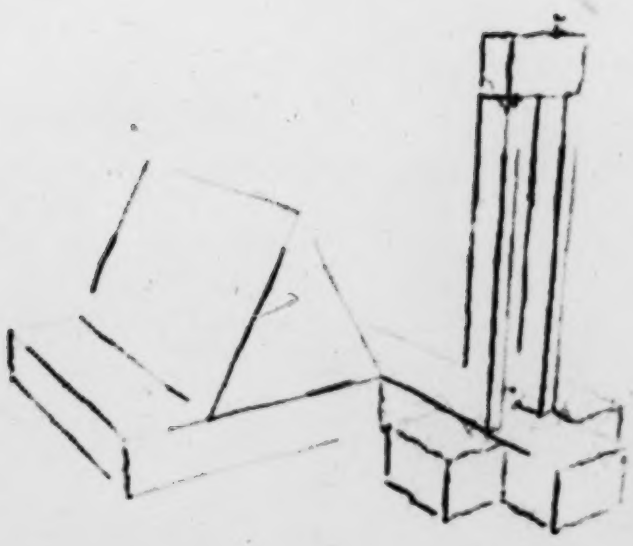

Figure 6.6: Accented outline using medium-soft pencil over smooth paper. Model of church has 62 vertices on 8 primitives with 93 edges in total (20 sec. to render).

traditional practices and guidelines in pencil rendering. Each entry in $tvc_i$ has the following information (see fig. 6.8):

(a) Lightness intensity range $v_{min}, v_{max}$.

(b) Average intensity value: $av = \frac{(v_{min}+v_{max})}{2}$

(c) Pencil hardness $ph$.

(d) Pressure value $p$.

(e) Number of pencil passes (or layers of marks) $np$.

We implemented two traditional approaches used to create charts of a graded tone from value 0 (black) to 10 (white). Figure 6.8 illustrate examples for the two approaches with $i = 11$ tone values:

(a) Use one pencil hardness that will make a dark enough tone to create a solid black. Changing the pencil pressure and varying the number of pencil passes creates all tone values from 0 to 9. The pressure applied to the pencil is adjusted according to the averaged tone intensity value and is given by: $p = 1.0 - av$. This means that in order to achieve a darker intensity more pressure is required (fig. 6.8 top chart).

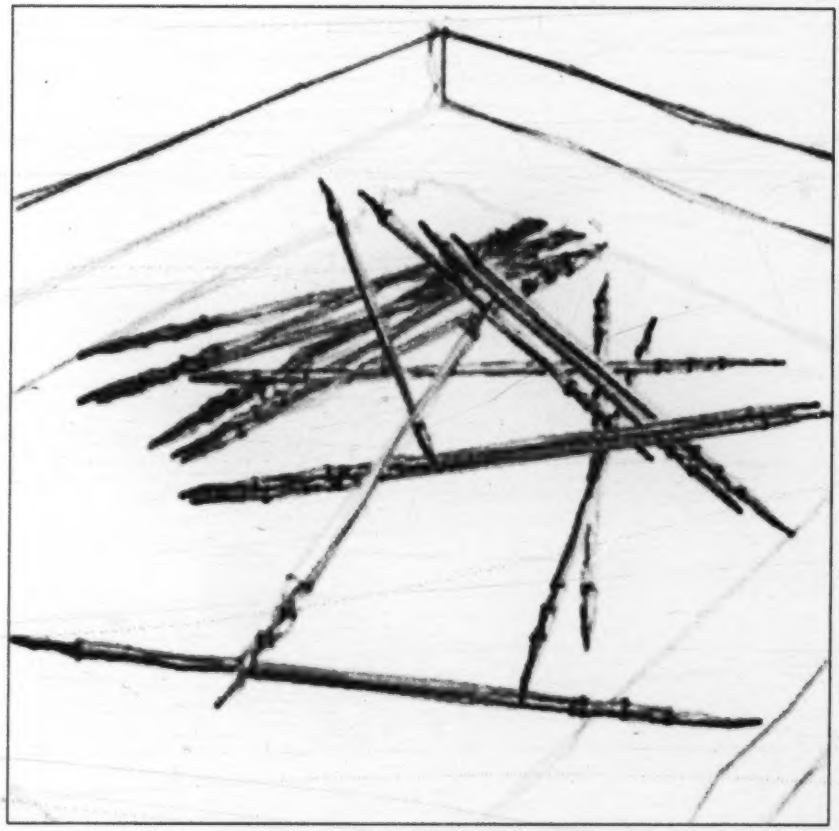

Figure 6.7: Outlining result using medium-soft pencils. Model has 5 groups with 822 vertices on 22 primitives, and a total of 1624 edges (2 min. to render).

(b) Use seven pencils of grades 6B, 4B, 2B, HB, 2H, 4H, and 6H. Pencils are changed to create a gradual blending of the tones. There are slight or no variations on the pencil pressure and variations on the number of pencils passes from one value to the next (fig. 6.8 bottom chart).

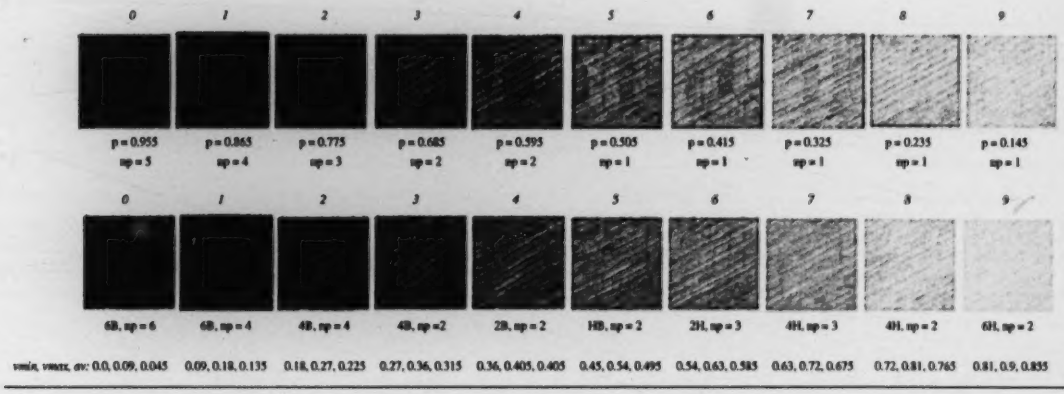


Figure 6.8: Examples of tone values charts generated by our system for $i = 11$ values. The values of $v_{min}$, $v_{max}$, and $av$ for both tables are listed. The eleventh entry uses the white of the paper ($vmin = 0.9$, $vamx = 1.0$, $av = 0.95$). Pencil marks are rubbed using layers (indicated by $np$) of the hatching mark-making primitive over a medium-rough paper texture. Using the same pencil (4B) for the values created the chart on the top row. Using the same pressure (0.5) for the values created the chart on the bottom row.

### 6.3.2 Placing linear marks

Linear marks allow the creation of tones. For each visible face and shadow in the 3D model the following steps are followed:

(a) Compute the shading direction. This direction expresses the form and depth of the planes of the subject being drawn and there are no fixed rules to determine it [Gupt77, Misa94, Mayw98]. The default shading direction is the projected surface normal $P(N)$ in the projection plane (fig. 6.9(a)).

(b) Place a mark-making primitive:

i. The path $P(t)$ is defined in the projection plane as being orthogonal to the shading direction and passing over the center of the face being shaded (fig. 6.9(b)).

ii. Generate collection of parallel strokes along $P(t)$ with angle $\theta$ with respect to the computed shading direction (fig. 6.9(c)). The distance $d$ between every

pair of strokes should be the same. It has been observed that this is the case for most shading approaches using graphite pencil [Salw25, Mayw98].

iii. Collection of strokes along $P(t)$ are clipped against the surface being shaded (fig. 6.9(c)).

The parameters of the mark-making primitive can now be adjusted in order to match the target tone (next subsection) and according to a particular shading method (see subsecs. 6.3.3 and 6.3.4).

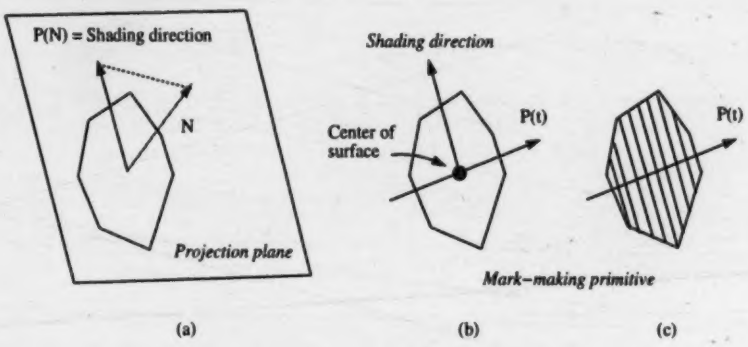


Figure 6.9: Main steps on placing linear marks.

### 6.3.3 Matching the target tone

Every visible face and shadow from the 3D model are flat shaded resulting in a target tone *tt*. Tone values that match the target tone can be created with the same methods that were used to make the value charts. Given a target tone *tt* we find the necessary parameters in the pre-computed look-up tone value chart *tvc* (fig. 6.1, subsec. 6.3.1, fig. 6.8). These parameters are *np*, *p*, and *ph*, where *np* defines the number of times the mark-making primitive will be placed on the surface being shaded, *p* defines the pressure applied to the stroke, and *ph* defines the pencil hardness.

### 6.3.4 Tone Rendering Results

In this subsection we present results from our implementation of two fundamental graphite pencil tone rendering categories: "realistic" and line-based methods.

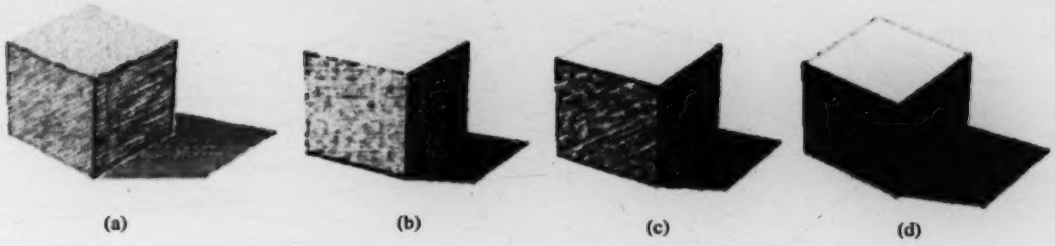


Figure 6.10: Four variations of tone value study with mass, hatching/crosshatching, and feathering shading over a cube using different charts. With a 2H pencil (a) the light value, the middle value, and the dark value are indicated. A stronger light effect is obtained with a 2B pencil (b), or (c) by keeping the light side white, the middle tone a 6th value with a 2H pencil, and the dark side a 2nd value by using a 4B pencil. In order to create the strongest effect of light possible (d), the light side is left white and the middle tone a 2nd value with a 2B pencil and the dark a 1st value with a 4B pencil.

### "Realistic" methods

Of the various methods of toning or shading, perhaps the most natural for the beginner's first use is what might be called the "realistic" method [Gupt77]. In this method, the artist renders, by "mass" shading every visible tone in the subject as literally as possible. In *mass shading* the component pencil lines are so merged that their individual identity is wholly or largely lost [Gupt77]. The zigzag mark-making primitive (see chap. 5, fig. 5.6) is used with the strokes very close together to make a continuous tone. The side of the pencil is used by slanting it to 30 - 40 degrees (see chap. 5, fig. 5.1(e)), bringing the tone out very smoothly. Layers of the mark-making primitive can be repeatedly placed over the surface in different shading directions until all traces of line disappeared. Another "realistic" method is smudging or burnishing [Pric93, Camh97, Team97]. We implemented it for automatic and interactive image-based pencil rendering using our blender and eraser model (chap. 4).

Figures 6.11 and 6.16 illustrate examples of real pencil work in mass shading. Figures 6.10, 6.12, 6.17(a), 6.19, and 6.20(b) illustrate mass-shading of 3D models generated by our system. These results use default parameters which are given in Table 6.2.

### Line-based marking methods

These are methods where at least some lines are plainly visible. We implemented two techniques:

**PENCIL**

| | | *Mass* | *Hatching* | *Feathering* |
|---|---|---|---|---|
| **Pencil hardness** | | B, 2B | F, HB, B, 2B | HB, 2B, 4B |
| **Point** | **Shape** | Typical | Typical, Broad | Broad, Chisel |
| | **Size** | Lead thickness | Lead thickness | Lead thickness |
| | **Pressure distribution coefficients** | 1.0 | 0.8, 1.0 | 0.3, 0.7, 1.0 |

**STROKE**

| | *Mass* | *Hatching* | *Feathering* |
|---|---|---|---|
| $C_p(t)$ | Tone value chart | Tone value chart | Tone value chart |
| $C_{ps}(t)$ | Typical, Broad | Typical | Typical, Broad, Chisel |
| $C_{pdc}(t)$ | 0.7, 0.8, 1.0 | 0.7, 1.0 | 0.5 ... 1.0 |
| $C_w(t)$ | *w2, w3* with *noise* | *w1, w2, w4* with *turbulence* | Any *w* with *noise, turbulence* |
| $C_{fd}(t)$ | 0.4 ... 0.7 | 0.4 ... 0.7 | 0.3 ... 0.8 |
| $C_\alpha(t)$ | 30 ... 40 | 45 .. 70 | 10 ... 50 |
| $C_\beta(t)$ | Perpendicular with the path | Perpendicular with the path | Perpendicular with the path |

**MARK-MAKING**

| | *Mass* | *Hatching* | *Feathering* |
|---|---|---|---|
| *l* | 1.0 | 0.9 – 1.0 | 0.7 – 1.0 |
| $\theta$ | shading direction + range of –45 ... +45 degrees | shading direction + range of –5 ... +5 degrees | shading direction + range of –15 ... +15 degrees |
| *d* | 0.01 ... 0.2 | 0.05... 0.3 | 0.03 ... 0.5 |
| *t1, t2* | t1: 0.8 ... 1.0<br>t2: 0.0 ... 0.2 | — | t1: 0.7 ... 1.0<br>t2: 0.0 ... 0.3 |
| *a, b, c* | — | — | a: 0.1 ... 0.3<br>b: 0.4 ... 0.8<br>c: 0.1 ... 0.4 |

Table 6.2: Default range values for the shading parameters. Waviness functions are given in Table 6.1.

Figure 6.11: Example of mass shading in real pencil work [Gupt77].

(a) **Hatching/Crosshatching:** the principle of hatching is drawing lines with one definite and continuous movement, parallel to each other, and very near together to produce an even tone. The hatching mark-making primitive (see chap. 5, fig. 5.6) is used with the collection of strokes in the shading direction and equal distance $d$ between every pair of strokes. Cross-hatching is the rendering of tone values by superimposing one series of parallel lines diagonally across another series of parallel lines [Salw25]. It can be achieved by placing additional layers of the hatching mark-making primitive at different shading directions on top of the current pencil marks.

(b) **Feathering or scumble:** With this technique the strokes are plainly visible because the pencil is used with a greater degree of freedom, blending tones optically so that while individual strokes are retained, they are also overlaid to create smoother tones [Gupt77, Pric93, Team97]. The feathering mark-making primitive (see chap. 5, fig. 5.6) is used.

Figures 6.13 and 6.16 illustrate real pencil work in feathering shading. Figures 6.10, 6.17(b), 6.19, 6.20(b) illustrate hatching, and Figures 6.10, 6.14, 6.15, 6.17, 6.19(b, step 2) illustrate feathering tone rendering of 3D models generated by our system. The default variations for the pencil, stroke, and mark-making parameters are given in Table 6.2.

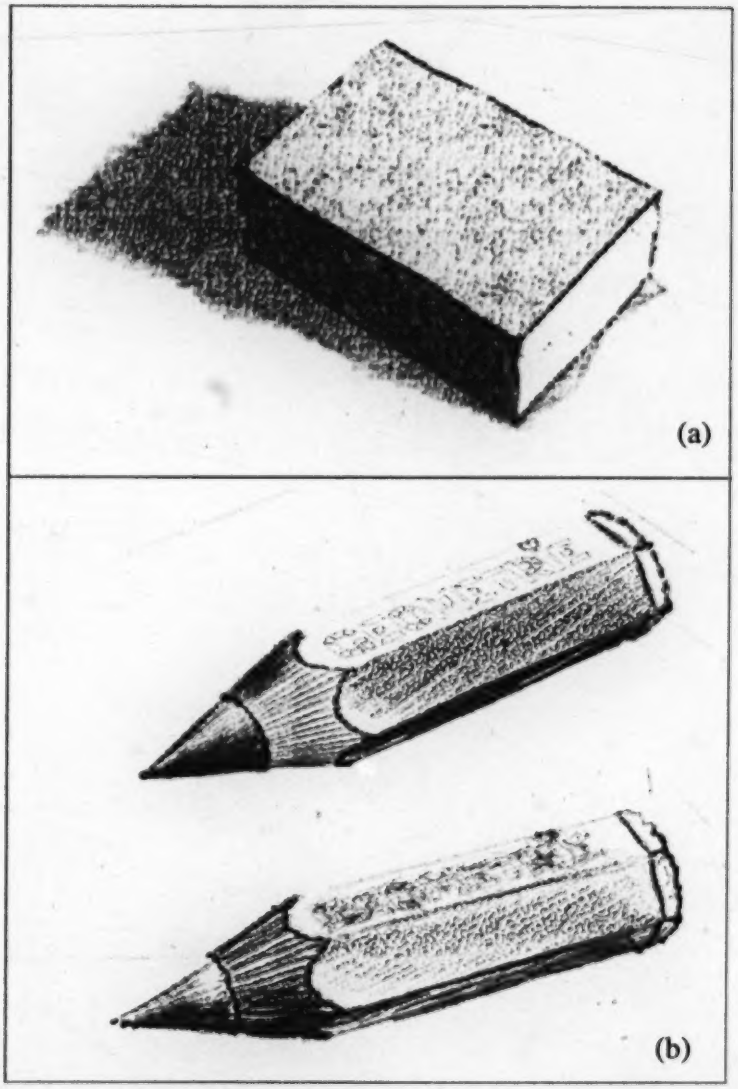


Figure 6.12: Examples of pencil rendering of 3D objects in mass shading using our system: (a) parallelepipeds, 3H, 2H, HB, and B pencils used firmly over rough paper (22 sec.), (b) pencil (602 edges, 206 faces), 2B pencil used lightly over semi-rough paper, (1.20 min for top pencil, 1.10 min for bottom pencil).

Figure 6.13: Example of hatching and feathering in real pencil work [Lewi84].

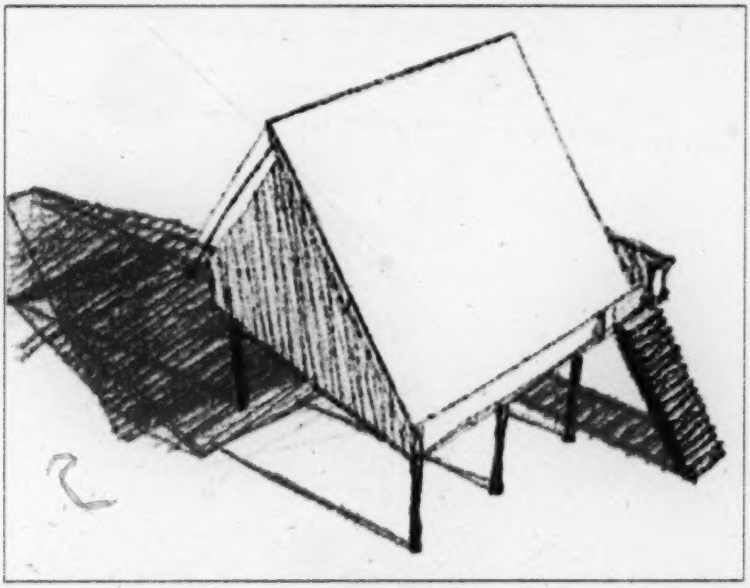

Figure 6.14: Feathering shading using H and 4B pencils over semi-rough paper. The H pencil with a broad point is applied firmly across the shadow to smooth the strokes. Model has 510 edges and 238 faces (1.25 min. to render).

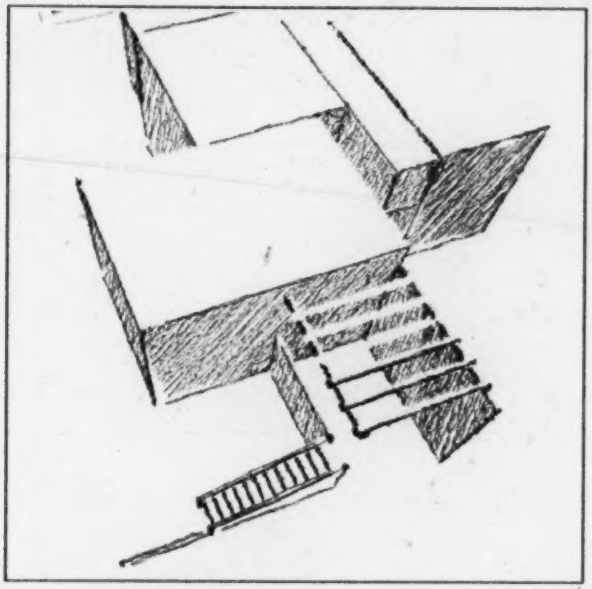

Figure 6.15: Initial stages of feathering shading using tone value chart with three values (7th and 8th values from chart on fig. 6.8 and white of the paper). Model has 450 edges and 224 faces (1 min. to render).

Figure 6.16: Example of mass shading and feathering in real pencil work [Gupt77].

(a)

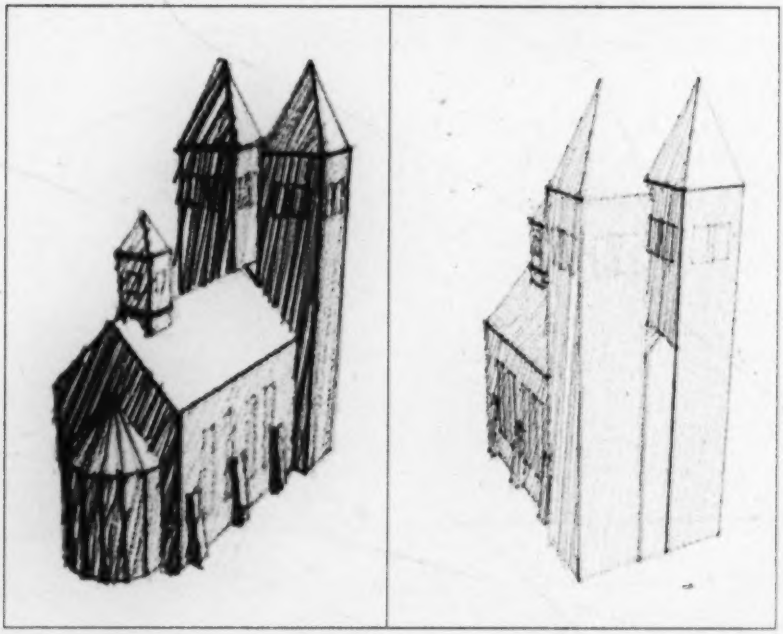

(b)

Figure 6.17: Examples of pencil rendering of 3D objects in tonal contrast using our system: (a) computer desk (3374 edges, 1195 faces), The three shading methods with 8H, 5H, B, and 5B pencils over rough paper. Accented outline (48 sec.), mass shading (1.23 min), hatching/cross-hatching, and feathering (1.10 min), total time is 3.20 min, (b) church (298 edges, 100 faces), mass and feathering shading with B, 2B, and 4B pencils over medium-rough paper (left church, 50 sec.); light mass and feathering shading with B, 2B, and 4B pencils over smooth paper (right church, 33 sec.).

## 6.4 Drawing steps control

The control of the drawing composition is an important aspect of both traditional illustration practices and non-photorealistic rendering methods. Composing an illustration means putting together things and arranging them in order, to make one unit out of them all. Composition issues include proportion of the picture space according to the subject, focal points in the drawing, tone value studies, atmospheric effects, and so on [Gupt77, Lewi84, Fran88, Pric93]. Figure 6.18 illustrate real pencil work in drawing steps. Some of these issues have been investigated in NPR research. Strothotte et al. [Stro94] control the placement of lines depending on the areas of the image needing more attention. Winkenbach and Salesin [Wink94] interactively control the placement of strokes indicating where details should appear on the surfaces of the objects. Streit and Buchanan [Stre98] present techniques for creating non-photorealistic half toned images by controlling importance functions and the type and number of drawing primitives. Seligmann and Duncan [Seli91] describe an automated intent-based approach to illustration which fulfills high-level description of the communicative intent and stylistic choice.

With our system it is possible to control the composition of a drawing work from the initial sketch to the finished rendering, a process achieved in a variety of drawing steps [Gupt77, Lewi84, Fran88, Pric93]. The rendering proceeds in layered steps emulating the process that artists take to make sure that the composition is correct at specific steps. Each drawing step is implemented by configuring the parameters of the pencil and the rendering methods described (see tabs. 6.1 and 6.2). Each step can be repeated a number of times before moving to next step. Figure 6.19 shows an example of how an illustration is improved by rendering in progressive steps in this way. The parameters for each step are configured according to the guidelines found on pencil drawing literature and by using the values from Tables 6.1 and 6.2. Figure 6.20 illustrates different steps on a rendering study of a chair.

## 6.5 Wrap-up

In this chapter we presented non-photorealistic rendering methods that simulate the basic rendering techniques used by artists and illustrators familiar with graphite pencil rendering. The methods are based on traditional pencil illustration techniques

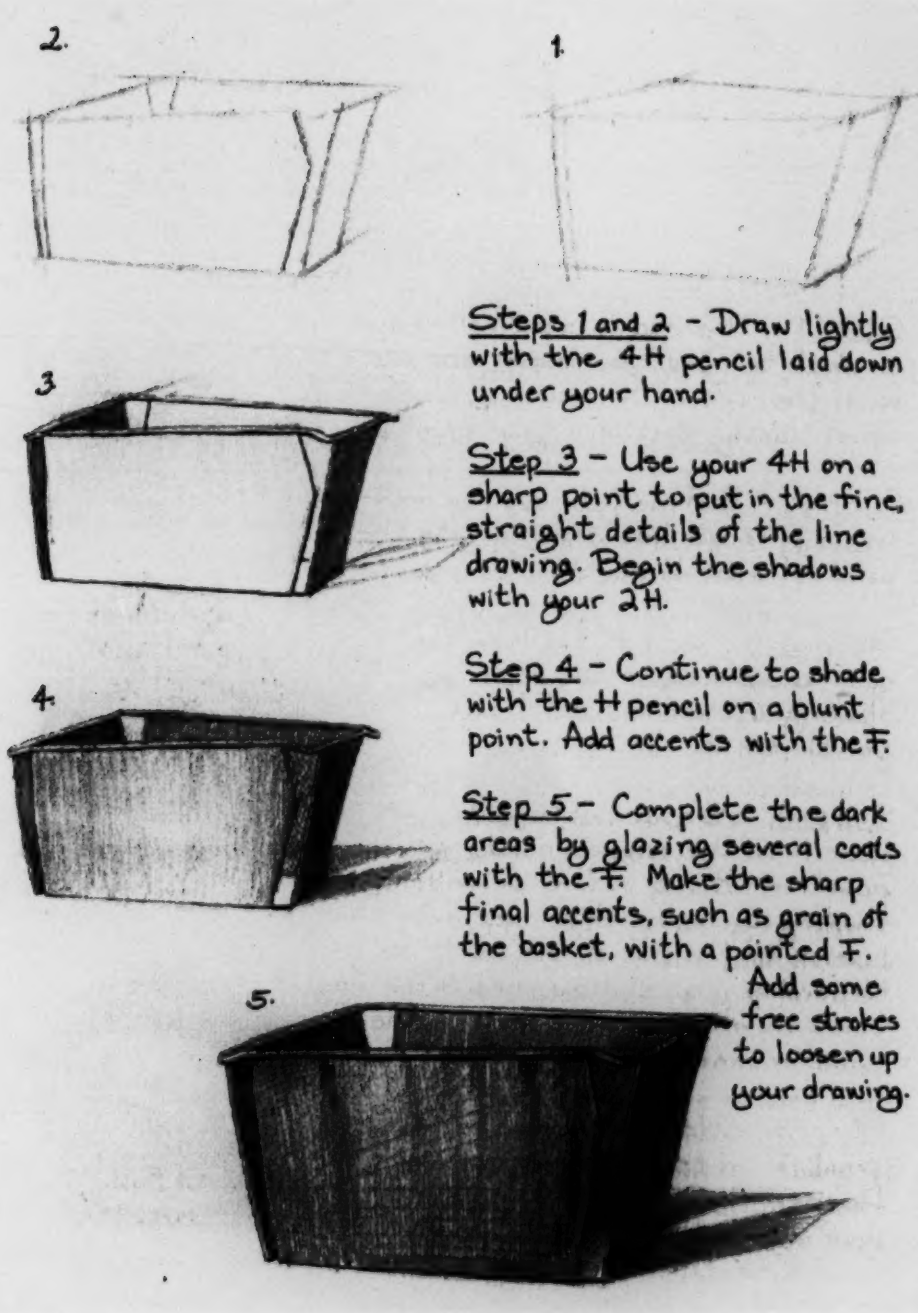
2.
1.
Steps 1 and 2 - Draw lightly with the 4H pencil laid down under your hand.
3
Step 3 - Use your 4H on a sharp point to put in the fine, straight details of the line drawing. Begin the shadows with your 2H.
4.
Step 4 - Continue to shade with the H pencil on a blunt point. Add accents with the F.
Step 5 - Complete the dark areas by glazing several coats with the F. Make the sharp final accents, such as grain of the basket, with a pointed F.
Add some free strokes to loosen up your drawing.
5.

Figure 6.18: Example of drawing steps in real pencil work [Fran88].

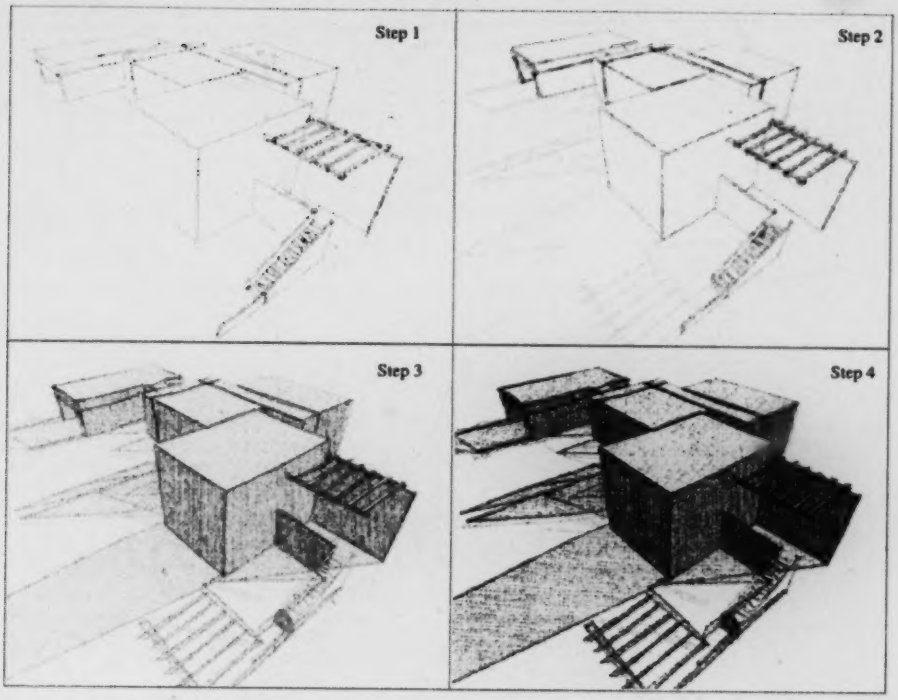


(a)

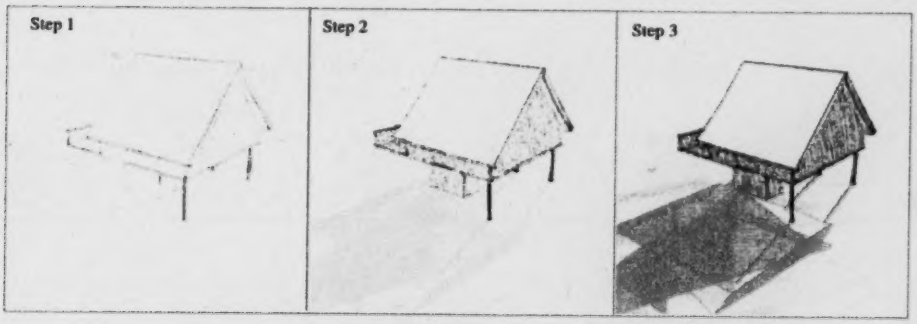


(b)

Figure 6.19: The evolution of a pencil drawing over semi-rough paper in traditional steps [Gupt77, Lewi84, Fran88, Pric93] implemented in our system: (a) *step 1*, B pencil, accented outline (7 sec.); *step 2*, 55 sec. later, HB, 2H pencils, uniform outline, delineation of shadows. This step is repeated 2 times; *step 3* after 1.40 min., HB, 3B pencils, mass shading, light hatching and feathering. This step is repeated 2 times; *step 4* after 2 min., 3B pencils with increased pressure. Steps 2 and 3 are repeated 2 times. (b) *step 1*, HB pencil, uniform outline (45 sec.); *step 2*, 1.05 min. later, 3H, B pencils, light mass shading, very light feathering; *step 3* after 1.15 min., 2B, 3B pencils with increased pressure, with high pencil slanting in the shadow. Step 3 is repeated 3 times.

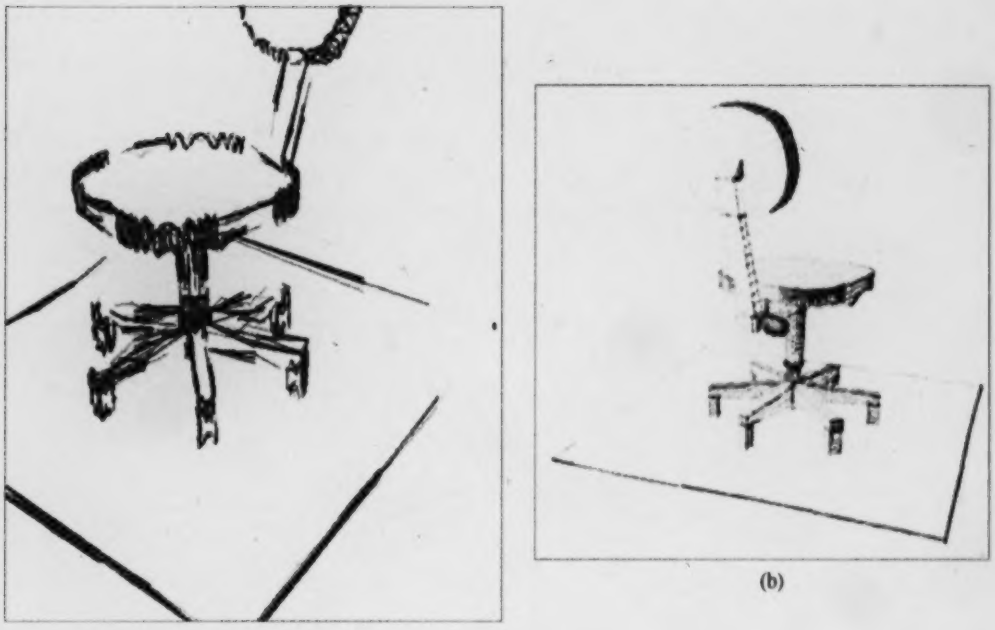

(a) (b)

Figure 6.20: Examples of a pencil rendering study of a chair using our system. Model has 2 groups, 624 vertices on 27 primitives, 976 edges, and 406 faces. (a) sketchy outline using 4B pencil (40 sec. to render), (b) hatching and mass shading with various pressures applied to B and 2B pencils (50 sec. to render).

recommended by review of pencil literature. We implemented rendering techniques for automatic outlining and shading of 3D polygonal models. These techniques are built on top of an observational model of graphite pencil and drawing paper (chap. 3), and on the mark-making and stroke primitives (chap. 5). We also describe the partial control of the drawing composition through ordering and repeating of drawing steps from preparatory sketches to finished rendering results.

# Chapter 7

# Conclusions

## 7.1 Summary

In this thesis we presented results from our research in pencil illustration methods for non-photorealistic rendering. The main motivation for this work is to investigate graphite pencil as a useful technical and artistic NPR production technique to provide alternative display models for users. We chose the pencil because it is a flexible medium, providing a great variety of styles in terms of line quality, hand gesture, and tone building. It is excellent for preparatory sketches and for finished rendering results. Many people in different contexts such as scientific and technical illustration, architecture, art, and design use pencil renderings.

### 7.1.1 Methodology

Our approach is based on an observational model of how real graphite pencils interact with drawing paper. The goal was to capture the essential physical properties and behaviors observed to produce quality pencil marks at interactive rates. Our intention was not to develop a highly physically accurate model, which would lead to a computationally expensive simulation.

The images from the results show that our simulation model produces similar results to the strokes and swatches generated with real graphite pencils over drawing papers. To evaluate the system we chose representative swatches of real pencil drawings and used our system to duplicate the effect. Our evaluation is thus conducted by observing how close to the original swatches are the computer-generated ones. Besides this we used a thresholded contour display that bestowed us some further insights into the

distribution of the graphite. The evaluation of the higher level modules of the system was done less rigorously. We simply tried to make images in the same style as those found in the pencil literature.

This thesis has many applications in computer graphics. The models for the pencil drawing materials presented in this thesis (pencil, paper, blender, eraser) can be straightforwardly adapted to existing interactive illustration systems [Verm89, Scho93, Sali94] and 3D NPR systems for technical illustration, art, and design [Dool90a, Dool90b, Wink94, Stro94, Hall95, Deca96a, Mark97, Elbe98, Gooc98a]. The higher-level models (primitives, rendering methods) can be used to extend the capabilities of existing 3D modelers/renderers, to be used in the context of illustrators, architects, designers, and artists.

### 7.1.2 Modeling approach

Our approach was to break the problem of simulating pencil drawings down into the following sub-problems:

(a) **Drawing materials** (chaps. 3 and 4): low-level simulation models for wood-encased graphite pencil and drawing paper, and for blenders and kneaded eraser. The model for interaction between the pencil and paper took into account the composition of the lead pencil and the texture and weight of the paper. Assuming that clay and wax are optically neutral elements we also presented an observational illumination model for pencil lead. The model for interaction between blenders and erasers with lead and paper took into account parameters such as the particle composition of the lead over the paper, the texture of the paper, the position and shape of the blender and eraser, and the pressure applied to them. We have illustrated the results of our models by duplicating pencil swatches and by generating images. The images were generated using methods for pencil, blenders, and kneaded erasers recommended by review of pencil literature and contact with artists and illustrators. The images were generated online using reference images as input.

(b) **Drawing primitives** (chap. 5): pencil stroke and mark-making (for tones and textures) built on top of the drawing materials.

(c) **Rendering methods built on top of the drawing primitives** (chap. 6): Algorithms for outlining, shading, shadowing, and texturing of reference images and 3D objects with a look that emulates real pencil renderings. We have also presented non-photorealistic rendering methods that simulate the basic rendering techniques used by artists and illustrators familiar with graphite pencil rendering. The methods are based on traditional pencil illustration techniques recommended by review of pencil literature. We implemented rendering techniques for automatic outlining and shading of 3D polygonal models. These techniques are built on top of an observational model of graphite pencil and drawing paper, and on the mark-making and stroke primitives.

(d) **High-level tools** (chap. 6): partial control of the drawing composition through ordering and repeating of drawing steps. We also describe the partial control of the drawing composition through ordering and repeating of drawing steps from preparatory sketches to finished rendering results.

## 7.2 Extensions and future directions

Several research issues remain open for future work in computer-generated pencil drawing:

**User interface** The user interface to our system can be improved by providing a more intuitive way for controlling the automatic rendering of 3D models to emulate traditional graphite pencil illustration methods. A possible direction is to model the metaphor of a drawing studio where the user specifies the materials (pencil grade, paper texture, blenders, and erasers), the kind of outlining and shading methods, and also the number of drawing steps.

**Rendering techniques**

(a) **Outlining and shading** Other pencil outlining and shading techniques may also be explored and extended to render various classes of 3D models from different contexts (architecture, art, design). One important aspect that should be investigated is the merging of individual faces to enable outlining and shading an area with large strokes.

(b) **Tone and texture** Often several quite different surfaces in the same subject call for correspondingly diversified mark-making handling. Texture representation for

natural materials (glass, wood, fur, stone, water), architectural details (cornices, roof, wall surfaces).

(c) **Graded tones** Graded tones prove of value in innumerable ways when representing small details, shadows, and in composing entire drawings. Graded tones emphasize value contrasts where most needed to express the subject effectively. Almost any object can be represented satisfactorily by graded tones (rounded forms, architectural moldings, natural shapes, etc.). There is another use for graded tones that is of great importance - to achieve certain visual effects in drawing composition:

i. To give a sense of distance and detachment or separation of one object from another.

ii. To bring attention to a desired spot in the drawing.

**Drawing composition** The word "composition" means putting together things and arranging them in order, to make one unit out of them all. The control of drawing steps presented in Chapter 6 helps on composing a drawing from initial sketch to finished rendering. Additional work is necessary in the composition of each individual step:

(a) *Center of interest*: This means to decide where you want the observer's attention to be primarily directed (foreground, middle distance, far distance, above, at the center, below, right, left). Having determined this, a "center of interest" can be developed at that point, making this area "in focus" while throwing other areas "out of focus".

(b) *Creating an attention point*: Certain techniques are used in combination to create certain attention points in the composition:

- Vigorous or unusual technical handling (bold strokes, individual arrangements of stroke marking), extreme means of representing textures.
- Detailed handling of some part of a subject.

(c) *Value studies*: Provide many tone value schemes to a single subject, which diversifies the tone effects.

(d) *Recomposing forms*: Rearrange parts of the subject matter, one in relation to another, modifying the sizes of individual objects, alter the original shapes of objects.

(e) *Contrast effects*: Adapt the plan of light against dark or dark against light to the overall composition. This helps to create the focus of attention in the composition.

**Materials and techniques**

(a) The pencil combines perfectly with many media, frequently playing an important part in conjunction with pen-and-ink, brush and ink, wash, watercolor, etc. Our model can be extended and combined with other media simulated media such as watercolor [Curt97] and pen-and-ink [Wink94].

(b) The pencil embodies rendering features presented in other media: drawing in fine line (pen and ink and etching); broad line shading, together with shading in mass (crayon, charcoal, and other chalky media). Our drawing primitives can be extended to have specific features from other media drawing primitives.

# Bibliography


[Appe79] A. Appel, F.J. Rohlf, and A.J. Stein. "The haloed line effect for hidden line elimination". *Computer Graphics (Proc. of SIGGRAPH '79)*, Vol. 13, No. 2, pp. 151–157, August 1979.

[Bles88] T.W. Bleser, J.L. Sibert, and J.P. McGee. "Charcoal sketching: returning control to the artist". *ACM Transactions on Graphics*, Vol. 7, No. 1, pp. 76–81, January 1988.

[Borg85] H. Borgman. *Drawing in Pencil.* Watson-Guptill Publications Inc., New York, (ISBN 0-8230-1388-X), 1985.

[Camh97] S.W. Camhy. *Art of the Pencil: A Revolutionary Look at Drawing , Painting, and the Pencil.* Watson-Guptill Publications, (ISBN 0-8230-1373-1), 1997.

[Curt97] C.J. Curtis, S.E. Anderson, J.E. Seims, K.W. Fleischer, and D.H. Salesin. "Computer-generated watercolor". *Proc. of SIGGRAPH '97*, pp. 421–430, August 1997.

[Deca96a] P. Decaudin. "Cartoon-looking rendering of 3D-scenes". *Research Report INRIA 2919.* June 1996.

[Deca96b] P. Decaudin. *Modeling using fusion of 3D shapes for computer graphics – cartoon-looking rendering of 3D scenes.* Ph.D. thesis, Universite de Technologie de Compiegne (FRANCE), December 1996.

[Dool90a] D. Dooley and M.F. Cohen. "Automatic illustration of 3D geometric models: lines". *Symp. Interactive 3D Graphics*, Vol. 24, pp. 77–82, March 1990.

[Dool90b] D. Dooley and M.F. Cohen. "Automatic illustration of 3D geometric models: surfaces". *Proc. of IEEE Visualization '90*, pp. 307–314, October 1990.

[Doug93] D. Douglas and D. van Wyk. *The Drawing Process: Rendering.* Prentice Hall, Inc., (ISBN 0-13-219833-9), 1993.

[Elbe90] G. Elber and E. Cohen. "Hidden Curve Removal for Free Form Surfaces". *Proc. of SIGGRAPH '90*, pp. 95–104, August 1990.

[Elbe95a] G. Elber. "Line art rendering via a coverage of isoparametric curves". *IEEE Transactions on Visualization and Computer Graphics*, Vol. 1, No. 3, pp. 231–239, September 1995.

[Elbe95b] G. Elber. "Line illustrations in computer graphics". *The Visual Computer*, Vol. 11, No. 6, 1995.

[Elbe98] G. Elber. "Line art illustrations of parametric and implicit forms". *IEEE Trans. Visualization and Computer Graphics*, Vol. 4, No. 1, pp. 71–81, January 1998.

[Fran88] G. Franks. *Pencil Drawing.* Walter Foster Publishing, Inc., Laguna Hills, CA, (ISBN 0-929261-03-8), 1988.

[Glae94] G. Glaeser. *Fast algorithms for 3D-graphics.* Springer-Verlag New York, Inc., 1994.

[Gooc98a] A. Gooch. "Interactive non-photorealistic technical illustration". *MSc thesis.* Dept. of Computer Science, University of Utah, December 1998.

[Gooc98b] A. Gooch, B. Gooch, P. Shirley, and E. Cohen. "A non-photorealistic lighting model for automatic technical illustration". *Proc. of SIGGRAPH '98*, pp. 447–452, August 1998.

[Gupt33] A.L. Guptill. *Sketching and Rendering in Pencil.* The Pencil Points Press, Inc., New York, 1933.

[Gupt77] A.L. Guptill. *Rendering in Pencil.* Watson-Guptill Publications Inc., New York, (ISBN 0-8230-4531-5), 1977.

[Hall95] P.M. Hall. "Comic-strip rendering". *Tech. Report CS-TR-95/2.* Dept. of Computer Science, Victoria University of Wellington, New Zealand, January 1995.

[Hert98] A. Hertzmann. "Painterly rendering with curved brush strokes of multiple sizes". *Proc. of SIGGRAPH '98*, pp. 453–460, August 1998.

[Hort94] J. Horton. *An Introduction to Drawing.* Dorley Kindersley Limited, (ISBN 0-13-123902-3), 1994.

[Kama87] T. Kamada and S. Kawai. "An enhanced treatment of hidden lines". *ACM Transactions on Graphics*, Vol. 6, No. 4, pp. 308–323, October 1987.

[Lali69] N. Lalibert and A. Mogelon. *Drawing with Pencils, History and Modern Techniques.* Van Nostrand Reinhold Company, New York, 1969.

[Leis94] W. Leister. "Computer generated copper plates". *Computer Graphics Forum*, Vol. 13, No. 1, pp. 69–77, September 1994.

[Lewi84] D. Lewis. *Pencil Drawing Techniques.* Watson-Guptill Publications Inc., New York, (ISBN 0-8230-3991-9), 1984.

[Loha93] F. J. Lohan. *The Drawing Handbook: Comprehensive, Easy-To-Master Lessons on Composition and Techniques using Pencil and Pen Ink.* Contemporary Books, Inc., Chicago, (ISBN 0-8092-3786-5), 1993.

[Mark97] L. Markosian, M.A. Kowalski, S.J. Trychin, L.D. Bourdev, D. Goldstein, and J.F. Hughes. "Real-time nonphotorealistic rendering". *Proc. of SIGGRAPH '97*, pp. 415–420, August 1997.

[Mayw98] B. Maywood. *Personal communication.* Dept. Art and Design, University of Alberta, 1998.

[Meie96] B.J. Meier. "Painterly rendering for animation". *Proc. of SIGGRAPH '96*, pp. 477–484, August 1996.

[Misa94] H. Misawa. *Introduction to Pencil Techniques (Easy Start Guide).* Books Nippan, (ISBN 4766107144), 1994.

[Pric93] G. Price. *Pencil Drawing.* (from the Art is... Video Series). Crystal Productions (SBN 1-56290-077-3), August 1993.

[Ruff69] C. Ruffino. *A Guide to Pencil Drawing.* Van Nostrand Reinhold Company, New York, 1969.

[Sait90] T. Saito and T. Takahashi. "Comprehensible rendering of 3D shapes". *Proc. of SIGGRAPH '90*, pp. 197–206, August 1990.

[Sait94] T. Saito. "Real-time previewing for volume visualization". *Symp. Volume Visualization*, pp. 99–106, October 1994.

[Sali94] M.P. Salisbury, S.E. Anderson, R. Barzel, and D.H. Salesin. "Interactive pen-and-ink illustration". *Proc. of SIGGRAPH '94*, pp. 101–108, July 1994.

[Salw25] J. Salwey. *The Art of Drawing in Lead Pencil.* B.T. Batsford, Ltd., London, 1925.

[Sasa87] T.T. Sasada. "Drawing natural scenery by computer graphics". *Computer Aided Design*, Vol. 19, No. 4, pp. 212–218, May 1987.

[Schl96] S. Schlechtweg and T. Strothotte. "Rendering line-drawings with limited resources". *Proc. of GRAPHICON '96, 6th International Conference and Exhibition on Computer Graphics and Visualization in Russia*, Vol. 2, pp. 131–137, July 1996.

[Scho93] S. Schofield. *Non-photorealistic rendering: a critical examination and proposed system.* Ph.D. thesis, Middlesex Univ., England, October 1993.

[Schu96] J. Schumann, T. Strothotte, A. Raab, and S. Laser. "Assessing the Effect of Non-Photorealistic Images in Computer-Aided Design". *ACM Human Factors in Computing Systems, SIGCHI '96*, pp. 35–41, April 1996.

[Seli91] D.D. Seligmann and S. Feiner. "Automated generation of Intent-Based 3D Illustration". *Proc. of SIGGRAPH '91*, pp. 123–132, July 1991.

[Smal91] D. Small. "Simulating watercolor by modeling diffusion, pigment, and paper fibers". *Proc. of SPIE, Image Handling and Reproduction Systems Integration*, Vol. 1460, pp. 140–146, August 1991.

[Sous99a] M.C. Sousa and J.W. Buchanan. "Computer-generated graphite pencil rendering of 3D polygonal models". *Computer Graphics Forum (Proc. of Eurographics '99, to appear)*, September 1999.

[Sous99b] M.C. Sousa and J.W. Buchanan. "Observational model of blenders and erasers in computer-generated pencil rendering". *Proc. of Graphics Interface '99*, pp. 157–166, June 1999.

[Sous99c] M.C. Sousa and J.W. Buchanan. "Observational models of graphite pencil drawing materials". *Submitted for publication*, May 1999.

[Stre98] L. Streit and J.W. Buchanan. "Importance driven halftoning". *Proc. of Eurographics '98*, pp. 207–217, August 1998.

[Stro94] T. Strothotte, B. Preim, A. Raab, J. Schumann, and D.R. Forsey. "How to render frames and influence people". *Computer Graphics Forum (Proc. of Eurographics '94)*, Vol. 13, No. 3, pp. 455–466, August 1994.

[Taka97] S. Takagi and I. Fujishiro. "Microscopic structural modeling of colored pencil drawings". *SIGGRAPH '97 Visual Proc.*, p. 187, August 1997.

[Team97] Parramon Editorial Team. *Barron's Art Handbooks Drawing.* Barron's Educational Series, Inc., New York, (ISBN 0-7641-5007-3), 1997.

[Verm89] A.H. Vermeulen and P.P. Tanner. "PencilSketch – a pencil-based paint system". *Proc. of Graphics Interface '89*, pp. 138–143, June 1989.

[Very99a] O. Veryovka. *Texture Control in Digital Halftoning.* Ph.D. thesis, Dept. of Computing Science, University of Alberta, Canada, March 1999.

[Very99b] O. Veryovka and J.W. Buchanan. "Comprehensive halftoning of 3D scenes". *Computer Graphics Forum (Proc. of Eurographics '99, to appear)*, September 1999.

[Wats78] E. W. Watson. *Course in Pencil Sketching, Four Books in One.* Van Nostrand Reinhold Company, New York, (ISBN 0-442-29230-9), 1978.

[Wats83] E. W. Watson. *Gallery of Pencil Techniques.* Van Nostrand Reinhold Company, New York, (ISBN 0-442-29209-0), 1983.

[Wink94] G. Winkenbach and D.H. Salesin. "Computer-generated pen-and-ink illustration". *Proc. of SIGGRAPH '94*, pp. 91–100, July 1994.

[Wink96a] G.A. Winkenbach. *Computer-generated pen-and-ink illustration.* Ph.D. thesis, University of Washington, December 1996.

[Wink96b] G.A. Winkenbach and D.H. Salesin. "Rendering parametric surfaces in pen-and-ink". *Proc. of SIGGRAPH '96*, pp. 469–476, August 1996.